Incorporating the Effects of Gas Slippage and Non-Darcy Flow in the Measurement of Permeability using Pressure Pulse Decay Technique

by

Muhammad Noman Khan

A Thesis Presented to the

FACULTY OF THE COLLEGE OF GRADUATE STUDIES

KING FAHD UNIVERSITY OF PETROLEUM & MINERALS

DHAHRAN, SAUDI ARABIA

In Partial Fulfillment of the
Requirements for the Degree of

MASTER OF SCIENCE

In

PETROLEUM ENGINEERING

April, 2000

INFORMATION TO USERS

This manuscript has been reproduced from the microfilm master. UMI films the text directly from the original or copy submitted. Thus, some thesis and dissertation copies are in typewriter face, while others may be from any type of computer printer.

The quality of this reproduction is dependent upon the quality of the copy submitted. Broken or indistinct print, colored or poor quality illustrations and photographs, print bleedthrough, substandard margins, and improper alignment can adversely affect reproduction.

In the unlikely event that the author did not send UMI a complete manuscript and there are missing pages, these will be noted. Also, if unauthorized copyright material had to be removed, a note will indicate the deletion.

Oversize materials (e.g., maps, drawings, charts) are reproduced by sectioning the original, beginning at the upper left-hand corner and continuing from left to right in equal sections with small overlaps.

Photographs included in the original manuscript have been reproduced xerographically in this copy. Higher quality 6" x 9" black and white photographic prints are available for any photographs or illustrations appearing in this copy for an additional charge. Contact UMI directly to order.

Bell & Howell Information and Learning
300 North Zeeb Road, Ann Arbor, MI 48106-1346 USA
800-521-0600

UMI®

Incorporating the Effects of Gas Slippage and Non-Darcy Flow in the Measurement of Permeability using Pressure Pulse Decay Technique

BY

MUHAMMAD NOMAN KHAN

A Thesis Presented to the

DEANSHIP OF GRADUATE STUDIES

KING FAHD UNIVERSITY OF PETROLEUM & MINERALS

DHAHRAN, SAUDI ARABIA

In Partial Fulfillment of the
Requirements for the Degree of

MASTER OF SCIENCE

In

PETROLEUM ENGINEERING

APRIL 2000

KING FAHD UNIVERSITY OF PETROLEUM & MINERALS
DHAHRAN, SAUDI ARABIA

DEANSHIP OF GRADUATE STUDIES

This thesis, written by

MUHAMMAD NOMAN KHAN

under the direction of his Thesis Advisor and approved by his Thesis Committee, has been presented to and accepted by the Dean of Graduate Studies, in partial fulfillment of the requirements for the degree of

MASTER OF SCIENCE IN PETROLEUM ENGINEERING

Thesis Committee:

H.Y. Al-Yousef
Dr. Hasan Y. Al-Yousef
Thesis Advisor

M. A. Al-Marhoun
Dr. Muhammad A. Al-Marhoun
Member

Dr. Hasan S. Al-Hashim
Member

A. A. Almajed
Dr. Abdulaziz A. Al-Majed
Department Chairman

18/4/2000
Dr. Abdallah M. Al-Shehri
Dean of Graduate Studies

Dedicated to

My Parents, Brothers and Sisters

Acknowledgment

First and the foremost, all praise to the Almighty Allah Who gave me the courage and patience to carry out this work. I am happy to have had a chance to glorify His name in the sincerest way through this small accomplishment and ask Him to accept my efforts. May He guide us and the whole humanity to the right path (*Aameen*).

Acknowledgement is due to King Fahd University of Petroleum and Minerals for providing support to this work.

My deep appreciation goes to my thesis advisor Dr. Hasan Y. Al-Yousef for his constant help, guidance and the countless hours of attention he devoted throughout the course of this work. His priceless suggestions made this work interesting and learning for me. He was always kind, understanding and sympathetic to me. Working with him was indeed a wonderful and learning experience, which I thoroughly enjoyed.

Thanks are also due to my thesis committee members Dr. Hasan S. Al-Hashim and Dr. Muhammad A. Al-Marhoun for their interest, cooperation, advice and constructive criticism.

I am also indebted to Dr. Abdul-Aziz Al-Majed as the department chairman, and other faculty members for their support.

Thanks are due to my family members for their moral support throughout my academic career. This work is dedicated to my parents for taking pains for my academic pursuits and my personality.

Lastly, I also acknowledge my fellow graduate students, and all my friends in the campus, especially, Shariq, Zeeshan, Hamid, Shazli, Izzat, Ahmar and Dr. Asad-ur-Rahman, from whom I learned a lot and who made the long work hours pleasant.

TABLE OF CONTENTS

CHAPTER 7

CONCLUSIONS AND RECOMMENDATIONS

LIST OF TABLES

LIST OF FIGURES

THESIS ABSTRACT

NAME OF STUDENT: MUHAMMAD NOMAN KHAN

TITLE OF STUDY : Incorporating the Effects of Gas Slippage and Non-Darcy Flow in the Measurement of Permeability using Pressure Pulse Decay Technique.

MAJOR FIELD : Petroleum Engineering

DATE OF DEGREE : April 2000

In recent years the pressure pulse decay technique became a frequent tool for fast and convenient measurement of permeability of tight rocks. The method is superior to conventional steady state method as it is much faster and easier to perform. A lot of work has been done on the development of this technique, however, only few investigators considered the effect of gas-slippage and non-Darcy flow and gave approximate solutions. Neglecting these effects may introduce errors when analyzing laboratory pressure pulse decay data.

The objective of this work is to develop a computer model to analyze the pressure pulse decay data by taking into account the effects of gas-slippage and non-Darcy flow. For this purpose a computer simulator has been developed based on the numerical solution of the mathematical model in which gas-slippage and non-Darcy flow effects are incorporated. Based on the developed simulator, a data analysis computer program is developed, that analyses the pressure pulse decay laboratory data using non-linear regression technique for the estimation of permeability, Klinkenberg constant and Forchheimer constant.

The simulation results have shown that due to the opposite effects of gas-slippage and non-Darcy flow on the pressure pulse decay, it is not reliable to find the values of permeability (k), Klinkenberg constant (b) and Forchheimer constant (β), simultaneously from a single pressure pulse decay test. Hence, separate tests should be designed and performed to find b and β with permeability. Laboratory pressure pulse decay experiments have been designed and performed under the conditions where the data were influenced by the gas-slippage and non-Darcy flow effects separately, and the data obtained were analyzed by the developed computer program to obtain k, b and β values for the core samples. A technique has also been presented for the estimation of permeability and b from multiple pressure pulse decay tests. The results obtained are compared with the Jones approximate method, which is the most commonly used method for the analysis of pressure pulse decay data.

MASTER OF SCIENCE DEGREE
KING FAHD UNIVERSITY OF PETROLEUM & MINERALS
Dhahran, Saudi Arabia

مُلخص

اسم الطالب : محمد نعمان خان

عنوان الدراسة : تضمين تأثيرات أنزلاق الغاز والتدفق الغير متوافق مع دراسي في حساب النفاذية باستخدام طريقة تلاشي النبض الضغطي .

التخصص : هندسة البترول

تاريخ التخرج : ابريل ٢٠٠٠ م

لقد كثر استخدام طريقة تلاشي النبض الضغطي في حساب نفاذية الصخور المتماسكة جداً في الآونة الأخيرة وذلك لسهولتها وسرعة اجراءها مقارنة مع الطرق الاعتيادية . ولقد اجريت دراسات عديدة في تطوير هذه الطريقة إلا أن معظم هذه الدراسات لم تتضمن على تأثيرات انزلاق الغاز والتدفق الغير متوافق مع دراسي وتلك التي تضمنت عليهما أخذت حلول تقريبية لهما . وأن عدم تضمين هذه التأثيرات في حساب النفاذية يؤدي إلى أخطاء في تحليل البيانات المستخلصة من أختبارات تلاشي النبض الضغطي في المختبر .

وتهدف هذه الدراسة إلى تطوير نموذج كمبيوتر لتحليل بيانات اختبارات تلاشي النبض الضغطي مع تضمين تأثيرات انزلاق الغاز والتدفق الغير متوافق مع دراسي في حساب النفاذية . ولأجل ذلك تم تطوير محاكي على أساس الحلول الرقمية لنموذج رياضي يتضمن تأثيرات انزلاق الغاز والتدفق الغير متوافق مع دراسي . واعتماداً على نتائج المحاكي تم تطوير برنامج كمبيوتر يقوم بتحليل بيانات اختبارات تلاشي النبض الضغطي باستخدام طريقة التردد اللاخطي في تقدير ثابت كلنكنبيرج وثابت فورشهيمر .

ولقد أظهرت النتائج أنه بسبب تضاد تأثير انزلاق الغاز وتأثير التدفق الغير متوافق مع دراسي على تلاشي النبض الضغطي فانه لا يستحسن حساب النفاذية وثابت كلنكنبيرج وثابت فورشهيمر آتياً من نفس بيانات اختبار تلاشي النبض الضغطي . فعليه يجب عمل اختبارات منفصلة لحساب النفاذية وثابت كلنكنبيرج وأخرى للنفاذية وثابت فورشهيمر . ولقد صممت واجريت تجارب تلاشي النبض الضغطي في المختبر تحت تأثير انزلاق الغاز وأخرى تحت تأثير التدفق الغير متوافق مع دراسي وتم حساب النفاذية وثابت كلنكنبيرج وثابت فورشهيمر لعينات لبية . وأيضاً أدرجت طريقة لتقدير النفاذية وثابت كلنكنبيرج من اختبارات متضاعفة لتلاشي النبض الضغطي كما قورنت النتائج مع نتائج طريقة جون التقريبية التي تستخدم في نطاق واسع في تحليل بيانات تلاشي النبض الضغطي .

درجة الماجستير في العلوم

جامعة الملك فهد للبترول والمعادن - الظهران

المملكة العربية السعودية

CHAPTER 1

INTRODUCTION

1.1 Pressure pulse decay technique

As numerous low permeability reservoirs worldwide still present a considerable potential for hydrocarbon production, attention was paid to the investigation of these rock types. Determination of their permeability is usually difficult by the conventional steady state methods because the achievement of the steady state condition is sometimes questionable, the flow rates are difficult to measure and to control, and measurements can last for a long time. This problem is more complicated as the low-permeability rocks usually have sensitive clay minerals and fines that are susceptible for damages caused by extended flow periods.

It has been estimated that between 400 Tcf and 1000 Tcf of natural gas are trapped in formations designated as 'tight sands' (permeability less than 0.1 md). In addition to this resource, another 300 Tcf to 2700 Tcf of natural gas may be trapped in other low permeability formations [12].

Brace et al.[5] introduced a transient technique, known as the pressure pulse technique for the measurement of permeability. Inlet and outlet vessels were connected to the core, the inlet vessel having a slightly higher initial pressure than the outlet one. The pressure pulse generated in this way was forced through the core and the pressure evolution at both ends of the core was recorded with time. It was the very first model and the authors made some assumptions, which however might not be valid under some circumstances.

The pressure decay curve is described by a differential equation for the flow of gas through the sample (Brace et al. [3], Hsieh et al. [20]). To enable calculation of the permeability from the measured pressure decay, the solution of this differential equation should be known for the boundary and initial conditions involved. An exact solution of the problem was given by Hsieh et al. [20]. This solution is, however, difficult to evaluate. Several researchers, therefore, have proposed approximate solutions to the problem (Brace et al. [4], Lin [5], Trimmer [6], Chen and Stagg [18], Bourbie and Walls [28], Haskett et al. [34] etc.), which are valid for certain ranges of the upstream, downstream and pore volumes. These solutions are only valid when the pore volume of the sample is negligibly small compared to the upstream and down stream vessel volumes. Some of these methods are valid only for certain experimental conditions, which are unfortunately not always fully mentioned [9].

1.2 Non-Darcy flow

At low flow rates (e.g., Reynold no. < 0.1), the flow in each pore is in the Stokes flow regime. The pressure drop across the porous medium is linearly proportional to the flow rate, i.e., Darcy's law followed. At high flow rates, the pressure drop exceeds that predicted by Darcy's law. This phenomenon is known as non-Darcy flow, though sometimes referred to as high-velocity flow [8]. The Forchheimer (1914) equation

$$-\frac{dP}{dx} = \frac{\mu}{k}v + \rho\beta v^2 \quad \text{.....1.1}$$

describes the relationship between the pressure gradient and velocity in isotropic porous media. β is called the non-Darcy coefficient and sometimes also known as velocity coefficient [8]. Also μ, ν and ρ are the viscosity, velocity and density of the flowing fluid. The above equation is a general momentum balance equation for steady state flow. It may also be rearranged to form

$$v = -\delta \frac{k}{\mu}\frac{dP}{dx} \quad \text{.....1.2}$$

where,

$$\delta = \left(\frac{1}{1 + \frac{\beta\rho kv}{\mu}}\right) \quad \text{.....1.3}$$

δ is known as the laminar inertial turbulent (LIT) factor. When δ = 1.0, equation 1.2 will be reduced to Darcy's equation.

1.3 Klinkenberg effect

Gas flow in porous media differs from liquid flow because of the large gas compressibility and pressure dependent effective permeability. For liquids flowing in a homogeneous medium, the permeability, k, is found to be independent of the flowing fluid and is, thus, a property of the medium. However, in the case of gas flow, Klinkenberg (1941) observed that when the pores of the medium were of the same order of size as the mean free path of the gas molecules, slippage occurred at the fluid solid boundary, and the permeability to gas was not constant. Under such conditions, which become significant at low pressures,

$$k_g = k_L(1+b/p) \quad \text{.....1.4}$$

where,

k_L = permeability of the medium to gas at infinite pressure (or permeability of the medium to a liquid)

b = a constant dependent on the gas porous medium system.

Despite the progress made so far in our understanding of porous medium gas flow, one important aspect, the Klinkenberg effect, has been ignored in most studies [37]. Even though efforts have been made to estimate errors introduced by neglecting the Klinkenberg effect, only a few studies addressed this phenomenon explicitly. The

Klinkenberg effect may have significant impact on gas flow behavior, especially in low permeability media [37].

The application of Darcy's law to gas flow in low permeability formations requires a correction for the Klinkenberg effect [12]. Incorporating the Klinkenberg effect as expressed in the above equation into a gas flow model introduces nonlinear terms that preclude the development of analytical solutions. Thus the conditions under which the Klinkenberg effect can be neglected were investigated by different workers to impose on their experimental setup.

CHAPTER 2

BACKGROUND OF THE WORK

2.1 Literature review

2.1.1 Pressure pulse decay technique

Neilson [31] initially proposed the idea of pressure pulse decay technique for measuring permeability of rocks. He did not present any mathematical details but only discussed the idea of pressure pulse decay technique, its advantages and the experimental setup. For interpretation he relied heavily upon the empirical interpretation methods based largely upon the time lapse between triggering and completion of the pressure decay.

Brace et al. [5] were the pioneers of the pressure pulse decay technique for permeability measurement. In those times permeability was generally determined from measurements of flow rate through a sample under constant pressure gradient. They suggested a transient method, which was more convenient as the pressure and time are more easily measured in a high pressure experiment than flow rate.

They showed that the decay characteristics depend on the permeability, the dimensions of the sample, reservoir volumes and the physical characteristics of the fluid. The permeability of the sample was obtained by comparing the observed decay of pressure in the upstream reservoir with the behavior predicted theoretically.

They showed that the pressure gradient decays exponentially to zero. The pressure P_1 in the upstream reservoir was given as

$$(P_1-P_f) = \Delta P[(V_2/V_1)+V_2]e^{-\alpha t} \quad \text{.....2.1}$$

where,
$$\alpha = (kA / \mu cL)(1/V_1+1/V_2) \quad \text{.....2.2}$$

A = cross sectional area

L = Length of the sample

V_1 , V_2 = Volumes of upstream and downstream reservoirs

P_f = Final pressure

ΔP = Step change of pressure in reservoir at t=0

μ = viscosity of fluid

c = compressibility of fluid

The permeability of a sample is found by plotting the pressure decay (P_1-P_f) on semilog paper against time. The slope of the resulting line is -α. Permeability is found from above equation of α, where it is the only unknown.

Yamada and Jones [35] suggested a different approach to find the exponential pressure decay prescribed by Brace et al.[5] and associated constraints. They reviewed the Brace et al. approach of ignoring sample pore volume by assuming it negligibly small. They concluded that the pressure decay may look exponential, but it is only a fraction of an exponential curve, and the interpretation by Brace et al. cannot be applied.

Hsieh et al. [20] gave a general, analytical solution for the transient pulse testing. The mathematical analysis adopted by Brace et al.[5] for the transient pulse test assumed that there is no compressive storage in the rock sample. According to Hsieh et al., although this assumption may be reasonable for some crystalline rocks, it is generally poor for rocks such as shales and argillites, which have significant porosity and compressive storage. Plots of dimensionless variables were used to illustrate the general nature as well as the limiting behavior of the solution. It was shown that solutions for several special cases, which have been examined by the previous investigators, are limiting forms of the general solution.

Neuzil et al. [32] in continuation of Hsieh et al.'s work, presented a method for analyzing the time history of pressure changes in the upstream and downstream reservoirs

to determine the hydraulic properties (permeability and specific storage) of the sample. They also compared the general solution with the Brace et al. analysis (in which compressive storage was assumed negligible) and examined the error in permeability calculation. The solution was expressed in four dimensionless quantities:

1. Dimensionless hydraulic head in the upstream and downstream reservoirs, h_u/H and h_d/H respectively.
2. Dimensionless time, $\alpha = kt/L^2S_s$

   where, S_s is the specific storage of the core sample (with the dimension, L^{-1})
3. Parameter 1 (expresses the ratio of compressive storage in the sample to the upstream reservoir).
4. Parameter 2 (expresses the ratio of compressive storage in the downstream reservoir to the upstream reservoir).

The authors showed that in order to minimize the time required for the test, the sample length should be kept as small as possible. Also they concluded that for calculating both permeability and specific storage, ideally $0 <$ (Parameter 1) ≤ 0.1. For a sample with significant compressive storage, a large upstream reservoir is required.

Lin [28] performed analysis to compare the two approaches of using the transient method to determine permeability of rocks. the simplified version (Brace et al., 1968) and the numerical version developed by himself. The author used TRUMP (A computer code, originally developed for calculating thermal diffusion problems) to generate solutions and compared them with those of Brace et al. [5].

He concluded that:

1. $P_1(t)$ is generally not a simple exponential function of time as shown by Brace et al (1968).
2. The simplified analytical version is not generally suitable to all systems of measuring permeability. If the experimental setup could be adjusted to meet the conditions of the simplified analytical version (namely, small fluid storage), then the convenience of his version would make determination of permeability far easier.
3. For relative fluid storage < 0.01, the difference in permeability between the two versions is very small; when relative fluid storage > 0.03, then the permeability determined by these two versions differs significantly.
4. The curve matching procedures used in the numerical version is not as convenient as his simplified version.

Trimmer [34] discussed the advantages and limitations of the techniques described by Brace et al. (1968), Trimmer et al. (1980), Lin (1981). He concluded that:

1. In designing permeability experiments, the technique described by Brace et al. (1968) should be used when possible. This requires that the sample pore volume be small compared to the reservoir volume.
2. If the experimental parameters cannot be adjusted to take advantage of the Brace et al. technique, then the technique described by Trimmer et al. (1980) and Lin (1981) may be used.

Bourbie and Walls [4] presented an analytical solution based on certain assumptions and specific boundary conditions. They described Lin's [28] and Yamada and Jones' [35] numerical solution as inconvenient to use. They took the upstream reservoir volume much greater than the pore volume or the volume of the downstream reservoir. Thus the pressure in upstream reservoir remains essentially constant during the decay. They concluded that error resulting from using the exponential solution was about 25%, and permeabilities calculated from their solution were within ±5% of steady state measurement over a wide range of permeability.

Chen and Stagg [6] presented an alternative solution that is not restricted by t_D ($kt/\phi\mu cL^2$) or γ (ratio of pore volume to downstream volume), as concluded by Bourbie and Walls [4]. It reduces to an exponential decay solution similar to Brace et al.'s [5] solution when $t_D > 0.3$. Pore volume was also not neglected as neglected by Brace et al. The exponential series solution presented is valid for all t_D and γ. This solution can be used to analyze most core samples except those having extremely low permeability on the order of 10^{-9} micro m^2 ($\sim 10^{-6}$md). Here either the full solution given or the error function solution must be used. They also concluded that the Brace et al. [5] solution underestimates the permeability and the degree of under estimation is dependent on the ratio of the pore volume to the downstream volume.

Haskett and Narhara [18] used the dimensionless pseudo-pressure and pseudo-time terms, and described an analytical model for gas flow through a core and proposed a method for simultaneous determination of both the porosity and permeability of low permeability cores. They concluded that the use of a pressure transient technique utilizing gas flow and small pore volume, results in a test that is sensitive to both porosity and permeability.

Dicker and Smits [9] showed that fast and accurate measurements are possible when taking the volumes of the upstream and downstream vessels in the equipment approximately equal to the pore volume of the sample. They also assumed that gas slippage effect is negligible, because high pore pressure is used. The permeability can be calculated from the relation

$$k = \frac{c\,\mu\phi\,L^2 s}{f(a,b)} \qquad \text{.....2.3}$$

Where,

s = semi-log slope of the pressure decay (sec^{-1})

$f(a,b) = (a+b+ab) - (a+b+0.4132ab)^2/3 + 0.0744(a+b+0.0578ab)^3$ 2.4

$a = Vs/V_1$ and $b = Vs/V_2$

Vs = sample pore volume, V_1 & V_2 = upstream and downstream reservoir volumes

The method consists of plotting the measured pressure difference versus time on semi logarithmic paper, determining the slope of the straight line part of this plot, and

calculating k from the above relation. The factor f(a,b) is a constant dependent on the choice of a and b. They also suggested to take the volume of the upstream and downstream vessels slightly higher than the pore volume, such that a and b are relatively large, resulting in fast measurements, whereas the simple analytical approximation is still valid.

Kamath et al. [25] summarized the work done in the area of pressure pulse decay technique and presented the solution of the problem by Hsieh et al. [20] in dimensionless variables. Some of their important conclusions are :

- The effective permeability calculated from a transient test could be a function of the direction of the pressure disturbance and could differ significantly from the effective steady state value for heterogeneous cores.
- The pressure transient response of heterogeneous core appears similar to that of a homogeneous core for small F_{cu} (F_{cu} = Ratio of the compressive storage of core to upstream vessel = $A\phi cL/S_u$). As F_{cu} increases, the response deviates. Therefore, their pressure transient testing system contains variable volume vessels.

Jones [22] proposed an approach to reduce the total time significantly in pulse decay permeability measurements of tight rocks. He suggested calculating the permeability from "late time" measurements. He concluded that the reservoir volumes should be equal. This produces the desirable effects of maintaining a constant mean pore pressure during the single exponential portion of the decay. Also the average fluid viscosity and

compressibility remain constant. According to Jones, even employing high mean pressure, the gas permeabilities obtained are not corrected for gas slippage, and may be somewhat high. To minimize the inertial flow resistance, the author recommended 10 psi as the maximum ΔP for gas measurements.

2.1.2 Klinkenberg effect

Klinkenberg [26] identified the gas slippage phenomena at the fluid solid boundary in case of gas flow through a porous medium. He performed steady state experiments and proposed the method to find the permeability and gas slippage constant using the equation:

$$k_g = k_L(1+b/p) \quad \text{.....2.5}$$

By plotting k_g vs $1/p_m$ we can find equivalent liquid permeability, k_L, and Klinkenberg constant, b, from the intercept and slope of the straight line.

Ertekin et al. [12] developed a mathematical formulation, applicable to both numerical simulation and transient well test analysis, describing the flow of gas in very tight (k< 0.1 md) porous media. They combined the two flow mechanism namely flow due to concentration field and flow due to pressure field. This yields a composition, pressure and saturation dependent slippage factor. Before this work, no detailed

investigation theoretical or experimental had been conducted regarding the dynamic behavior of gas slippage. Klinkenberg's [26] experimental data indicated that the slippage factor increased with increasing pressure, however, in practice it was regarded as being constant. When the mean free path of the gas molecules is small compared to the capillary radius (r_c), the flow of a gas through a capillary is governed by Hagen Poiseuille law [12]:

$$q = \frac{\pi r_c^4 \overline{p} \Delta p}{8 \mu p L} \quad \text{.....2.6}$$

This criterion of the mean free path being small compared with the capillary radius is met for large radii capillaries or flow at high pressures.

When the mean free path is large compared to the capillary radius, the flow is governed by the Knudsen equation as

$$q = \frac{4}{3} \frac{r_c^3}{p} \sqrt{\frac{2RT}{MW} \frac{\Delta p}{L}} \quad \text{.....2.7}$$

In the intermediate range the flow rate is governed by

$$q = \frac{\pi r_c^4 \overline{p} \Delta p}{8 \mu p L} + K \frac{4}{3} \frac{r_c^3}{p} \sqrt{\frac{2RT}{MW} \frac{\Delta p}{L}} \quad \text{.....2.8}$$

Where, K is a constant and approximately equal to 0.9, MW is the molecular weight, R is the gas constant and T is the absolute temperature.[12].

They derived the relation for 'b' as

$$b = \frac{8.52\ K\mu}{r_c}\sqrt{\frac{RT}{MW}} \qquad \text{.....2.9}$$

They derived the equation that describes the single phase, dual mechanism flow of gas through porous media with appropriate initial and boundary conditions.

$$\frac{1}{r}\frac{\partial}{\partial r}\left[\frac{\alpha r k_{\infty} p\left(1+\frac{b}{p}\right)}{\mu z}\frac{\partial p}{\partial r}\right] = \frac{\phi \rho c_g}{z}\frac{\partial p}{\partial t} \qquad \text{.....2.10}$$

They suggested to solve the above equation either numerically or after linearization. analytically using standard reservoir engineering techniques.

Freeman and Bush [14] recommended using downstream volume to be equal to the pore volume of the sample and measured its pressure buildup during the experiment. They used the Darcy's equation in one dimension and corrected it for the Klinkenberg effect by Klinkenberg relation for slippage. It was mentioned that the method was not particularly sensitive to values of 'b' because of the relatively high mean pressure.

Kaluarachchi [24] presented an exact solution to gas flow in a two-dimensional axi-symmetric flow domain with anisotropic gas permeability that includes the

Klinkenberg effect. His results suggest that the Klinkenberg effect is important with low permeable materials such as clay and silt. He presented the permeability relationship given by Klinkenberg in explicit r and z coordinates as follows

$$k_{rr} = k_{rr_\infty}\left(1 + \frac{b}{\sqrt{\Phi}}\right) \quad \text{.....2.11}$$

Where, $\Phi = p^2$ and k_{rr} is the principal permeability in r direction and $k_{rr\infty}$ is the permeability at infinite pressure. The differential equation he derived then was

$$\frac{\partial}{\partial z}\left[k_{zz}\frac{\partial \Phi}{\partial z}\right] + \frac{1}{r}\frac{\partial}{\partial r}\left[rk_{rr}\frac{\partial \Phi}{\partial r}\right] = 0 \quad \text{.....2.12}$$

As direct solution to the above equation became difficult due to the non-linearity, he used the Kirchhoff transformation on Φ which was denoted as U

$$U = \int_{\Phi_*}^{\Phi}\left(1 + \frac{b}{\sqrt{\tau}}\right)d\tau \quad \text{.....2.13}$$

Thus he got the linear partial differential equation in U, and non-linearity due to Klinkenberg effect had been eliminated due to the Kirchhoff's transformation.

$$\frac{\partial}{\partial z}\left[k_{zz}\frac{\partial U}{\partial z}\right]+\frac{1}{r}\frac{\partial}{\partial r}\left[rk_{rz}\frac{\partial U}{\partial r}\right]=0 \quad \text{.....2.14}$$

Hence, pressure, P can be written as

$$P(r,z)=-b+\sqrt{b^2+2bP_a+P_a^2+U(r,z)} \quad \text{.....2.15}$$

Where, P_a is the atmospheric pressure, (~1 atm.)

He finally concluded after his analysis that the Klinkenberg effect is dominant with less permeable soils due to large predicted pressure drawdown. The errors produced by neglecting the Klinkenberg effect are highest at the center of the well for any given soil type and also increase with decreasing permeability. The errors in gas-phase velocities produced by neglecting Klinkenberg effect may affect correct estimation of gas permeability and/or overall predictions of contaminant mass recovery.

Yu-Shu Wu et al. [37] presented a set of analytical solutions developed to analyze steady state and transient gas flow through porous media with Klinkenberg effect. They used a new variable (pressure function) to simplify the gas flow governing differential equation with the Klinkenberg effect. As examples of application. the analytical solution was used to verify the numerical solutions for simulating Klinkenberg effects and to provide linear correlations according to which, laboratory data can be plotted to determine the values of k and b. They did not include the turbulent effects on gas flow in the analysis. According to them, it can be shown that effects of turbulent flow

can in general be ignored when Klinkenberg effects are significant. They wrote the mass balance equation for gas flow in porous media as

$$\nabla.(\nabla P_b^2) = \frac{1}{\alpha}\frac{\partial P_b^2}{\partial t} \quad \text{.....2.16}$$

Where using a new variable

$$P_b = P_{avg} + b \quad \text{.....2.17}$$

and α is gas diffusivity

$$\alpha = \frac{k_\infty P_b}{\phi\mu} \quad \text{.....2.18}$$

They gave the transient solution by linearizing the conventional approach for transient gas flow analysis, i.e. by setting

$$\alpha = \frac{k_\infty P_b}{\phi\mu} \approx \frac{k_\infty \overline{P_b}}{\phi\mu} \quad \text{.....2.19}$$

Where $\overline{P}_b = P_{avg} + b$, is a function of average gas pressure, P_{avg}, and is treated as a constant. With this approximation, equation 2.16 becomes linear with respect to P_b^2.

If $P_{avg} = P_i$ is used throughout in the solution in evaluating the diffusivity term, it remains constant. This may introduce significant errors in the solution, in particular, at late time when pressures and their distributions in the system are very different from the initial condition.

The second approach they proposed, using a history dependent average pressure within the pressure changed (disturbed) domain instead of a constant diffusivity, evaluated using $P_{avg} = P_i$. The history dependent averaged pressure is defined as

$$\overline{P} \approx \frac{\sum A_j p_j}{\sum A_j} \quad \text{.....2.20}$$

Where, A_j is a controlled area at the geometric center of which the pressure was P_j at the immediate previous time when the solution was calculated.

The third approach they used was a comparison study using a numerical model, TOUGH 2 (Pruess [37]) to examine the approximate transient gas flow solution. It has been found that the conventional linearization procedure of deriving gas flow equation, using an initial gas pressure for the diffusivity term, will result in acceptable solutions, when the overall pressure variations in the system are small. However, the linearization assumption may introduce considerable errors when pressure changes are significantly different from the ambient condition. In this case, Yu-Shu Wu et al. proposed to use the third approach for the diffusivity term using a history-dependent averaged pressure with the analytical solution, which will still give accurate solutions even under high pressure change in the system.

2.1.3 Non-Darcy flow

Jones [21] developed an unsteady state apparatus and related theory for measuring the Klinkenberg permeability, Klinkenberg slip factor and Forchheimer turbulence factor of core plugs. He combined Darcy's equation and Klinkenberg equation to calculate the permeability from the experimental data. By plotting the resulting equation k and b could be found. However, there was difficulty in the evaluation of the pressure derivative with respect to time. He approximated that term to get the results.

For higher velocities, he derived a working equation for non-Darcy flow using Forchheimer equation, that gave a straight line for the correct value of b. In his solution, k_L, b and α were not separable and thus not convenient to use. Therefore, he approximated the solution, and his approximation becomes exact for b=0. ($\alpha = \beta k_L$ and β= turbulent factor in Forchheimer equation). Further he concluded that certain rocks, especially those that have high α factors deviate from a linear plot, then he modified the equation for higher velocities and accounted for non-Forchheimer flow behavior. He also correlated the slippage factor, b, and permeability, k_L, and obtained the following relation

$$b(psi) = 6.9\, k_L^{-0.36} \quad \text{.....2.21}$$

Geertsma [15] introduced an empirical correlation to estimate Forchheimer constant (β) in terms of permeability (k) and porosity (ϕ). His work based on

experimental data, dimensional analysis and other physical considerations. The data he used, covered the porosity range of 0.07 to 0.24 and the permeability range of 0.1md to 1000 md. He proposed the following correlation:

$$\beta = 4.8512\times10^{4}\, k^{-0.5}\, \phi^{-5.5} \quad \text{.....2.22}$$

Jones [23] suggested that the inertial coefficient, β, is influenced by the degree of permeability heterogeneity in a reservoir rock. He conducted permeability and pore volume measurement on 355 sandstone and 29 limestone core plugs using Helium in an unsteady state Klinkenberg permeameter/porosimeter. All permeabilities reported were slip corrected Klinkenberg permeabilities. Jones also measured the permeabilities of core plugs less than 0.01 md but that were not reported because according to him, inertial coefficients for these tight samples were probably unreliable. The reason was that under the experimental conditions employed, deviation from Darcy flow in these plugs was very small, and computation of the inertial coefficient becomes unstable as the quadratic term approaches zero. He concluded that porous, permeable rocks have three characteristic length dimensions that can be determined from gas flow measurements, $(k/\phi)^{1/2}$, c/b (c is constant), and $\beta k\phi$. Also the reciprocal slip factor, 1/b, is approximately proportional to $(k/\phi)^{1/2}$, and inertial coefficient, $\beta k\phi$ appears proportional to $(k/\phi)^{1/2}$ with increasing permeability and/or increasing homogeneity. He also gave the correlation for β which is valid for k = 0.01md to 1000 md.

$$\beta = 6.15\times10^{10}\, k^{-1.55} \quad \text{.....2.23}$$

Yildiz [36] developed an analytical model describing the transient non-Darcy flow in a reservoir. He presented the partial differential equation describing the unsteady state, non-Darcy fluid flow by combining the continuity equation, Forchheimer equation and an equation of state for fluid. He recognized that the transient, non-Darcy flow in porous media is a complex phenomenon and the partial differential equation is not amenable to analytical treatment. Therefore, the equation had been solved either numerically or semi-analytically. He applied the Boltzman transformation to the momentum and continuity equations in his derivation. His model has shown that the slope of the straight lines obtained from pressure drawdown and buildup tests are independent of non-Darcy flow component as long as fluid properties remain constant.

Milton-Taylor [30] investigated both the β factor and the Klinkenberg slip constant. He pointed out that the non-Darcy effects may be serious in the analysis of laboratory derived gas permeametery data, of reservoir cores and its extrapolation to the field. His data presented in the paper confirms Ertekin et al.'s [12] view that slip constant 'b' increases with increasing pressure. After his experimental study, Milton-Taylor concluded that the β-factor in both consolidated and unconsolidated media is independent of gas type used.

Al-Rumhy and Kalam [2] used experimental techniques, such as constant overburden pressure, changing overburden pressure, forward flow and back pressure flow to optimize and obtain accurate evaluations of Klinkenberg parameters and inertial

resistance coefficients for a selection of Omani reservoir cores. Thirteen reservoir core plugs from various Omani reservoirs were initially chosen. Klinkenberg permeabilities were determined for each of the cores used. Visco-inertial coefficients were also determined for each of the cores, by increasing the gas flow to extend through the transition region to visco-inertial flow. It was concluded that the inertial resistance coefficient derived from gas flow data in the transition from laminar to visco-inertial flow are always affected by gas slippage factor. Their laboratory derived non-Darcy coefficients show

$$\beta \propto k^{-1.50} \qquad \text{.....2.24}$$

after applying the gas slippage corrections, confirming close agreement with the non-steady state gas flow data of Jones [23].

Liu et al. [29] developed a general correlation for the non-Darcy flow coefficient with permeability, porosity and tortuosity (τ).

$$\beta = \frac{8.91 \times 10^{-8} \tau}{\phi k_l} \qquad \text{.....2.25}$$

Based on the analyses of a wide range of experimental flow data from various sources in the literature, Liu et al. has concluded that the effective stress should not be included in the correlation of the non-Darcy flow coefficient to avoid duplication. Because its effect

is implicitly included through the dependency of permeability, porosity and tortuosity on the effective stress. Also the dimensionless group ($\beta k\phi/\tau$) appears to be universal constant.

Firoozabadi et al. [13] summarized the previous literature on the high velocity flow in porous media. They performed flow experiments on a cylindrical Berea sandstone core and repeat the experiments after dividing the core into two equal parts. On the basis of their experiments they concluded that the effect of gas properties change over the length of a porous media, do not account for high velocity flow in porous media, and Darcy's law is inadequate to represent high velocity flow. They also concluded that β is a function of rock properties and does not depend on length.

A De Ville [1] studied the effect of the inertia and Forchheimer terms on a compressible Darcy flow. The motivation for his work had been the study of aeration of cereal stores. He concluded after his analytical solution that Forchheimer and inertial terms represent different physical effects. The Forchheimer term always resists the motion of the gas, whereas the inertia term may resists or accelerates the gas flow.

Grigg and Hwang [17] reported the results of non-Darcy flow experiments in a single and two-phase flow in porous media. They tried to extend the work of Al-Rumhy and Kalam and Firoozabadi et al. The Klinkenberg effect was ignored because of using high average internal core pressure (~1000 psig). They concluded that the effect of both

mobile and immobile liquid was significant for both decreasing the effective permeability and increasing β.

Coles and Hartman [7] presented transient flow for β measurements obtained in dry core samples and in samples containing different saturations of immobile liquid. They obtained the measurements of inertial coefficient β using the apparatus described by Jones[21] (1972) and employed unsteady state pressure transient analysis to generate values for porosity, permeability and β. They compared the results with the literature reported β-k relationship and concluded that use of existing literature reported permeability non-Darcy coefficient relationships to calculate β might not be appropriated and may lead to significant errors. The errors increase with increasing flow rate and decreasing permeability. They derived a relationship from dry core data that allows β to be estimated as function of effective porosity and effective permeability.

They also suggested the need for further work to identify additional parameters (such as tortuosity) which may be used to estimate and predict non-Darcy coefficient.

Cooper et al. [8] study was directed at combining the effects of non-Darcy gas flow in anisotropic porous media. They conducted experimental study on carbonate and Berea sandstone cores and used nitrogen for single-phase experiments. They used the integrated Forchheimer's equation and plotted it as an equation of a straight line with intercept 1/k and slope β.

$$\frac{(P_{in}^2 - P_{out}^2)MA}{2\mu\dot{w}RTL} = \frac{1}{k} + \beta\frac{w}{A\mu} \quad \text{.....2.26}$$

Where '*M*' is the molecular weight of the gas, '*A*' is the cross-sectional area and '*w*' is the mass flow rate. They concluded that their experimental data showed good linearity between β and 1/k for both single phase and two-phase experiments. Also the experimental data agreed well with the equation proposed by Thauvin and Mohanty [33], for predicting β from k and τ.

$$\beta = 3.1\text{x}10^{4}\, k^{-1}\, \tau^{3} \quad \text{.....2.27}$$

2.2 Statement of the problem

Literature survey shows that a lot of work has been done on the development of the pressure pulse decay technique for the measurement of permeability of tight rocks. But only a few of the authors actually considered the combined effects of gas slippage and non-Darcy's flow. Incorporating the effect of non-Darcy flow and gas slippage into a gas flow model introduces nonlinear terms that preclude the development of analytical solutions. Thus the conditions under which these effects can be neglected were selected by different workers to impose on their experimental test.

Errors can result when neglecting the effects of gas slippage and non-Darcy flow in the analysis of laboratory data. This is the reason that anomalies have been reported in the literature in laboratory determined equivalent liquid permeability, k_L, from single-phase gas permeability measurements. It is often found that k_L evaluated for the same dry reservoir core varies from laboratory to laboratory, and that, the repeatability of evaluated k_L from the same laboratory is difficult [2].

Therefore, under the experimental conditions where the laboratory pressure pulse decay data, to measure permeability, are influenced by gas slippage and non-Darcy flow, there effects should be taken into account in the analysis of such data.

2.3 Objective and approach of the study

The objective of this work is to develop a computer model to analyze pressure pulse decay data by taking into account the effects of non-Darcy flow and gas slippage.

To achieve the objective, the following approach is adopted:

- A mathematical model is developed to describe pressure pulse decay, taking into account gas slippage and non-Darcy flow effects with appropriate initial and boundary conditions.

- A numerical simulator is developed to solve the fluid flow equations with gas slippage and non-Darcy flow effects.

- A Computer program is developed that uses non-linear regression technique and numerical solution for the analysis of the data obtained from pressure pulse decay test, taking into account the effects of gas slippage and non-Darcy flow.

- The developed simulator is tested against the case where analytical solution available.

- Experimental conditions are determined where the gas-slippage and non-Darcy flow effects influence the pressure pulse decay data.

- Pressure pulse decay experiments are performed under the conditions where data are influenced by gas slippage and non-Darcy flow effects.

- The test data are analyzed using the developed computer program.

- The results obtained are compared with other approximate solution results available in the literature.

CHAPTER 3

MATHEMATICAL MODEL

3.1 Governing differential equation

The governing differential equation was derived for transient flow of compressible fluid through porous media. The basic assumptions are:

- The flow is single phase and isothermal;
- One dimensional flow; and
- Rock properties like porosity and permeability are constant.

The basic equation is derived by applying the mass balance for the porous media. Forchheimer equation was modified as

$$v = -\delta \frac{k}{\mu} \frac{dP}{dx} \quad \text{.....3.1}$$

where,

$$\delta = \frac{1}{\left(1 + \frac{\beta \rho k v}{\mu}\right)} \quad \text{.....3.2}$$

And the Klinkenberg relation was also used as

$$k_g = k_L(1+b/p) \quad \text{.....3.3}$$

Using the above relations and substituting into the mass balance equation for the system, we get the following partial differential equation for the one-dimensional transient flow of gas through porous media with gas-slippage and non-Darcy flow effects.

$$\frac{\partial}{\partial x}\left[\frac{p}{\mu z}(1+\frac{b}{p})\delta\frac{\partial p}{\partial x}\right]=\frac{\phi}{k_L}\frac{\partial}{\partial t}(\frac{p}{z}) \quad \text{.....3.4}$$

Further simplification using equation of state for gas, we get,

$$\frac{\partial}{\partial x}\left[\frac{p}{\mu z}(1+\frac{b}{p})\delta\frac{\partial p}{\partial x}\right]=\frac{\phi c_g}{k_L}\frac{p}{z}\frac{\partial p}{\partial t} \quad \text{.....3.5}$$

The detail derivation is presented in appendix A. Equation 3.5 is the partial differential equation that describes the transient one dimensional compressible fluid flow in a porous media with gas-slippage and non-Darcy flow effects.

3.2 Initial and boundary conditions

To get numerical or analytical solutions of equation 3.5, we must specify the boundary and initial conditions. These Initial and boundary conditions are given below:

$P_u(0) = P_i$ and $P_d(0) = P_o$ 3.6

$P(x,0) = P_d(0)$ for $0 < x < L$.....3.7

$P(0, t) = P_u(t)$ for $t \geq 0$.....3.8

$P(L,t) = P_d(t)$ for $t \geq 0$.....3.9

where,

P_u and P_d = pressure in the upstream and the downstream vessel.

and V_u and V_d = Volume of the upstream and the downstream vessel.

Also,

$$c_g V_u \frac{\partial p_u}{\partial t} = \frac{1}{\alpha} \frac{k_L A}{\mu} \frac{(b+p)}{p} \delta \frac{\partial p}{\partial x}\Big|_{x=0} \quad \text{for } t > 0 \quad \text{.....3.10}$$

$$c_g V_d \frac{\partial p_d}{\partial t} = \frac{-1}{\alpha} \frac{k_L A}{\mu} \frac{(b+p)}{p} \delta \frac{\partial p}{\partial x}\Big|_{x=L} \quad \text{for } t > 0 \text{ .....3.11}$$

Equation 3.7 states that at the start of the experiment, the pressure in the sample is equal to the downstream reservoir pressure. Equation 3.8 and 3.9 indicate that the upstream and downstream faces of the sample are in direct hydraulic contact with their respective adjacent reservoirs. Equation 3.10 and 3.11 express mass conservation at the sample faces. For example, fluid flow from the sample results in a pressure increase in the downstream resevoir.

3.3 Numerical model

Due to the non-linearity of the resulting partial differential equation and the complexity of boundary conditions, it is difficult to get an analytical solution, especially when gas-slippage and non-Darcy flow effects are also incorporated. Thus a numerical scheme has been developed to solve the partial differential equation.

Finite difference technique was used to solve equation 3.5 with the initial and boundary conditions described in equations 3.6 to 3.11. A detail derivation is shown in appendix B. The finite difference equations are presented below:

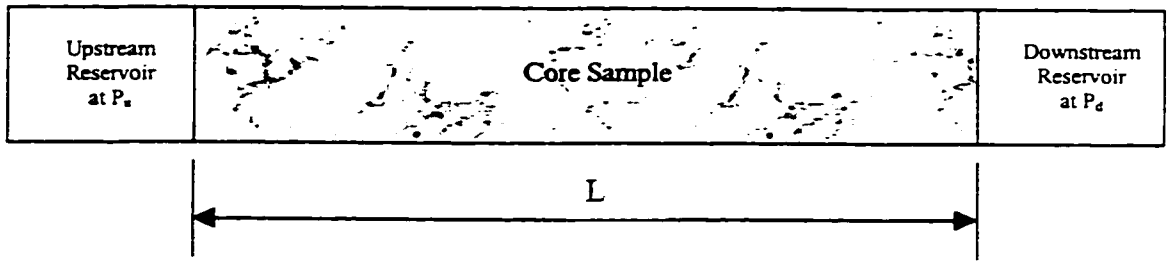

Figure 3.1 Core Sample with Upstream and Downstream Pressures

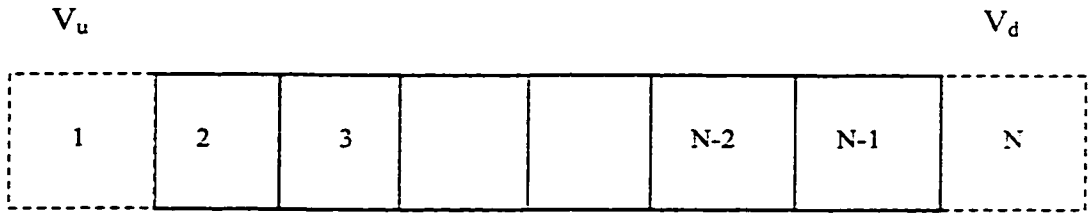

Figure 3.2 Block Centered Grid System for Numerical Scheme

I=1

$$-[(C_1)\delta_{i+\frac{1}{2}}F_{i+\frac{1}{2}}+G]P_i^{n+1}+[(C_1)\delta_{i+\frac{1}{2}}F_{i+\frac{1}{2}}]P_{i+1}^{n+1}=-GP_i^n$$

.....3.12

I=2

$$[2C_3\delta_{i-\frac{1}{2}}F_{i-\frac{1}{2}}]P_{i-1}^{n+1}-[C_3\delta_{i+\frac{1}{2}}F_{i+\frac{1}{2}}+2C_3\delta_{i-\frac{1}{2}}F_{i-\frac{1}{2}}+G]P_i^{n+1}+[C_3\delta_{i+\frac{1}{2}}F_{i+\frac{1}{2}}]P_{i+1}^{n+1}=-GP_i^n$$

.....3.13

I=3 to I=N-2

$$[C_3\delta_{i-\frac{1}{2}}F_{i-\frac{1}{2}}]P_{i-1}^{n+1}-[C_3\delta_{i+\frac{1}{2}}F_{i+\frac{1}{2}}+C_3\delta_{i-\frac{1}{2}}F_{i-\frac{1}{2}}+G]P_i^{n+1}+[C_3\delta_{i+\frac{1}{2}}F_{i+\frac{1}{2}}]P_{i+1}^{n+1}=-GP_i^n$$

.....3.14

I=N-1

$$[C_3\delta_{i-\frac{1}{2}}F_{i-\frac{1}{2}}]P_{i-1}^{n+1}-[2C_3\delta_{i+\frac{1}{2}}F_{i+\frac{1}{2}}+C_3\delta_{i-\frac{1}{2}}F_{i-\frac{1}{2}}+G]P_i^{n+1}+[2C_3\delta_{i+\frac{1}{2}}F_{i+\frac{1}{2}}]P_{i+1}^{n+1}=-GP_i^n$$

.....3.15

I=N

$$[(C_2)\delta_{i-\frac{1}{2}}F_{i-\frac{1}{2}}]P_{i-1}^{n+1}-[(C_2)\delta_{i-\frac{1}{2}}F_{i-\frac{1}{2}}+G]P_i^{n+1}=-GP_i^n$$

.....3.16

In the above equations, we have:

$$F=\frac{p+b}{\mu z}$$ 3.17

$$G = \frac{p}{z} c_g \quad \text{.....3.18}$$

$$C_1 = 2\frac{k_L A \Delta t}{\alpha V_u \Delta x} \quad \text{.....3.19}$$

$$C_2 = 2\frac{k_L A \Delta t}{\alpha V_d \Delta x} \quad \text{.....3.20}$$

$$C_3 = \frac{k_L \Delta t}{\alpha \phi \Delta x^2} \quad \text{.....3.21}$$

$\alpha = 1.47 \times 10^{4}$ (unit conversion factor)

CHAPTER 4

COMPUTER MODEL

4.1 Numerical simulator

A computer model is developed that is based on the finite defference equations of the transient one-dimensional flow equation for a compressible fluid in which gas-slippage and non-Darcy flow effects have also been incorporated. The computer model or numerical similator can simulate the pressure pulse decay experiments and generate the data of pressure pulse decay with respect to time. The complete code listing is presented in the appendix C.

4.2 Data analysis program

Based on the developed numerical simulator, computer programs are developed that analyse the pressure pulse decay experimental data, using the non-linear regression technique. A subroutine DRNLIN from MSIMSL library is used, that fits a non-linear regression model using least squares.

4.3 Determination of the physical properties of Nitrogen

Nitrogen has been used as the flowing compressible fluid for the pressure pulse decay experiments. The gas physical properties that are functions of pressure and temperature are gas viscosity (μ) and gas compressibility factor (z). These properties are determined in the program for each set of pressure and temperature in subroutine FUNC.

4.3.1 Viscosity

The viscosity of gases as a function of pressure can be determined by the available equations in the literature. The viscosity of Nitrogen at temperature close to 25°C and pressure to 253 atmosphere can be calculated from the following equation [3].

$$\mu_{N_2}[T,P] = \mu_{N_2}[T,1] - 0.12474 + 0.123688P + 1.05452\times10^{-3}P^2 - 1.5052\times10^{-6}P^3 \quad .....4.1$$

where $\mu_{N_2}[T,1]$ is the viscosity of Nitrogen at 1 atmosphere pressure and can be obtained from Sutherland's equation [27] (equation 4.2) for which the constants are based on Licht and Stechert [27] work.

$$\mu_{N_2}[T,1] = \frac{13.85T^{1.5}}{T+102} \quad .....4.2$$

The pressure in equation 4.1 is in atmospheres and the temperature in equation 4.2 is in degrees Kelvin. Equation 4.1 was obtained by fitting the data of Gracki et al. [16] to within a maximum dviation of 1% in equation 4.1.

4.3.2 Gas compressibility factor

Gas compressibility factor which is also known as z-factor is equal to 1.0 for an ideal gas. Values of z-factor for Nitrogen as a function of pressure are calculated by fitting a polynomial of degree 3 to the data given in API RP-40 [3] for a temperature of 25°C. This data was actually generated from Beattie-Bridgema equation of state [19].

$$Z = 1.0 - 1.96929\times10^{-3}P + 1.50321\times10^{-6}P^2 - 6.73225\times10^{-11}P^3 \quad \text{.....4.3}$$

4.3.3 Compressibility of the gas

Gas compressibility values have been calculated by equation 4.4

$$c_g = \frac{1}{p} - \frac{1}{z}\frac{\partial z}{\partial p} \quad \text{..... 4.4}$$

where $\frac{dz}{dp}$ is obtained by differentiating equation 4.3.

4.4 Initial estimate of the gas slippage and non-Darcy flow coefficients

The values of Klinkenberg constant (b) and Forchheimer constant (β) have been initially calculated from the available correlations in the literature. These values have been taken as the initial estimate for the regression prgram. The final estimates are obtained from the developed data analysis program after convergence is achieved in the regression program. For the initial estimation of Klinkenberg constant (b), Jones [22] correlation has been used.

$$b\ (psi) = 6.9\ k_L^{-0.36} \qquad \text{.....4.5}$$

The above correlation can be used for permeability ranging from 0.01 md to 1000 md [22]. For the initial estimate of Forchheimer constant (β) two correlations have been used. Equation 4.6 is from Geertsma [15] work for permeability ranging from 0.1 md to 1000 md and porosity ranging from 0.07 to 0.24. For lower values of porosity equation 4.7 has been used which was suggested by Jones [23].

For k = 0.1md to 1000 md and ϕ = 0.07 to 0.24

$$\beta = 4.8512\times10^{4}\ k^{-0.5}\ \phi^{-5.5} \qquad \text{.....4.6}$$

For k = 0.01md to 1000 md

$$\beta = 6.15\times10^{10}\, k^{-1.55} \quad \text{.....4.7}$$

In the above equations, units for permeability (k), porosity (ϕ) and Forchheimer constant (β) are md, fraction and ft^{-1} respectively.

CHAPTER 5

EXPERIMENTAL EQUIPMENT AND PROCEDURE

To perform pressure pulse decay experiments for the determination of permeability, an experimental setup was constructed in the laboratory. Nitrogen was used as the flowing fluid. Core plugs were selected from a low permeability gas reservoir, whose estimated permeabilities were in the range of 0.01md to 25md. The schematic of the experimental setup for the pressure pulse decay testing is shown in figure 5.1.

5.1 Apparatus

5.1.1 Core holder

A Hassler type core holder was used in the experiments to hold the core samples during the test. This stainless steel core holder can accommodate 3 inches long and 2 inches diameter core plugs. The core plugs used in the pressure pulse decay tests were 2 inches long and 1.5 inches in diameter. The core was mounted inside the rubber sleeve and subjected to overburden pressure of about 500 psig. Two end pieces with a hole in their center and had grooves on the core plug side were used. These end pieces had O-rings on their surfaces to completely seal the overburden pressure from the flowing fluid

pressure. The other ends of the end pieces were connected to the respective inlet or outlet piping.

5.1.2 Upstream and downstream vessels

Two vessels were used, one on the upstream side and the other on the downstream side of the core. The volume of each vessel was approximately 250cc. The volume of the vessels can be decreased, by placing any solid material inside it.

5.1.3 Pressure gages

Pressure gages were needed to measure the pressures at various positions, for example overburden pressure, Nitrogen cylinder pressure, and pressure in the upstream vessel. For overburden pressure, a 0-5000psi gage was used and for upstream pressure measurement, 0-5000psi and 0-1250psi gages were used. For accurate measurement pressure gages with digital displays were used.

5.1.4 Piping

Stainless steel tubing was used to connect the Nitrogen cylinder, pump, upstream and downstream vessels, and the core holder. The tubing size was 1/8 inch and could stand a pressure of 2500 psig.

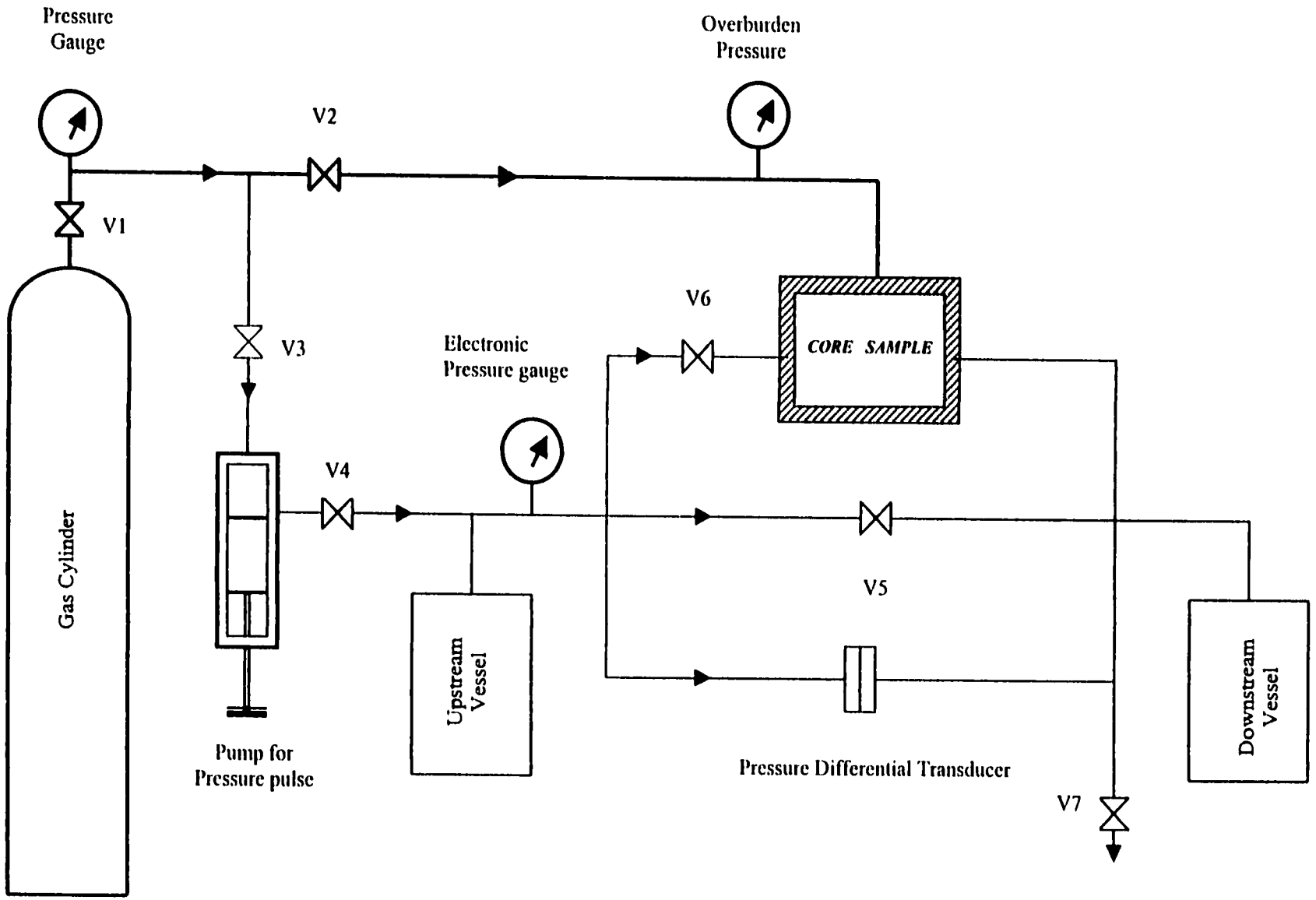

Figure 5.1 Experimental Set-Up for Pressure Pulse Decay Test

5.1.5 Valves and fittings

The valves and fittings available for the stainless steel piping were used and were of the same rating as the tubing was. About seven valves were needed, as shown in the figure 5.1.

5.1.6 Pump for pressure pulse

A mercury injection hand pump was used to create a small and controlled pressure pulse for the experiment. It was possible to create a pressure pulse of 1 psi up to 100 psi using this type of pump.

5.1.7 Nitrogen gas cylinder

A Nitrogen gas cylinder was required to have enough supply of gas during the experimental runs. The cylinder contained Nitrogen gas at about 2000 psig. A pressure regulator was used to regulate the pressure from the cylinder according to the requirements of the pressure pulse decay experiments.

5.1.8 Pressure differential transducers

Pressure differential transducers were used to measure the pressure difference across the core plug during the test. These transducers were calibrated with their respective digital indicators. The transducers used were of 32psi, 125psi and 1250psi

pressure-differential, as per the requirements of the experiments. The pressure drop data were transferred from the digital indicator to the computer.

5.1.9 Data acquisition system and personal computer

A personal computer was used to run the data acquisition software, which convert the voltage into pressure difference reading. The software records the pressure pulse decay with respect to time and displays it graphically on the computer screen. It also creates a data file on the hard disk of the computer for future record and analysis. From the data acquisition system we can control the time interval size for which we want to record the pressure value. The time interval size ranges from 0.1 second to 60 seconds and the maximum number of data points record are limited to 550. One has to select the proper combination of these parameters to get the complete pressure pulse decay data.

5.2 Consideration of the temperature effects

As gas expands, its temperature decreases, according to Charles' law. This temperature variation is not desirable as it violates our assumption of isothermal gas flow in the derivation of the governing flow equations. Moreover, it is not possible to correctly estimate the temperature variation during the test. To avoid these problems, glass wool insulation was used for piping, upstream and downstream vessels, and other fittings.

Copper tube bundles were placed in the vessels to minimize the cooling effect of gas due to expansion of gas in the upstream and downstream vessels. These copper tubes provided a larger surface area for the gas to contact, for transfer of heat from the metal in case of gas cooling. The high heat capacity of the copper reduces the temperature variation in the system, thus providing a reasonably constant temperature of the flowing gas.

5.3 Experimental conditions determination

Two types of experimental conditions were determined to perform the pressure pulse decay tests. These pressure conditions were based on the effects of gas-slippage and non-Darcy flow. One set of tests was performed with small initial pressure pulse and low mean pore pressure values (~100psi). The other set of experiments was at higher mean pore pressure and pressure difference (~1000psi). The detail discussion of these conditions is given in section 6.1.

5.4 Calibration and testing of the setup

Before performing the pressure pulse decay tests, the experimental setup (figure 5.1) was tested for any leak at a pressure of 1500 psig. Bubble test was used to detect any leakage instantly and the setup was left for one day under this pressure to ensure that the system is leak proof. Overburden pressure of 2000 psig was also imposed after insertion of a steel solid cylinder inside the sleeve of the core holder. After completing the pressure

testing, the system was calibrated for measuring the volumes of the piping and upstream and downstream vessels. The upstream and downstream volumes were determined by measuring the pressure drop after expanding the gas from one volume to the other volume (applying Boyle's law). The volume of tubing from the valve 6 (figure 5.1) to the core end face was also determined using the above procedure. This volume was required to determine the correct value of initial upstream pressure.

5.5 Experimental procedure

The procedure to perform the pressure pulse decay experiments is as follows:

- Insert the core sample inside the sleeve and then place it into the core holder.
- After tightening the core holder, apply a net overburden pressure of 500 psig.
- Close valve-7 and pressurize the system to some initial system pressure. Let the pressure be stabilized for few minutes. Valve-5 and valve-6 should be open during this time. Note that this pressure is the initial downstream pressure. Initial downstream pressure can also be the atmospheric pressure (14.7 psia).
- Provide the required parameters in the data acquisition program window, according to the transducers used. Also provide the required number of data points and time interval for recording the pressure readings.
- Close valves 5 and 6 and increase the upstream pressure to have some pressure difference between the upstream and downstream reservoirs. (e.g. 20 psi). Give few minutes for the stabilization of the pressure.

- Click on the start button on the data acquisition program window, and then open valve 6 to allow the gas to flow through the core. The pressure difference across the core with respect to time is recorded and shown graphically by the data acquisition program on the computer screen. This pressure pulse decay data along with other parameters are used as the input for the data analysis program that determines the permeability, Klinkenberg constant and Forchheimer constant simultaneously.

CHAPTER 6

RESULTS AND DISCUSSION

6.1 Comparison of numerical and analytical solutions

The parameters such as core length, core diameter, temperature, and upstream and downstream vessel volumes used to generate the simulation results are presented in Table 6.1. The estimated values of Klinkenberg constant (b) and Forchheimer constant (β) calculated from Equations 4.5, 4.6 and 4.7 are used in the simulation runs.

The developed numerical simulator is compared with an available analytical solution [20]. The analytical solution available in the literature did not consider the effects of gas-slippage and non-Darcy flow. Therefore, the simulator was also run for the same condition where gas slippage and non-Darcy flow effects are negligible and the results are shown in figure 6.1. The figure is showing an excellent match of the numerical results with the analytical solution.

Table 6.1 Parameters used in the simulator input data

S.No.	Parameter	Value
1	Temperature (T)	25 °C
2	Upstream reservoir volume (Vu)	251 cc
3	Downstream reservoir volume (Vd)	259 cc
4	Length of the core sample (L)	5.01 cm
5	Diameter of the core sample (D)	3.81 cm
6	Number of grids cells of core (Nx)	20
7	Molecular weight of Nitrogen (MW)	28
8	Universal gas constant (R)	1206.24 psi.cc./gmole/K

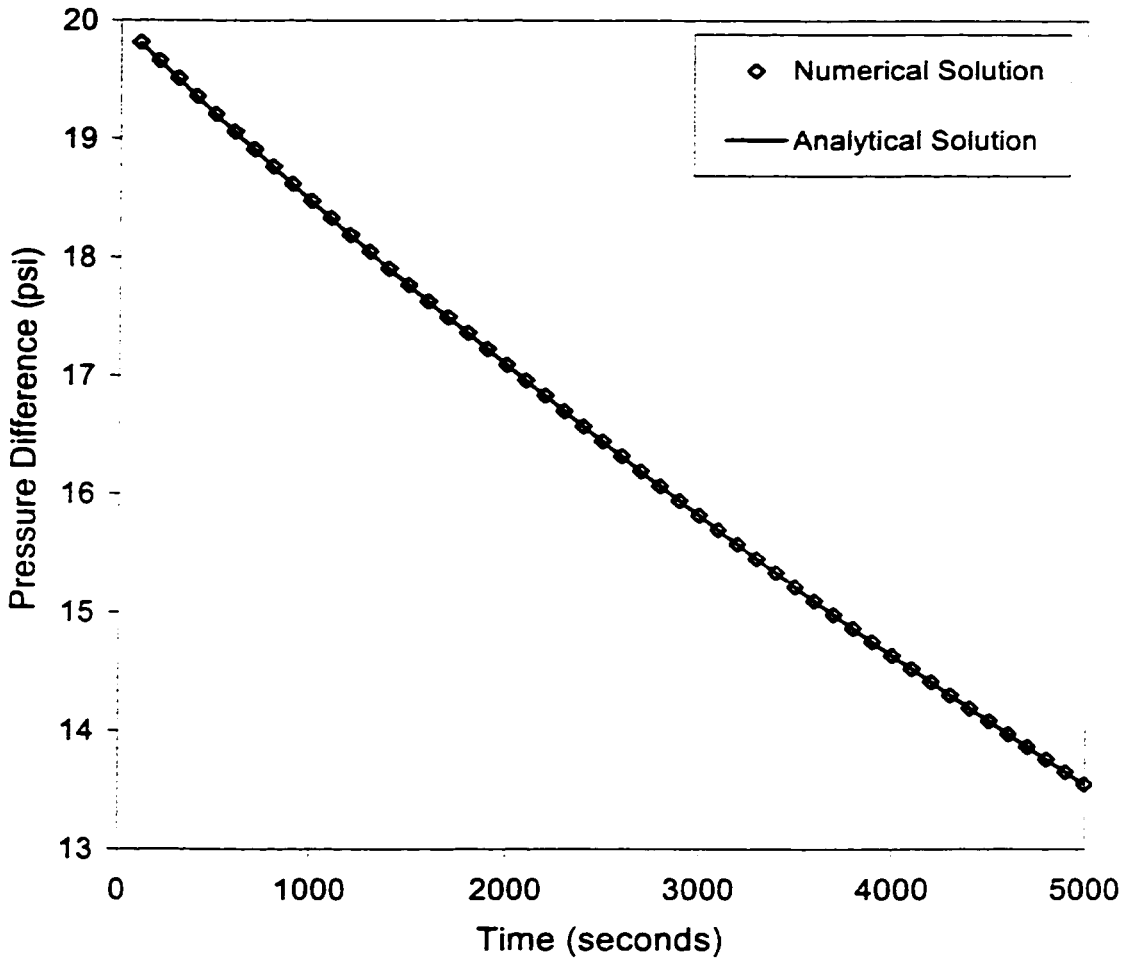

Figure 6.1 Comparison of numerical solution with the analytical solution without considering the effects of gas-slippage and non-Darcy flow (k=0.01md)

6.2 Effect of gas slippage and non-Darcy flow on pressure pulse decay curve

Using the developed simulator, pressure pulse decay (PPD) data were generated in which gas-slippage and non-Darcy flow effects were incorporated. The pressure pulse decay curves are plotted as pressure difference (between the upstream and down stream reservoirs) vs time for four conditions.

Case 1	Without considering the effect of gas slippage and non-Darcy flow.
Case 2	Considering the effect of gas slippage only.
Case 3	Considering the effect of non-Darcy flow only.
Case 4	Considering the effect of both gas slippage and non-Darcy flow.

Figures 6.2, 6.3 and 6.4 show that gas slippage and non-Darcy flow effects are acting opposite to each other in the case of gas flow through porous media.

Due to the slippage effect, the pressure decays faster as compared to no-slippage case and will give higher permeability values than the actual if we analyze the PPD data without taking into account gas-slippage. While due to the non-Darcy flow (NDF) effect the pressure decays slower as compare to no NDF effect and will give lower permeability value than the actual if we analyze the PPD data without taking into account NDF effects.

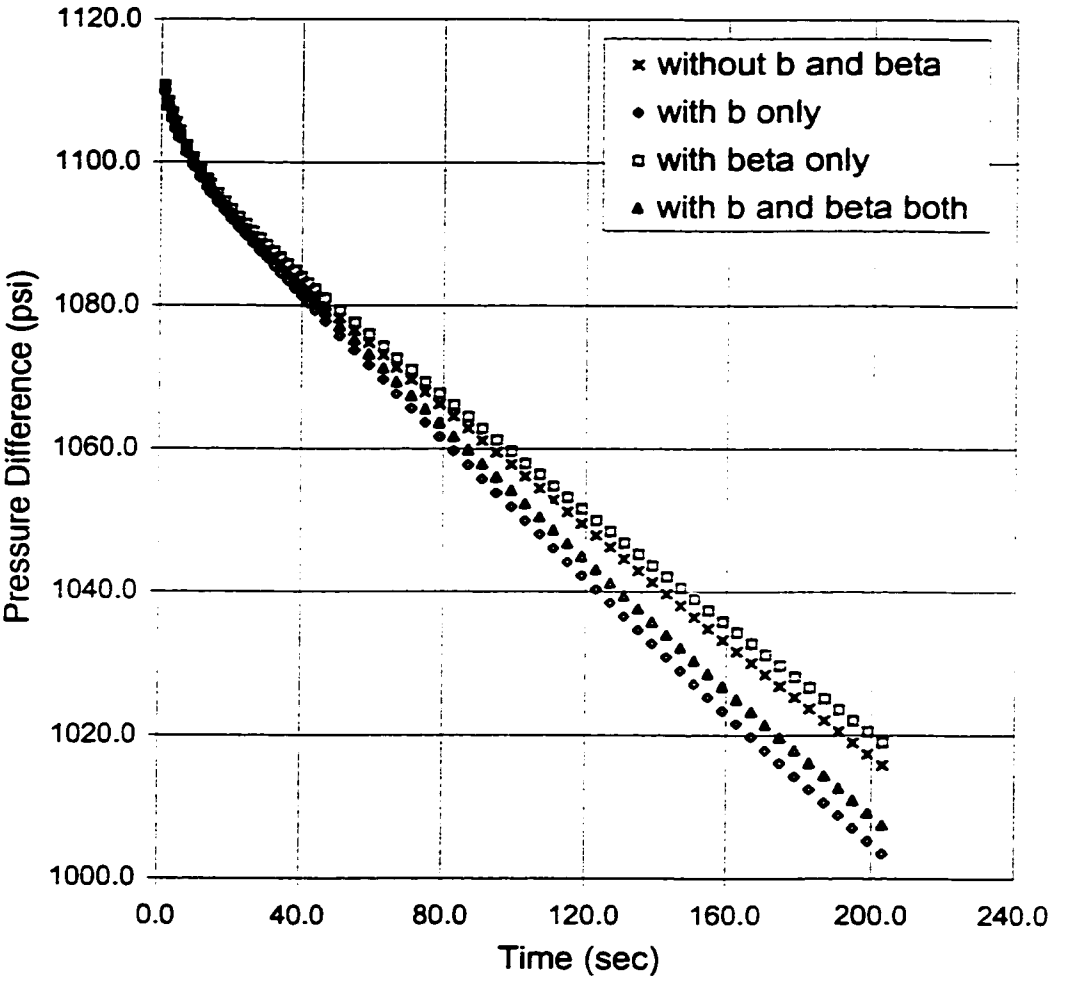

Figure 6.2 Effect of gas-slippage and non-Darcy flow on PPD curves (k=.01md and ΔPi=1100psi) (b = 36.21 psi, β = 7.7E13 ft^{-1})

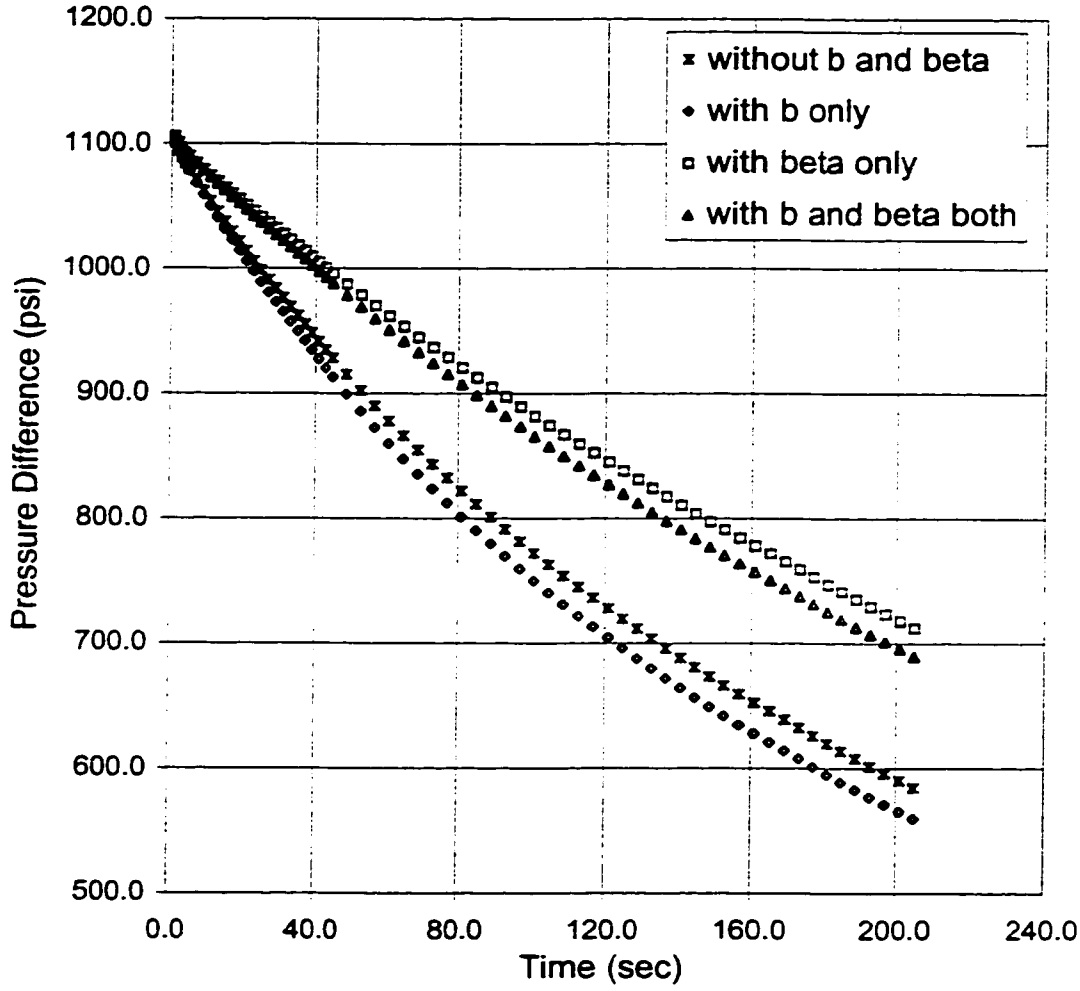

Figure 6.3 Effect of gas-slippage and non-Darcy flow on PPD curves (k=.1md and ΔPi=1100psi) (b = 15.81 psi, β = 2.2E12 ft^{-1})

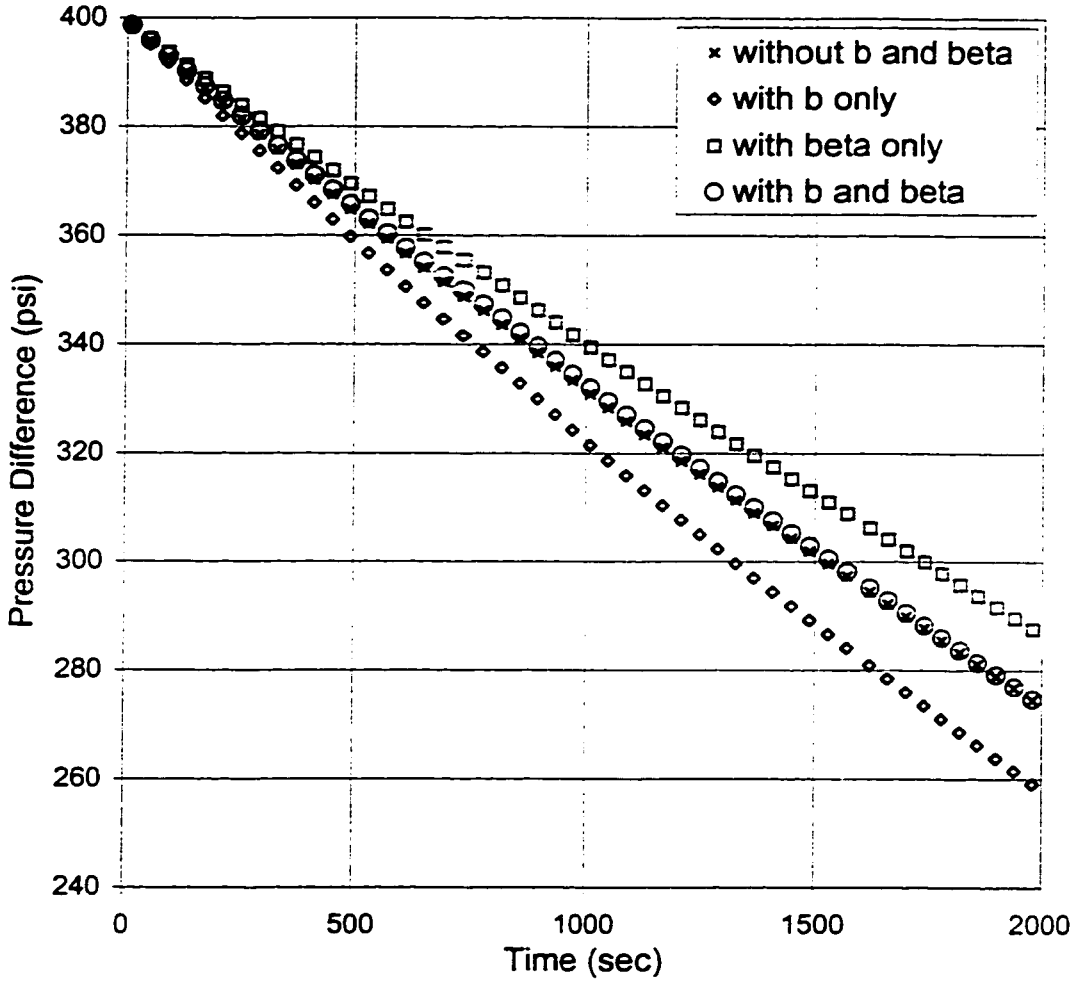

Figure 6.4 Effect of gas-slippage and non-Darcy flow on PPD curves (k=0.1md and ΔPi=400psi) (b=15.81 psi and $\beta = 2.2E12\ ft^{-1}$)

From figures 6.2 and 6.3 it can be concluded that in the real case (i.e. when considering both gas slippage and non-Darcy flow) the pressure pulse decays faster if gas slippage dominates over the NDF effect and vice versa for the case if NDF effect dominates the gas slippage effect.

Figure 6.4 is presenting the conditions where we can have both gas-slippage and non-Darcy flow effects considerably affecting the PPD data. But as both of these effects dragging the PPD data in opposite directions, the net effect can be seen as a very low or no effect of gas slippage or NDF. This type of condition can lead us to the values of k, b and β that are very much different from the actual values.

Hence, it is not reliable to find the values of k, b and β simultaneously from a single PPD test because of the nature of the influence of gas-slippage and non-Darcy flow on the pressure pulse decay data of porous media.

Based on the above discussion it was decided to find the conditions, where, the PPD data is influenced by gas-slippage and NDF separately.

6.2.1 Experimental conditions for the determination of k and b simultaneously

Using the developed simulator, a number of simulation runs have been made for permeability values ranging from 0.01 md to 1.0 md. For low mean pore pressure and low initial pressure difference (20 to 100 psi) the results are plotted in figures 6.5 to 6.8.

The plots clearly show a significant effect of gas slippage and negligible effect of non-Darcy flow on pressure pulse decay curve for lower values of mean pore pressure.

As the rock permeability increases, a decrease in the gas slippage effect can be seen. Also there is more gas slippage effect with decreasing the mean pore pressure from 100 to 20 psi for a fixed value of permeability.

Hence, it is clear that for lower mean pore pressure the effect of gas slippage cannot be ignored, even for 100 psi of mean pore pressure or pressure difference. To minimize this effect we need to have higher mean pore pressure ($\approx$1000 psi). But there are other problems that are associated with higher pressure and will be discussed in the next pages.

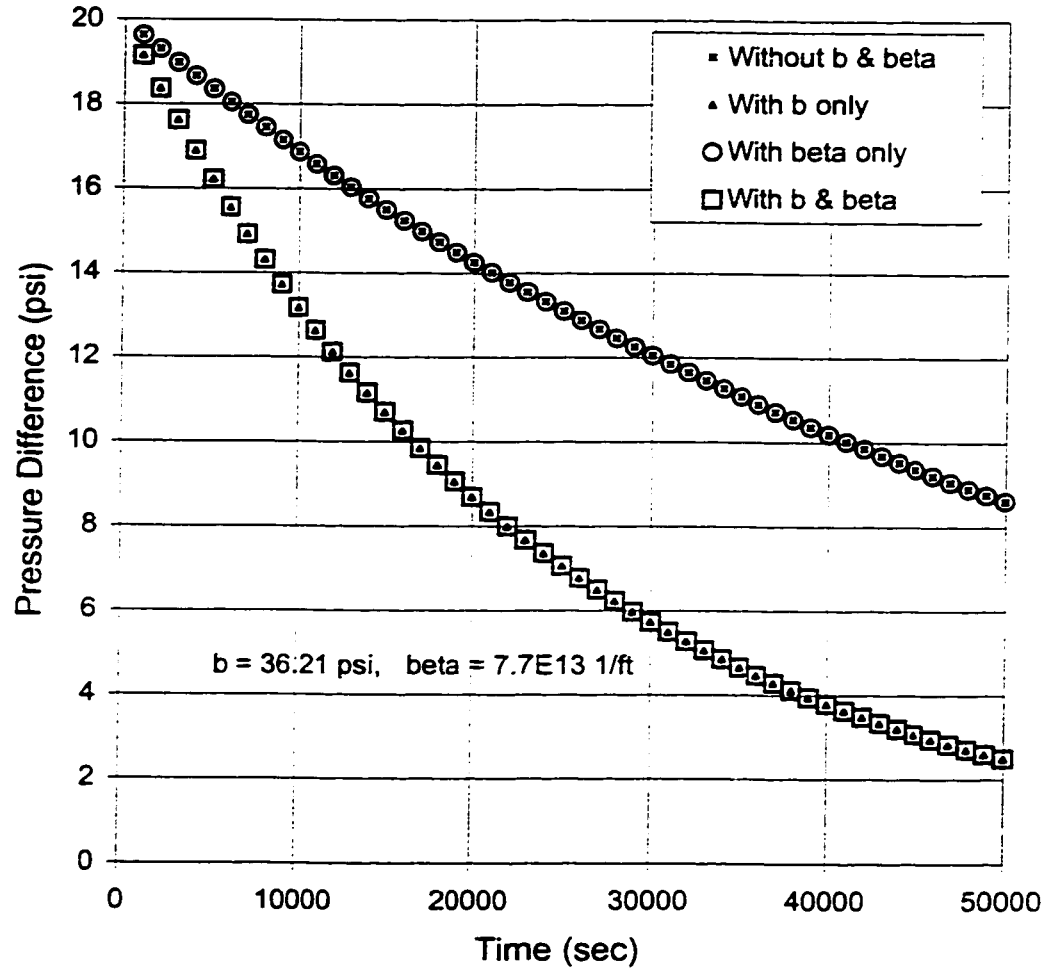

Figure 6.5 Effect of gas slippage on PPD curves with low mean pore pressure (k = .01 md & ΔP_i=20 psi)

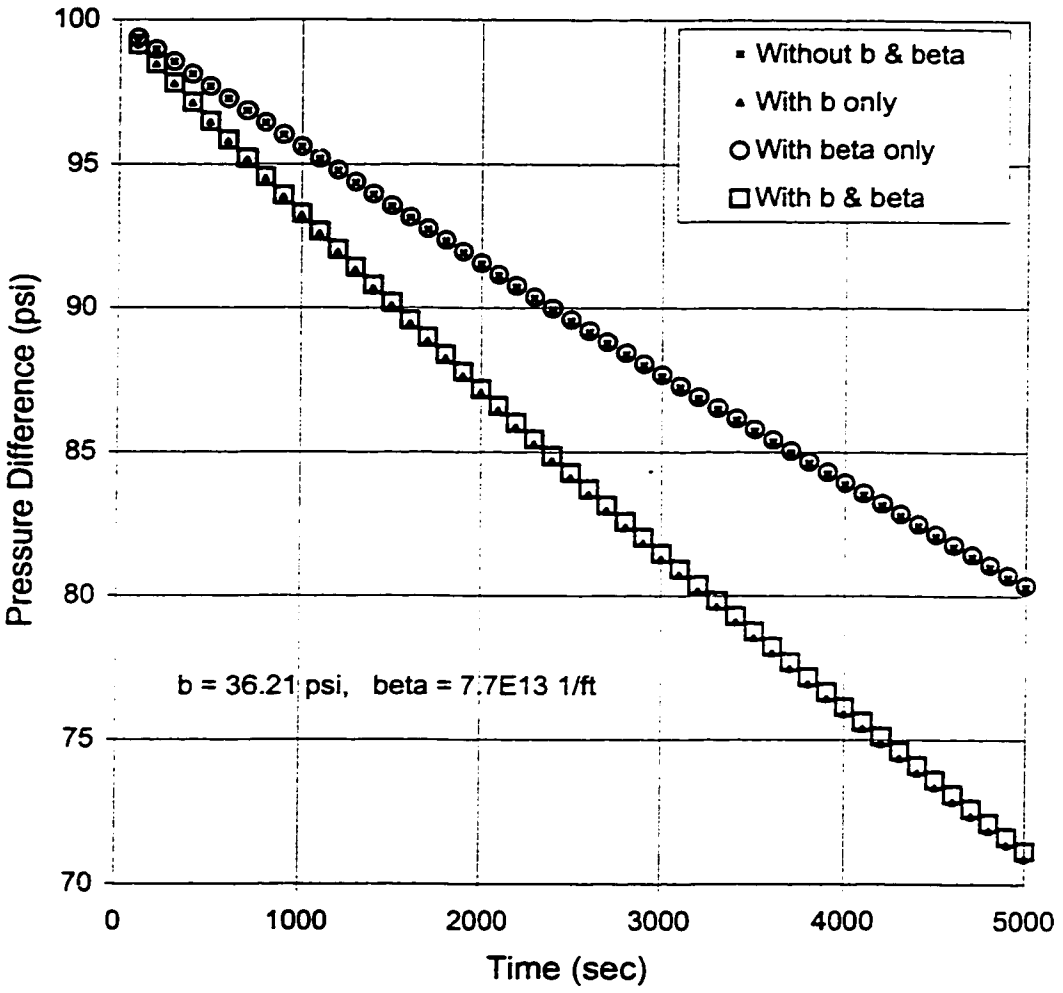

Figure 6.6 Effect of gas slippage on PPD curves with low mean pore pressure (k = .01 md & ΔPi=100 psi)

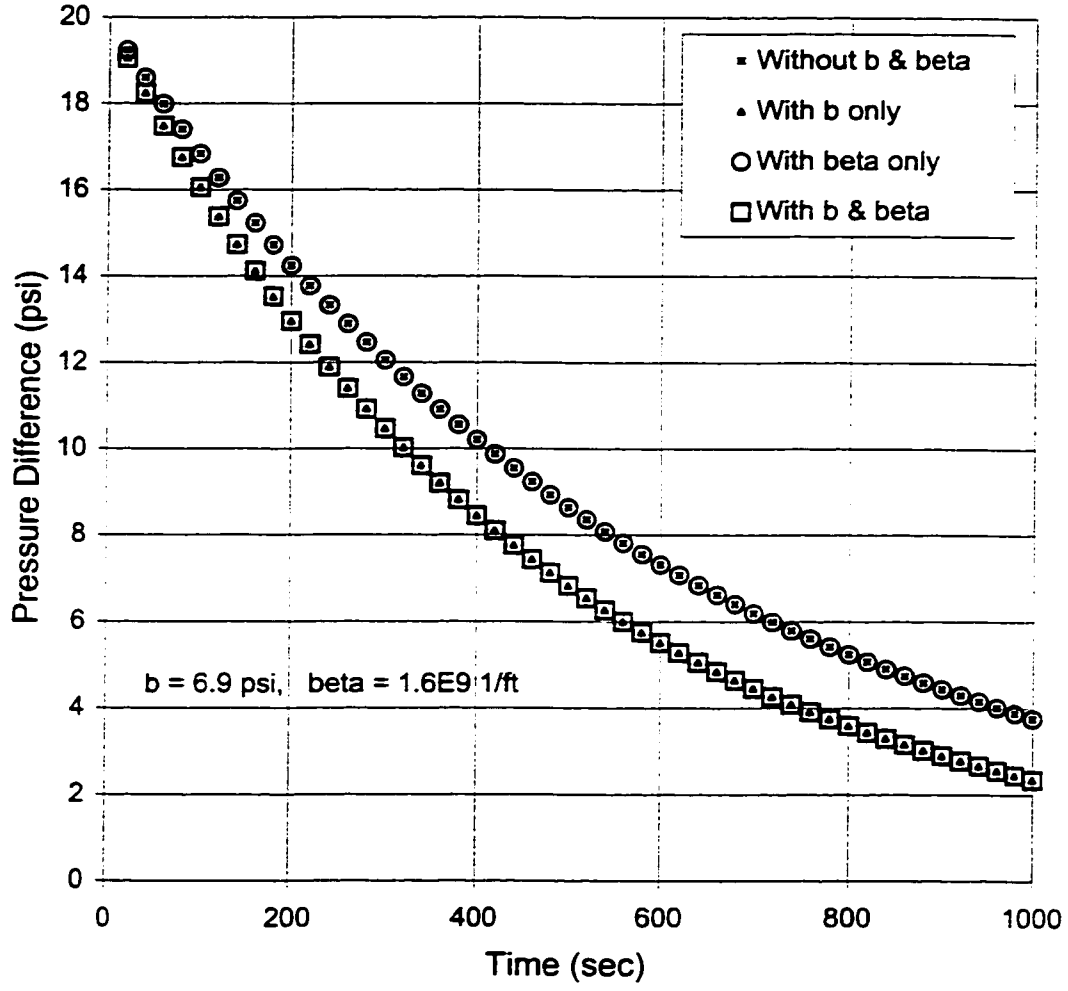

Figure 6.7 Effect of gas slippage on PPD curves with low mean pore pressure (k = 1.0 md & ΔP_i=20 psi)

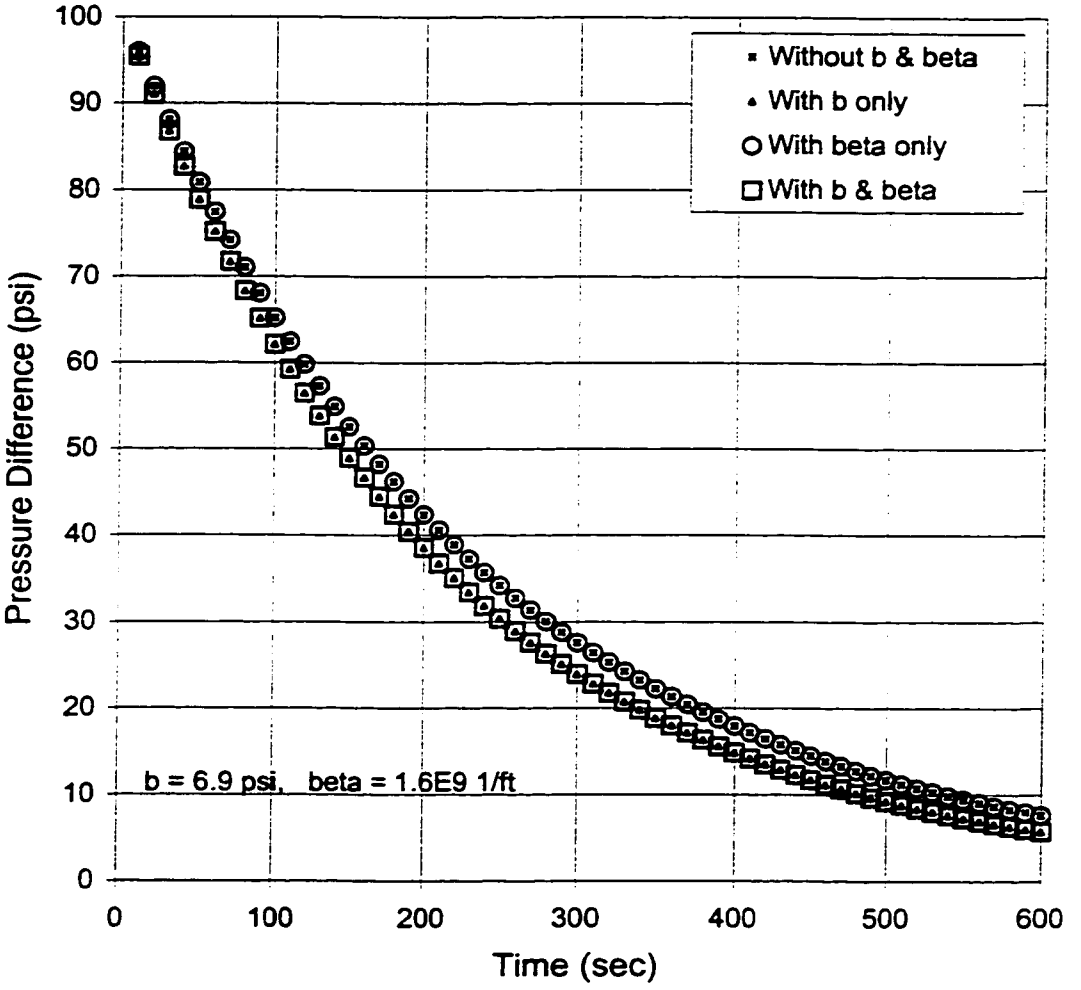

Figure 6.8 Effect of gas slippage on PPD curves with low mean pore pressure (k = 1.0 md & ΔPi=100 psi)

6.2.2 Experimental conditions for the determination of k and β simultaneously

Regarding the effect of non-Darcy flow, figures 6.5 to 6.8 show negligible effect on the pressure pulse decay curve and hence can be ignored without introducing any error in case of lower mean pore pressure and lower pressure difference (20 to 100psi). To see the effect of non-Darcy flow, simulation runs were made for higher mean pore pressure and higher initial pressure difference (500 to 1000 psi). The results are presented in figures 6.2, 6.3, 6.9 and 6.10.

Figure 6.2 shows that at higher pressure-difference (≈1000 psi), the NDF effect can be seen for k=0.01 md and ϕ=0.05, but still the slippage effect dominates the PPD curve. Also figure 6.9 shows negligible effect of NDF for higher mean pore pressure (≈1250 psi) and high pressure-difference (≈ 500 psi) for k=0.01 md and ϕ=0.1, but there is still some gas-slippage effect present. For high permeability values (>1.0md) the NDF effect is significant and gas-slippage effect is negligible (figure 6.10).

As the permeability of the core increases, the NDF effect also increases for the same conditions of mean pore pressure and pressure difference (figures 6.2 and 6.3).

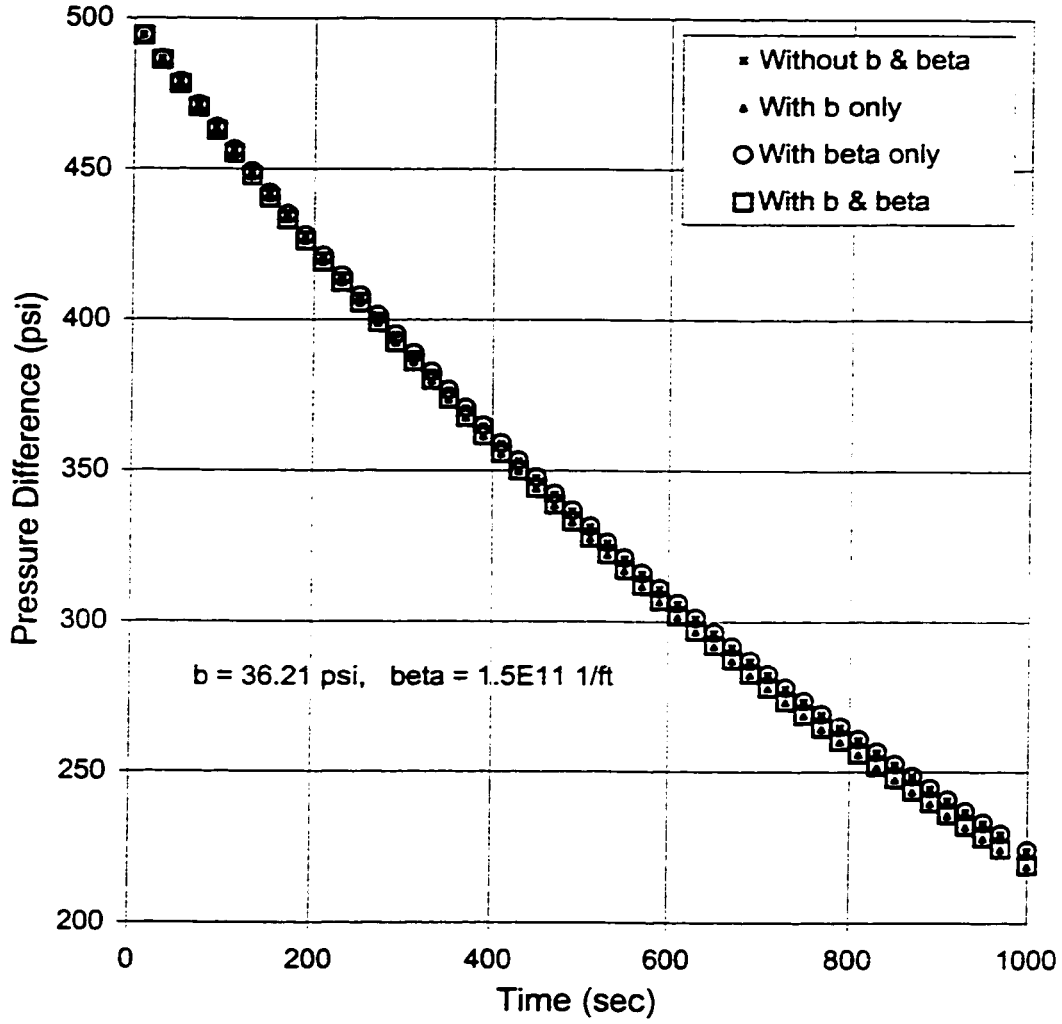

Figure 6.9 Effect of non-Darcy flow on PPD curves with high mean pore pressure and high pressure difference (k=.01md & ΔPi=500 psi)

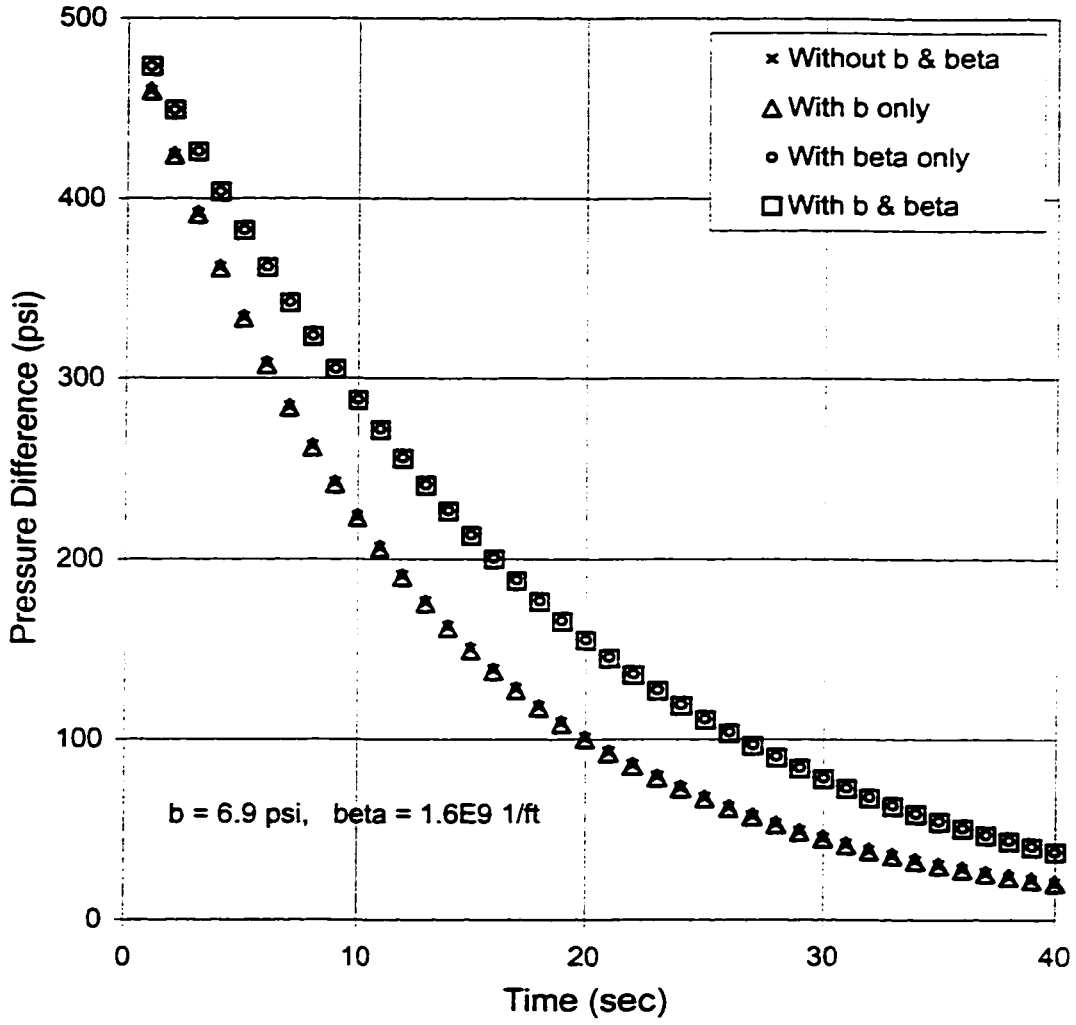

Figure 6.10 Effect of non-Darcy flow on PPD curves with high mean pore pressure and high pressure difference (k=1.0md & ΔPi=500 psi)

6.2.3 Effect of neglecting gas-slippage and non-Darcy flow

The synthetic data were obtained using the developed simulator considering both gas slippage and non-Darcy flow effects. The synthetic data were then analyzed using the data analysis software that does not include b and β effect to evaluate permeability.

Figure 6.11 shows the data, which was generated for the condition where it was influenced by significant gas-slippage effect. This data was then analyzed by using the data analysis program in which the gas-slippage effect was neglected. The result shows a 147% higher estimate of the permeability as compare to the original value (0.01 md) from which the data was generated. Hence, in pressure pulse decay experiments, ignoring the effect of gas-slippage may lead us to an error in the estimation of permeability as high as +150% of the original value.

Similarly, figure 6.12 shows the effect of neglecting non-Darcy flow effect. The synthetic data was generated for condition where it was influenced significantly by non-Darcy flow effect. This data was then analyzed by using the data analysis program in which the non-Darcy flow effect was neglected.

The result shows that decrease in the permeability estimate of about -25% of the original value (1.0 md) can be obtained if we neglect the effect of non-Darcy flow in the analysis of pressure pulse decay data.

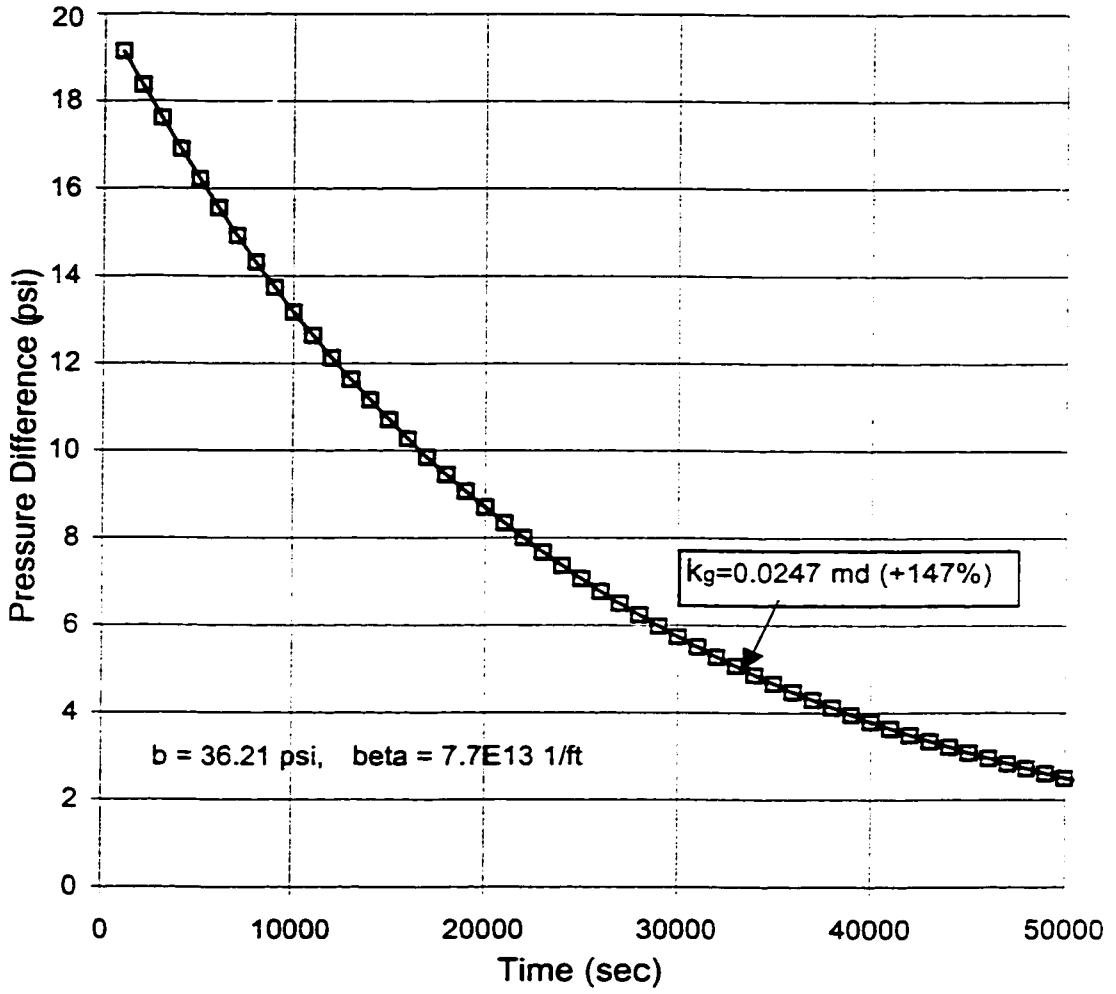

Figure 6.11 Effect of neglecting gas-slippage on the estimation of permeability from PPD test

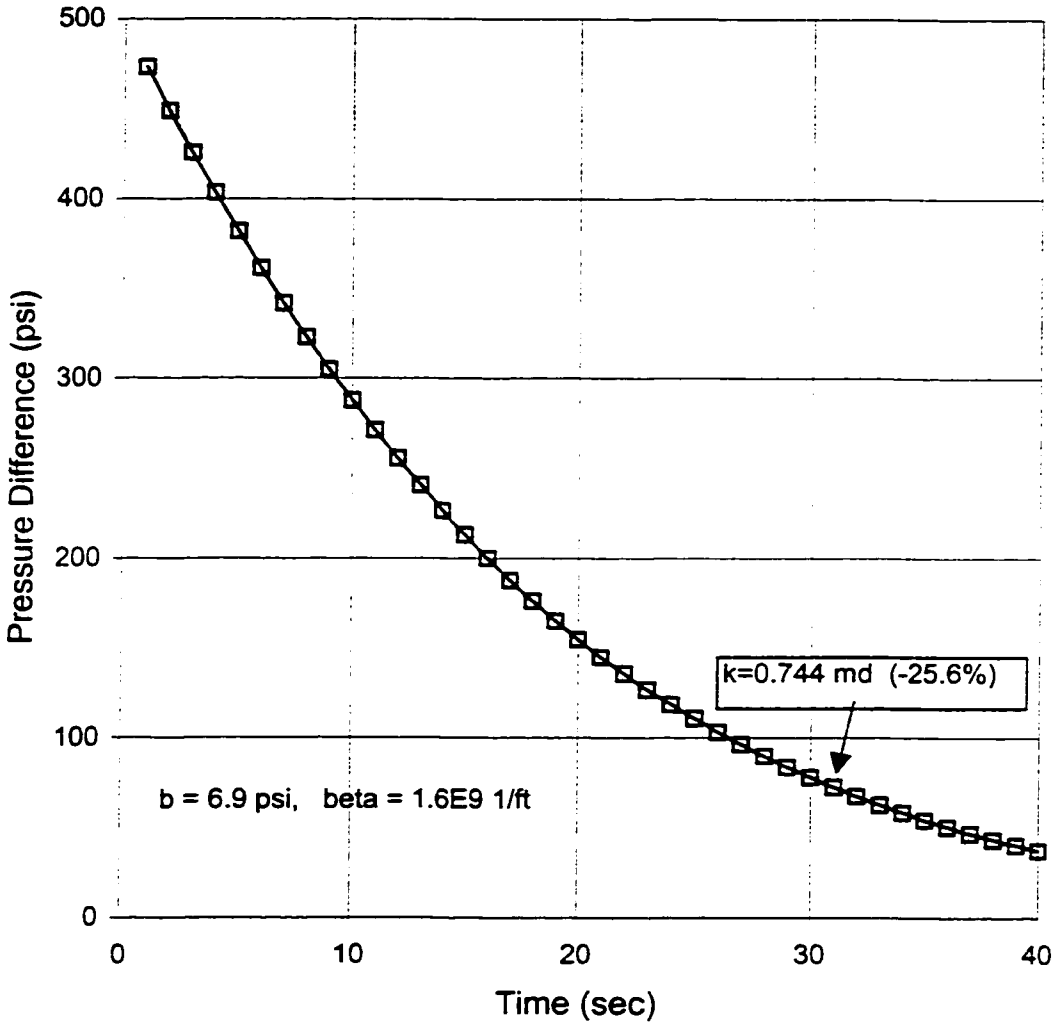

Figure 6.12 Effect of neglecting non-Darcy flow on the estimation of permeability from PPD test

6.3 Analysis of the simulation data using the developed computer programs

6.3.1 Estimation of k and b using the developed computer program from single test data

Synthetic data were generated for the conditions where the data were influenced by the gas-slippage effects and analyzed by the developed computer program. The results are presented in table 6.2. Synthetic data were generated for permeability of 10 md and Klinkenberg constant of 3.01 psi, for three different values of low initial upstream pressure (< 80 psi) with downstream side open to atmosphere. Analyzing this synthetic data using the developed data analysis program gives results with good accuracy (error<0.1%). Hence, our developed data analysis program is analyzing the PPD data with excellent accuracy for the case where gas slippage effects are significant and NDF effects are negligible.

6.3.2 Estimation of k and β using the developed computer program for single test data

Synthetic data were generated for the conditions where the data were influenced by the non-Darcy flow effects and analyzed by the developed computer program. The results are presented in table 6.3. The PPD synthetic data were generated for k = 10 md and $\beta = 1.1\times10^{8}$ ft^{-1} at three different higher initial pressure difference (500 to 1500 psi) with downstream side open to atmosphere.

Table 6.2 Results from the data analysis computer program, with input PPD data from the simulator (k=10 md and b=3.01psi)

Case	Pui (psia)	ΔPi (psi)	Program output		Error in %	
			k (md)	b (psi)	k	b
A	34.7	20	9.991	3.011	-0.1	0.0
B	54.7	40	9.999	3.013	0.0	0.1
C	74.7	60	9.999	3.014	0.0	0.1

Table 6.3 Results from the data analysis program with input synthetic PPD data influenced by NDF effect (k=10md, beta=1.1E8 1/ft)

Pui (psia)	ΔPi (psi)	Program output		Error (%)	
		k (md)	beta (1/ft)	k	beta
514.7	500	10.000	1.09E+08	0.00	-0.91
1014.7	1000	10.000	1.09E+08	0.00	-0.91
1514.7	1500	10.000	1.09E+08	0.00	-0.91

The results obtained by analyzing this PPD data using our developed data analysis program is showing good accuracy with errors of less than 0.91% in β values and nearly 0% error in the permeability values.

6.4 Effects of error in various parameters on the final estimate

The factors that affect the parameter estimation can be classified in many categories. For example, model error, test procedure, and measurement error. Here we will discuss only the measurement error.

For the case of measurement error, the effect of initial pressures (upstream and downstream) and porosity value on the final estimate of the unknown parameters (k, b and β) were studied. For this purpose, synthetic data was generated using the developed simulator and then the developed synthetic data was analyzed by changing the upstream pressure by ÷ 0.2%, which is the maximum error that our pressure differential transducer can give on its full scale. -2% error in the porosity values was used to study the effect of error in the porosity value.

6.4.1 Effect of error in initial upstream pressure measurement

Synthetic data was generated for permeability values of 0.01 and 1.0 md at a condition of low initial upstream pressure (ΔP=100 psi). After changing the initial upstream pressure value by +0.2%, the synthetic data was then analyzed by the developed data analysis program. The results are tabulated in table 6.4.

It is clear from table 6.4, that the final estimates of the unknown parameters (in this case k and b) are sensitive to the error in the initial upstream pressure values.

For two cases of permeability values (0.01 md and 1.0 md) with high gas slippage effect, the final estimate of the Klinkenberg constant is more sensitive to the error in initial pressure than the permeability. Moreover, low permeability ($\approx$0.01md) porous media are more sensitive to the error in upstream pressure value than the relatively higher permeability rocks (1 md).

Since, both permeability and Klinkenberg constant values are related to each other (i.e. when one increases, the other decreases), it is difficult to quantify the effect of initial upstream pressure, individually, on each parameter. But, it is clear from the study (table 6.4) that the output values of the parameters form the data analysis program are very sensitive to the error in the initial upstream pressure. Hence, to avoid the error in the final estimate of the parameters, it is necessary to measure the initial upstream pressure with a minimum error.

Table 6.4 Effect of error in upstream pressure value on the final estimate of the parameters

Synthetic Data			Data Analysis			Percentage Deviation			Confidence Interval	
Pui (psia)	k (md)	b (psi)	Pui (psia)	k (md)	b (psi)	ΔPui (%)	Δk (%)	Δb (%)	CI (k) (%)	CI (b) (%)
114.70	0.01	36.21	114.93	0.012	25.35	0.2	21.0	-30.0	1.0E+01	2.5E+02
114.70	1.00	6.90	114.93	1.043	5.87	0.2	4.3	-14.9	1.1E+00	8.7E+00

6.4.2 Effect of error in porosity value

Simulation data was generated for permeability values of 0.01, and 1.0 md and then analyzed after changing the porosity values by –2%. The results are presented in table 6.5, which shows that the error of –2% in the porosity value, is affecting the final estimate of the parameters.

The effect of error on the permeability estimate is lower (-5% to -14%) than its effect on the Klinkenberg constant estimate (40% to 61%). For the same value of permeability, the higher the value of original porosity, the higher will be the sensitivity of the final estimate of the permeability and gas-slippage constant with respect to the error in the porosity value. Hence, it is better to find the correct value of porosity for a core sample. For this purpose we should consider the effect of overburden pressure on the porosity values and the porosity should be measured at the same overburden pressure at which the pressure pulse decay experiments will be performed.

Table 6.5 Effect of error in porosity value on the final estimate of the parameters

Synthetic Data			Data Analysis			Percentage Deviation			Confidence Interval	
Por (frac)	k (md)	b (psi)	Por (frac)	k (md)	b (psi)	Δ(Por) (%)	Δk (%)	Δb (%)	CI (k) (%)	CI (b) (%)
0.050	0.01	36.21	0.049	0.009	50.70	-2.0	-13.0	40.0	0.83	1.90
0.075	0.01	36.21	0.074	0.009	52.70	-2.0	-14.3	45.5	1.36	3.05
0.150	1.00	6.90	0.147	0.943	10.99	-2.0	-5.7	59.3	0.96	6.40
0.175	1.00	6.90	0.172	0.941	11.16	-2.0	-5.9	61.7	1.10	7.60

6.5 Analysis of the pressure pulse decay experimental data

Some core plugs were selected to perform pressure pulse decay tests. The tests were run on the setup discussed before (chapter 5) for the conditions where the PPD data was expected to be influenced by the gas-slippage and non-Darcy flow effects. The PPD data was then analyzed using the developed computer programs using two approaches, and also by using the Jones approximate solution method to compare the results. Five samples were tested, and the results for two with minimum and maximum estimated permeability values are presented here. Table 6.6 shows the properties of the core samples.

As discussed before in section 6.2, due to the nature of the gas-slippage and non-Darcy flow effects on the pressure pulse decay data, two sets of experiments had to be conducted. First for the condition where the data is highly influenced by the gas-slippage and the non-Darcy flow effect is negligible. Secondly for the condition where the non-Darcy flow effects are dominant and gas-slippage is negligible.

Table 6.6 Properties of the core samples

Core #	Length (cm)	Dia (cm)	Porosity (fraction)
H4-275-3	5.070	3.810	0.1359
H4-113-3	5.008	3.810	0.0634

6.5.1 Determination of permeability and Klinkenberg constant simultaneously

Experiments were conducted for the conditions where the data is significantly influenced by slippage effect and then analyzed by three methods. Two types of approaches were used to find the permeability and Klinkenberg constant of the rock samples using the developed computer program, while Jones method was used as the third approach for comparison.

6.5.1.1 Determination of k and b from single test data using the developed computer program

Pressure pulse decay tests were conducted for each core sample for pressure difference of about 100 psi and the obtained PPD data were then analyzed by the developed computer program. The downstream side of the core was open to atmosphere, which gives the condition of constant downstream reservoir pressure of 14.7 psia. Since at these experimental conditions the non-Darcy flow effect was negligible, only permeability and Klinkenberg constant were used in the regression and β was taken as a constant (calculated from the Geertsma's correlation). Figures 6.13 and 6.14 show a pressure difference vs time curve fitting for the pulse decay data for the selected core samples.

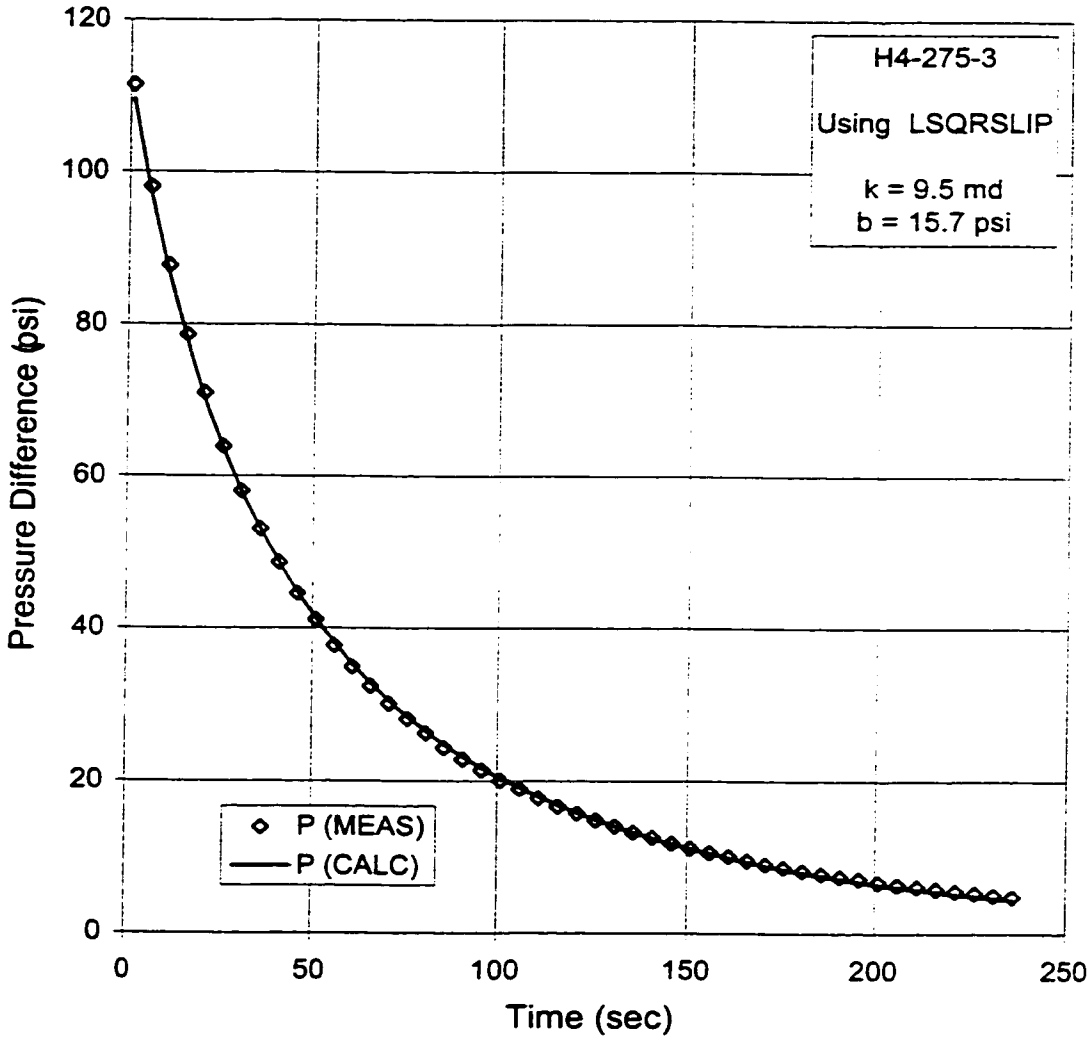

Figure 6.13 Experimental data analysis using the developed computer program for core # H4-275-3.

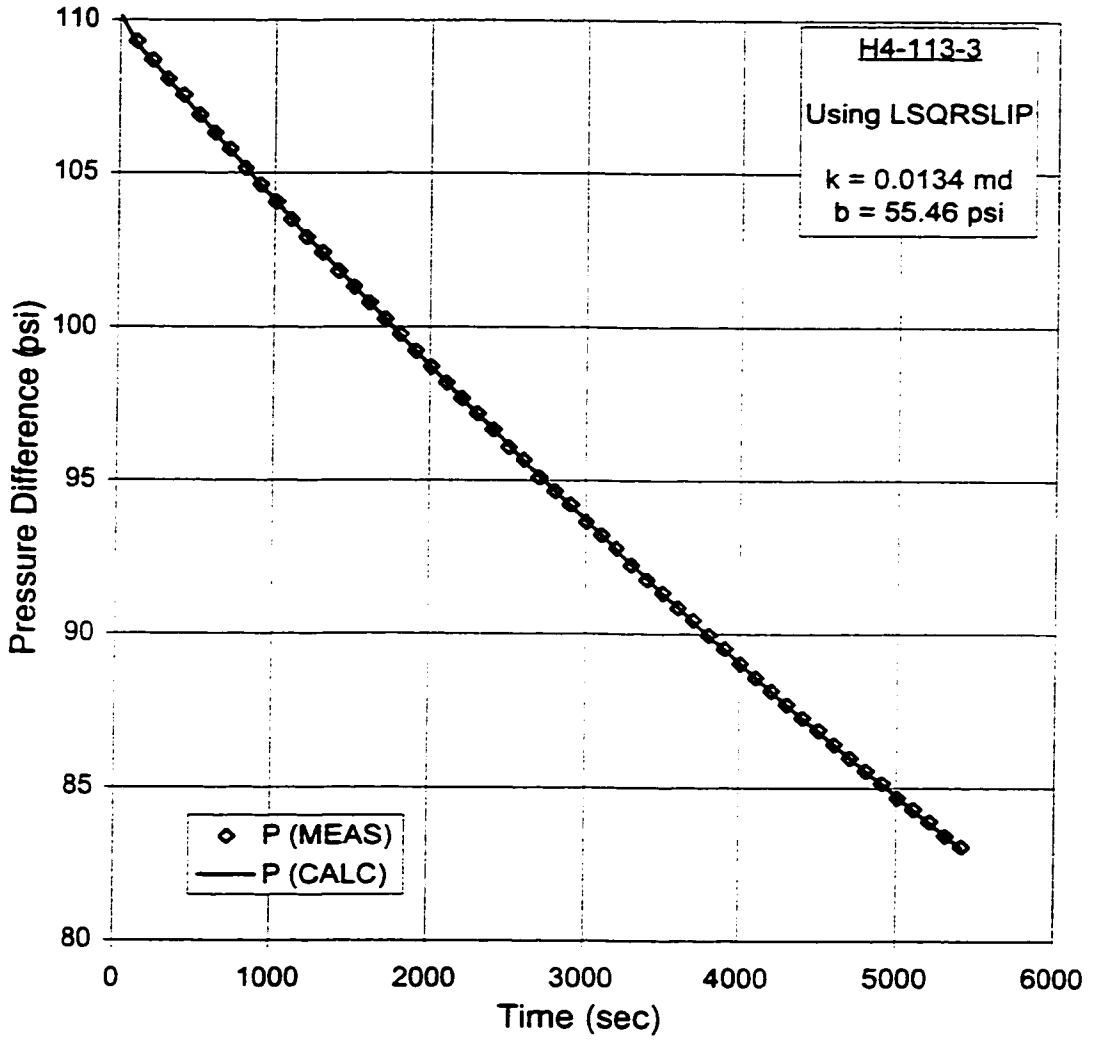

Figure 6.14 Experimental data analysis using the developed program for core # H4-113-3.

6.5.1.2 Problems faced in the experimental data analysis

Another set of experiments was performed with downstream side of the core connected to the downstream reservoir. This provided a variable downstream reservoir pressure. Lower values of pressure difference and mean pore pressure were used ($\Delta P \approx$ 40 to 60 psi and $P_m \approx$ 40 to 50 psi). The experimental data obtained under the above conditions were then analyzed using the developed computer program. Results are presented in table 6.7. Negative values of Klinkenberg constant were obtained, even after getting a good regression fit. The reason could be due to the relationship among gas permeability, liquid permeability and Klinkenberg constant, which is given

$$k_g = k_L (1+b/p)$$

For the experimental conditions under which we performed the experiments, mean pore pressure was nearly constant. Thus for a fixed value of k_g, we can have various combinations of k_L and b to get a regression fit for the test data. This is the reason that we were getting negative value of b and to adjust this, higher values of k were estimated by the non-linear regression of the experimental data. The errors in the values of P_{ui}, P_{di} or ϕ could also be the cause of this problem. To solve this problem a "non-linear regression and graphical technique" was used to analyze the same PPD data.

Table 6.7 Problems in experimental data analysis

Test #	P_m (psi)	k (md)	b (psi)
1	66.23	14.60	-7.74
2	55.27	13.85	-1.19
3	45.47	17.40	-8.30
4	37.42	15.10	-0.35

6.5.1.3 Proposed technique for multiple PPD tests for the estimation of k and b

Based on the Klinkenberg relation $k_g = k_L\ (1+b/p)$, a plot of k_g vs $1/P_m$ gives a straight line with intercept equal to "k_L" and slope equal to "bk_L".

This technique is generally used for the determination of liquid permeability and Klinkenberg constant when using gas in a steady state permeability measurement test.

Due to the error in single test analysis of PPD data, as discussed in section 6.5.1.2, it was decided to use the graphical method of plotting $1/P_m$ vs k_g for the multiple tests data of pressure pulse decay technique. In case of pressure pulse decay test, we can run a number of tests at different mean pore pressures. The pressure conditions should be such that the data is influenced by gas slippage effect. Analyzing these sets of data ignoring the effect of gas slippage will give us the value of gas permeability (k_g). By using the same plotting method (k_g vs $1/P_m$), we can find k_L and b from the graph. This approach is tested using the simulated data from the developed simulator and it is found that this method is giving the values of liquid permeability and Klinkenberg constant reasonably close to the values from which the synthetic data was generated. The results are presented in figure 6.15, which shows that the permeability value is only 0.4% less, and the gas-slippage constant is only 2.6% greater than the original values.

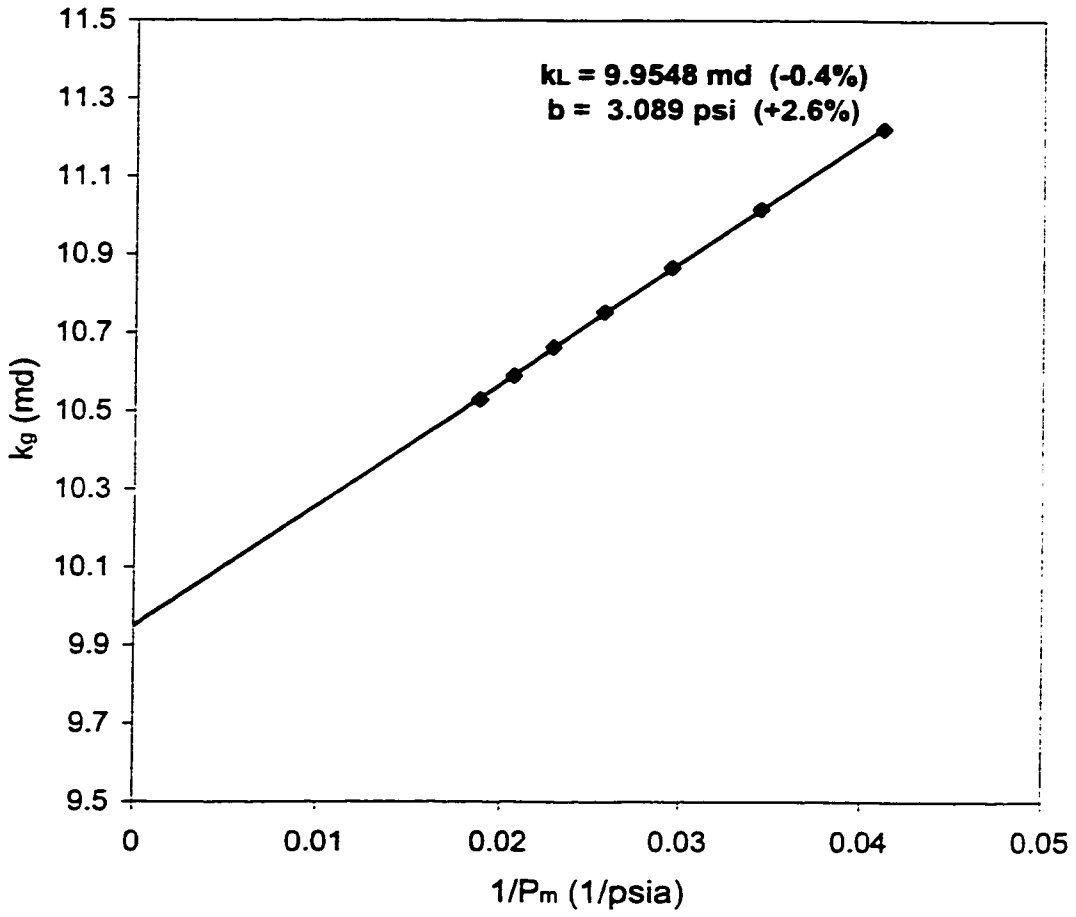

Figure 6.15 Varification of the graphical method for the determination of k and b, using synthetic data from the developed simulator.

6.5.1.4 Determination of k and b from the experimental PPD data using LSR and graphical technique

The proposed technique that had tested for the simulated data, was then used to estimate k and b from the experimental PPD data. At low pressure-difference, four or five PPD tests were performed for different values of low mean pore pressures. Each test data was analyzed using the developed computer program to get the permeability values at each mean pore pressure. The mathematical model used was the one that did not account for the gas-slippage and non-Darcy flow effects. The permeability value obtained was the gas permeability, k_g. Plotting k_g vs $1/P_m$ gave us the liquid permeability, k_L for the core and also the Klinkenberg constant, b. The results are given in figures 6.16 and 6.17.

6.5.1.5 Application of the Jones approximate solution on the simulation data

The synthetic data generated for higher gas-slippage effect was analyzed using Jones method by plotting the graph between P_g and Y_{Pg}, where

P_g = Geometric mean of upstream pressure P_o at time t_1 and t_2, (psig)

$$= \sqrt{P_o(t_1) \times P_o(t_2)}$$

and Y_{Pg} = volumetric rate function (ml/s)

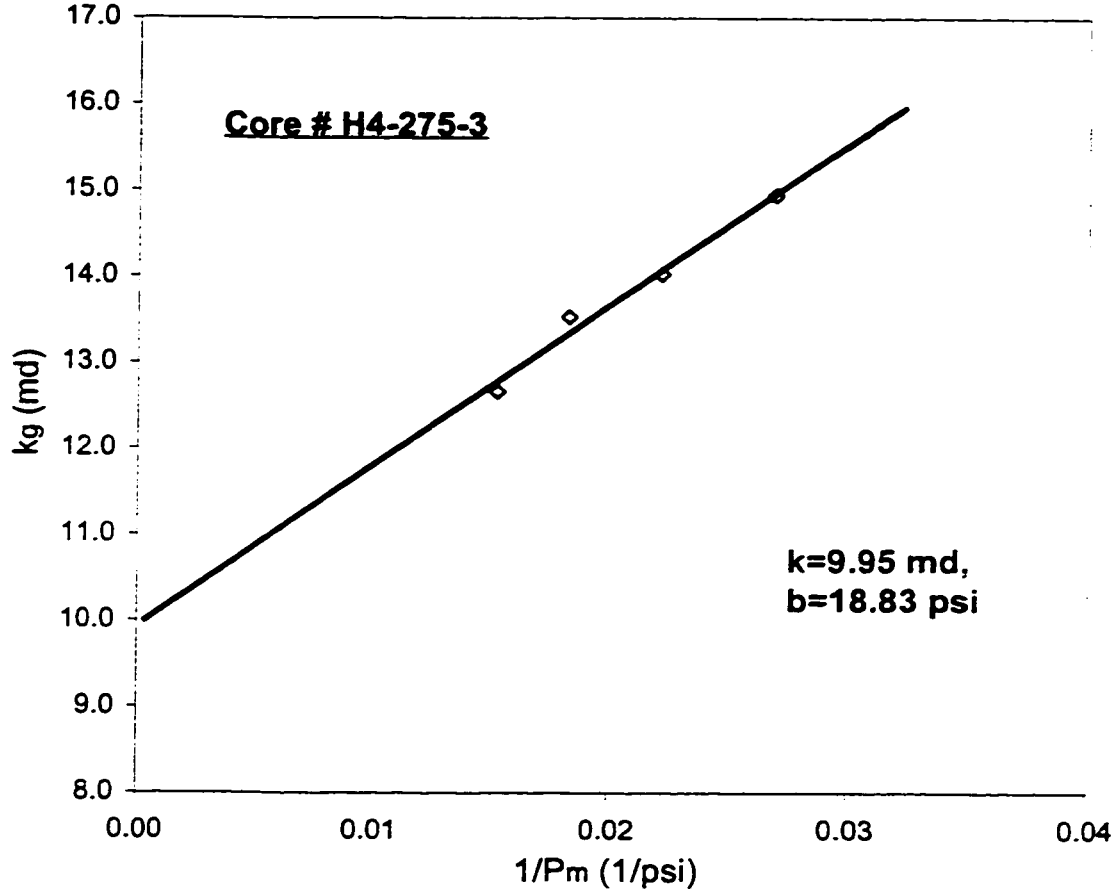

Figure 6.16 Determination of k and b using pressure pulse decay experiments with varying mean pore pressure

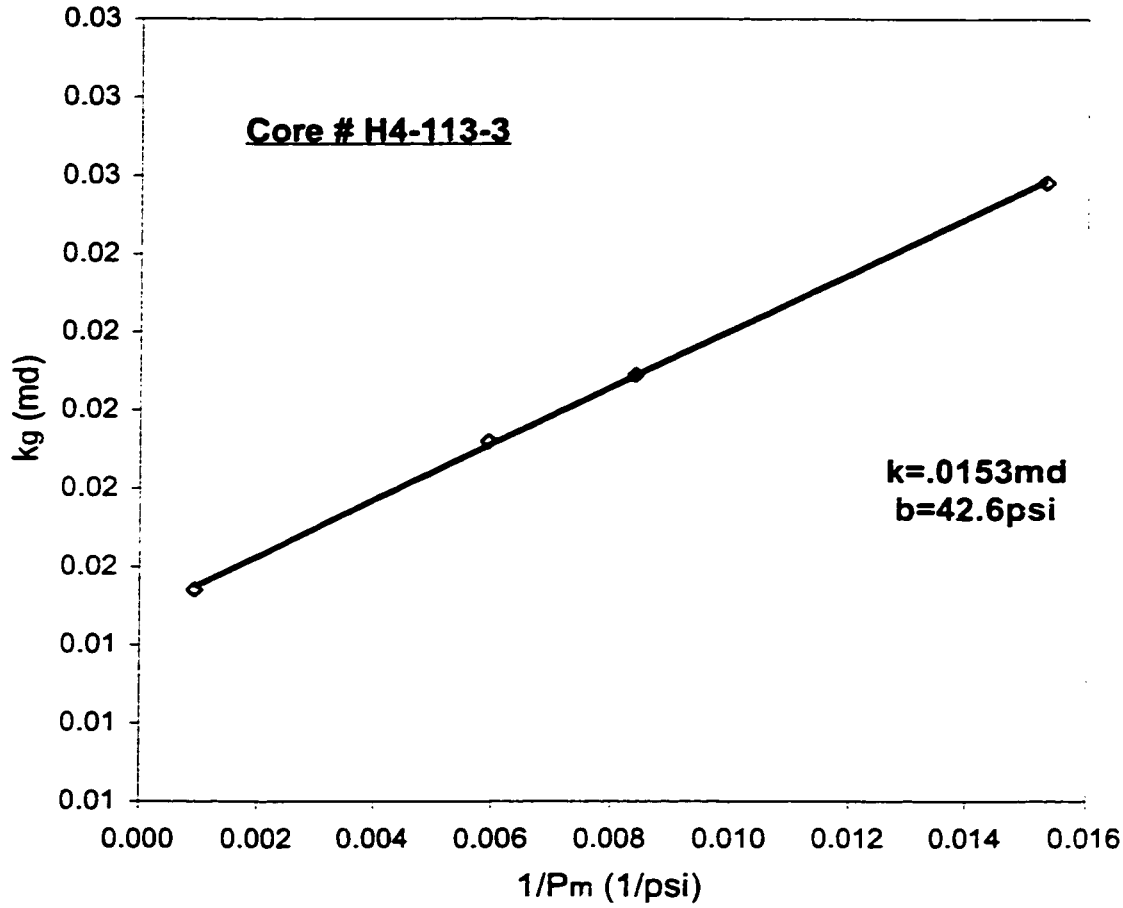

Figure 6.17 Determination of k and b using pressure pulse decay experiments with varying mean pore pressure

$$Y_{Pg} = \frac{V_t}{t_2 - t_1} \ln \frac{P_1}{P_2}$$ [where, V_t = upstream vessel volume (ml)]

These graphs are presented in figures 6.18 and 6.19 for permeability values of 0.01 md and 1.0 md. The early time data of the pressure pulse decay, shows deviation from the straight line as predicted by Jones. This is because of his assumption of initially taking constant mass flow rate and then applying a correction to obtain an approximate solution.

This assumption is not valid, especially for early time data, and this is clear from figures 6.18 and 6.19. Eliminating this early time data from experimental pressure pulse decay data is necessary to obtain a straight line. The inclusion of early time data can lead to a slope that will give incorrect permeability values.

It is evident from figures 6.18 and 6.19 that as the permeability of the core decreases the time before which the data deviates, increases. For 0.01 md core-sample the deviated data is lasting up to 400 seconds and 12 seconds for 1.0 md. Therefore, for very low permeability values (< 0.01md) this early time can have most of the pressure pulse decay data and thus the correct permeability value cannot be found using this method.

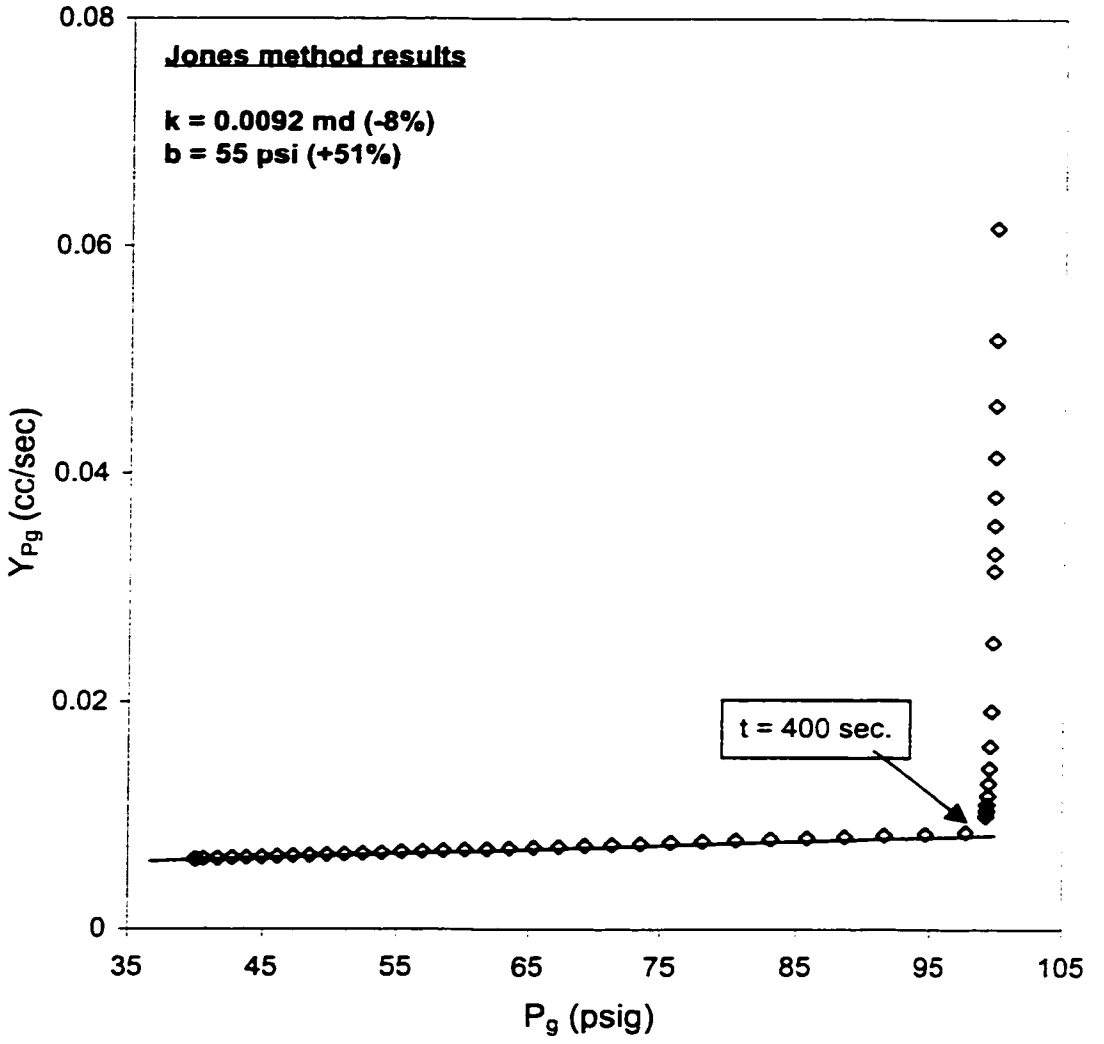

Figure 6.18 Comparison of the simulation results with Jones' approximate solution for the determination of k and b. (k=.01md)

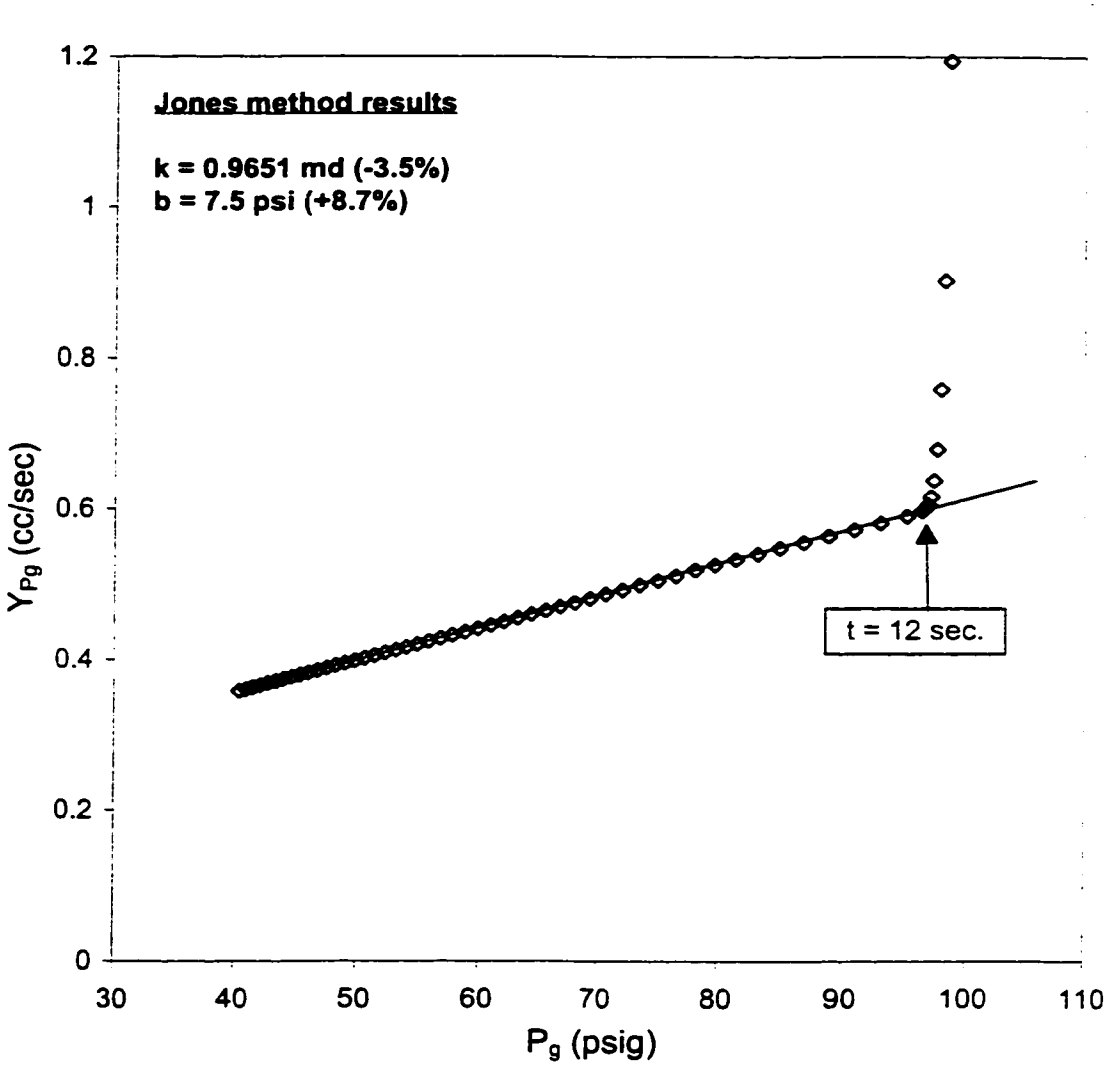

Figure 6.19 Comparison of the simulation results with Jones approximat solution for the determination of k and b. (k=1.0md)

Ignoring the early time data from the synthetic data, the values of permeability and Klinkenberg constant estimated from Jones method are in good agreement with the original values from which the synthetic data was generated. Jones method is underestimating the permeability values by 5% of the original value.

Jones method overestimated the Klinkenberg constant by 10 to 15% for permeabilities greater than 0.1md. For lower permeabilities (≈0.01 md), it gives about 50% higher estimate of the Klinkenberg constant.

6.5.1.6 Determination of k and b using Jones method from the experimental data

The same test data that was analyzed by the developed computer program (section 6.5.1.1), was also analyzed using Jones' method by plotting Y_{Pg} vs P_g. The values of permeability and slippage coefficient are obtained and presented in figure 6.20 and 6.21. There is too much scatter in the data because of the noisy derivative of Y_{Pg} of the pressure pulse data.

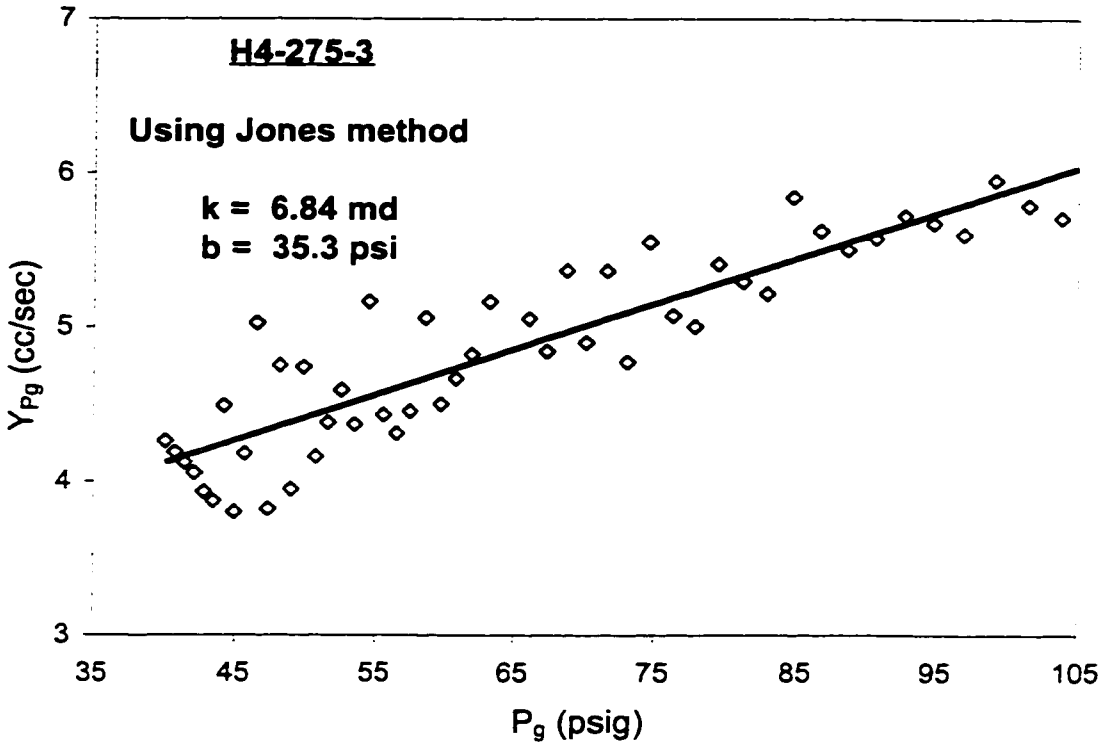

Figure 6.20 Jones approximate solution applied on experimental data for the estimation of k and b

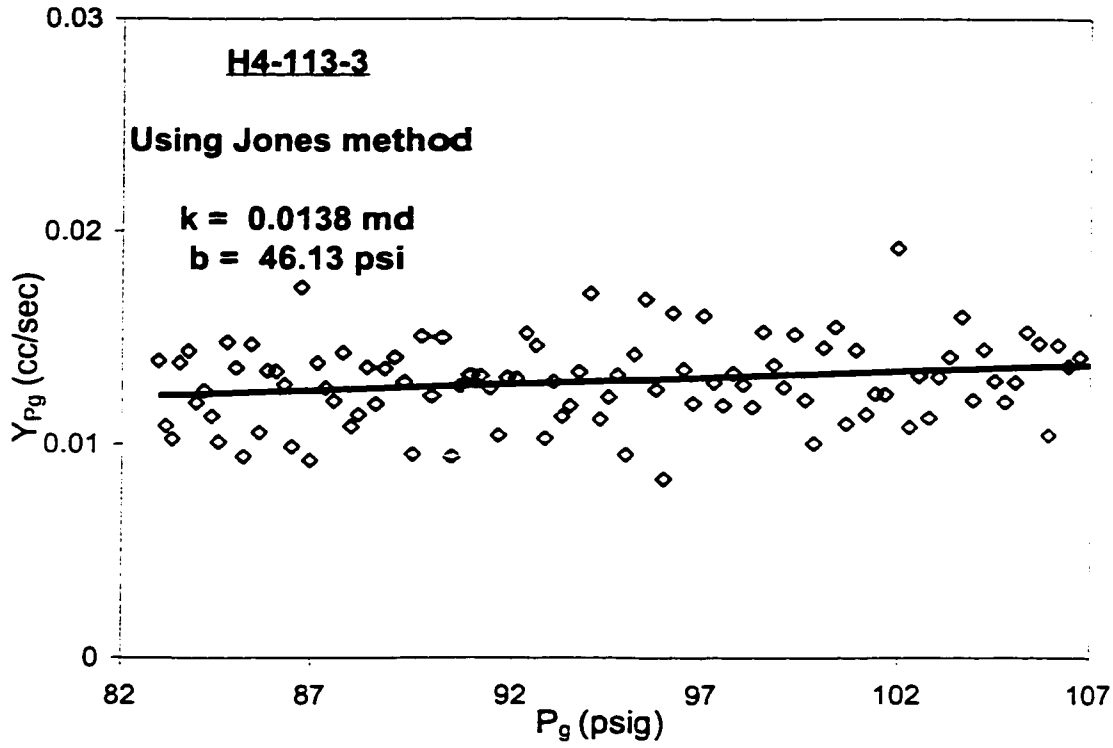

Figure 6.21 Jones approximate solution applied on experimental data for the estimation of k and b

6.5.1.7 Comparison and discussion of the experimental results

Table 6.8 shows the comparison of the results obtained using " non-linear regression and graphical technique", single test data analysis using the developed data analysis program and Jones method. For higher permeability value, the first two methods are giving k and b values nearly same, while Jones method is underestimating k and overestimating b. The estimated b value from the correlation is very low as compare to the values obtained from the three methods. For lower permeability cores, all three methods are giving comparable results.

6.5.2 Determination of permeability and Forchheimer constant simultaneously

The conditions at which the PPD experimental data is influenced by non-Darcy flow effects and nearly insensitive to the Klinkenberg constant were determined as discussed in section 6.2.2. For low permeability values (< 0.1 md) the NDF effects are not significant even for higher mean pore pressure (≈1000 psi) as compared to the gas-slippage effect. Therefore, we selected the core with higher estimated permeability for which the pressure pulse decay data was more likely to be effected by non-Darcy flow. Hence, one core sample was tested for this purpose.

Table 6.8 Comparative results from the developed computer program and the Jones method for k and b

Core #	Graphical result		Numerical Model		Jones Approx		Correlation*
	k (md)	b (psi)	k (md)	b (psi)	k (md)	b (psi)	b (psi)
H4-275-3	9.950	18.830	9.500	15.700	6.840	35.300	3.017
H4-113-3	0.015	42.600	0.013	55.460	0.014	46.130	31.071

Correlation :

Jones : b=6.9/K^(.36)

6.5.2.1 Determination of k and β from single test data using the developed computer program

The pressure pulse decay experiments were performed at the conditions where the data were influenced by non-Darcy flow effect and then analyzed by the developed computer program to estimate the values of permeability and Forchheimer constant. The result is presented in figure 6.22. The discussion and comparison of the obtained results are given in section 6.5.2.4.

6.5.2.2 Application of Jones approximate solution on the simulation data

According to Jones [21], when the pressure pulse decay data is influenced by non-Darcy flow, the plot of Y_{Pg} vs P_g deviates from straight line. Pressure pulse decay data was generated from the developed simulator for the conditions where it was influenced by non-Darcy flow, and plotted on the Y_{Pg} vs P_g plot for permeability ranges from 0.01md to 1.0 md (figures 6.23 to 6.26). The deviation from the limiting slope line can be seen, which shows that the flow is non-Darcy.

The same synthetic data was then plotted on Z vs X plot (figures 6.27 and 6.28) as proposed by Jones and the values of permeability, Klinkenberg constant and Forchheimer constant were determined simultaneously.

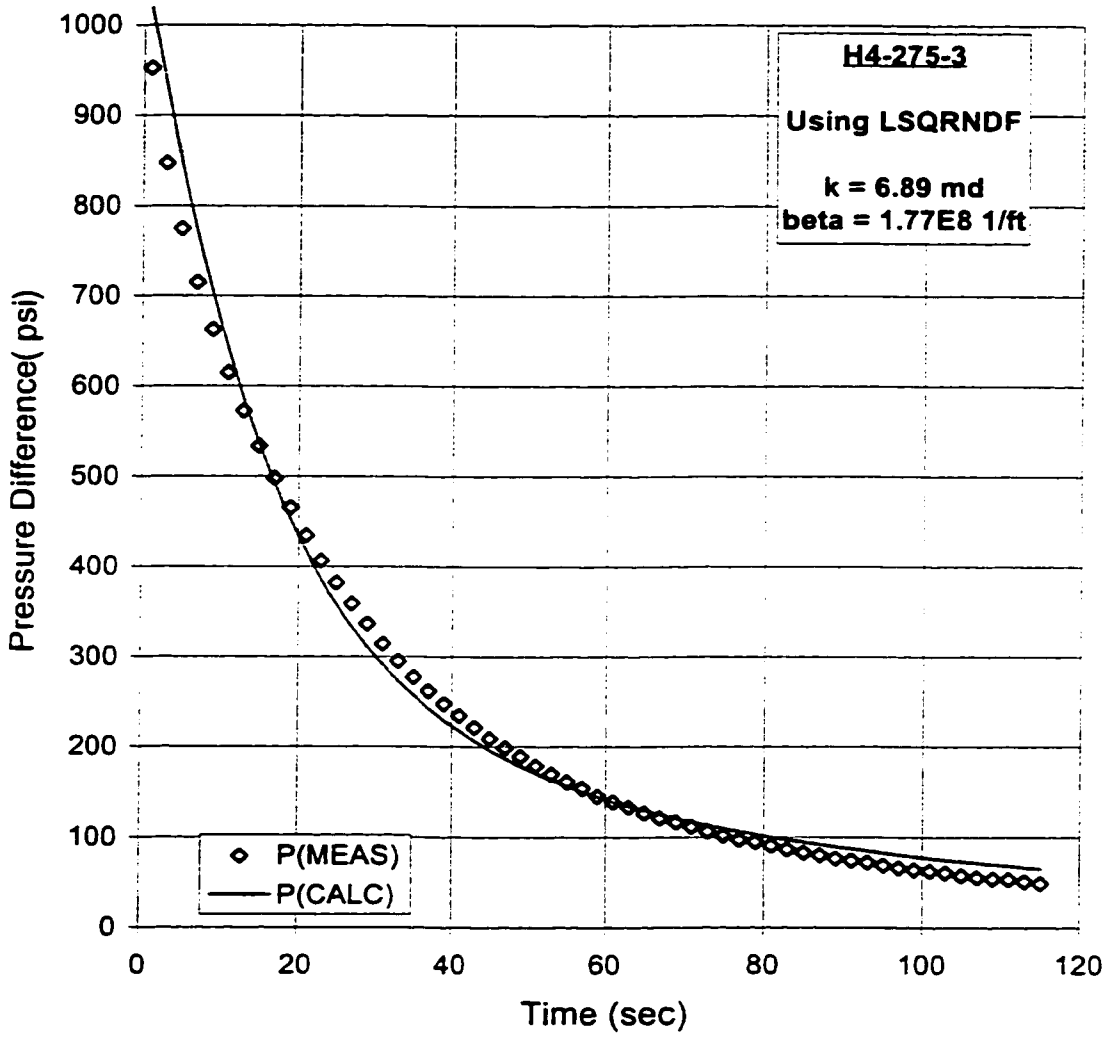

Figure 6.22 Experimental data analysis using the developed program for the determination of k and beta

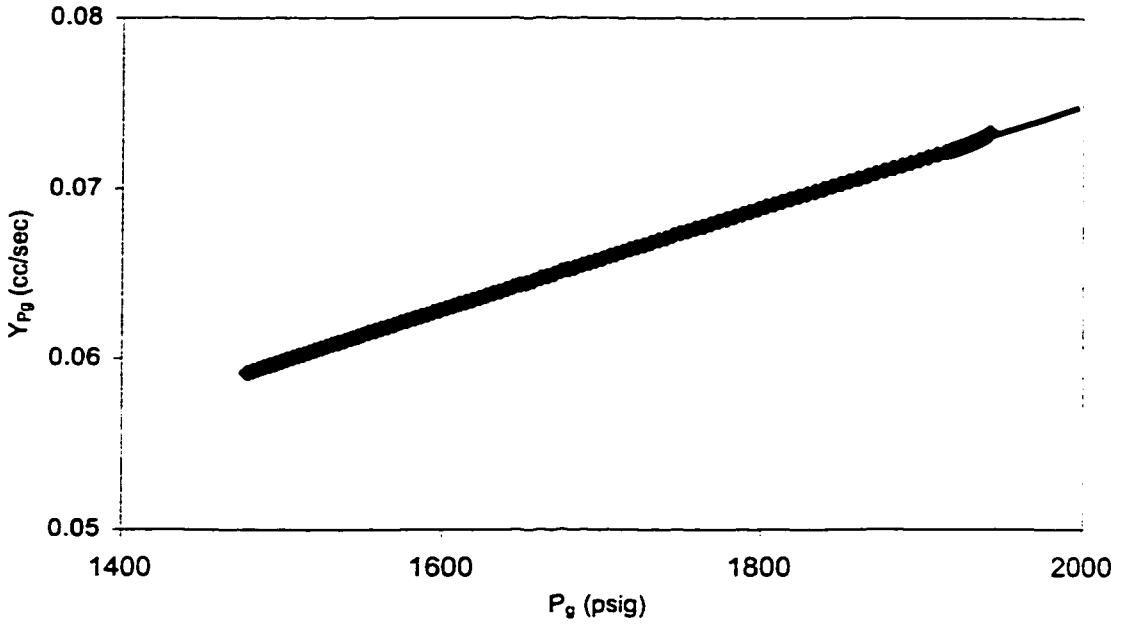

Figure 6.23 Comparison of simulation results with Jones approximate solution to check the presence of NDF effect (k=.01md & dPi=2000psi)

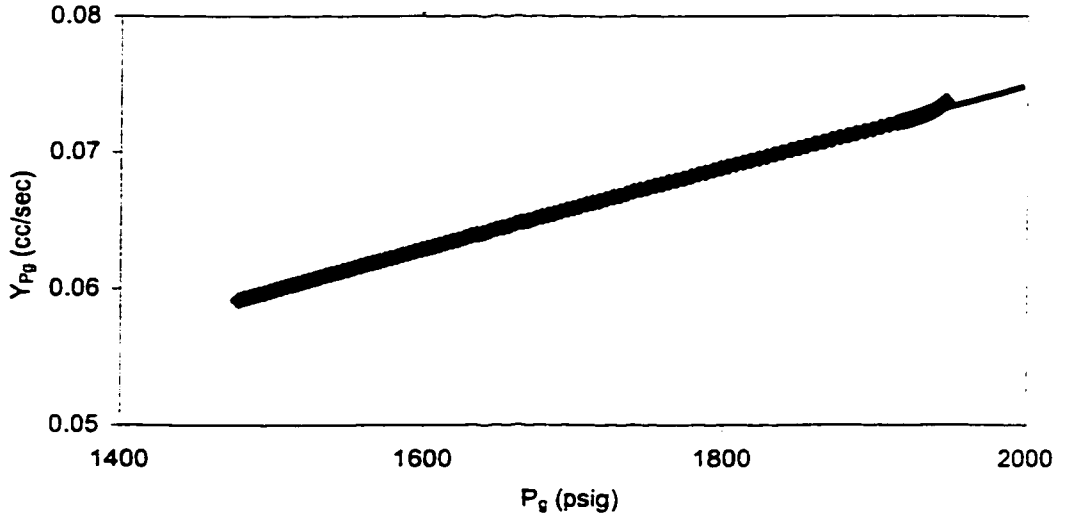

Figure 6.24 Comparison of simulation results with Jones approximate solution to check the presence of NDF effect (k=.01md & dPi=5000psi)

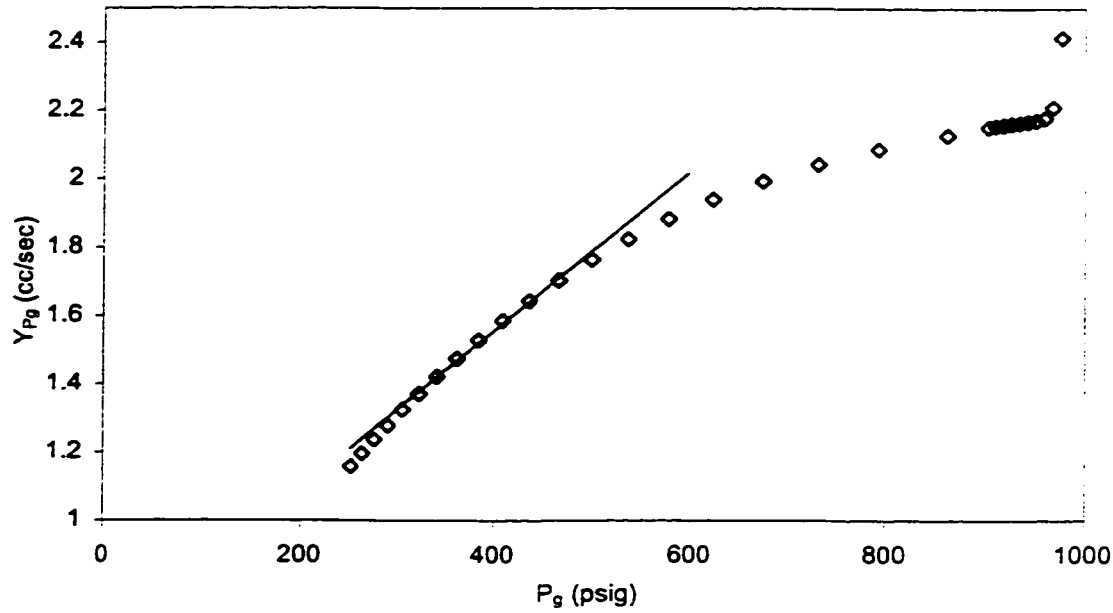

Figure 6.25 Comparison of simulation results with Jones' approximate solution to check the presence of NDF (k=1.0md & ΔPi=1000psi)

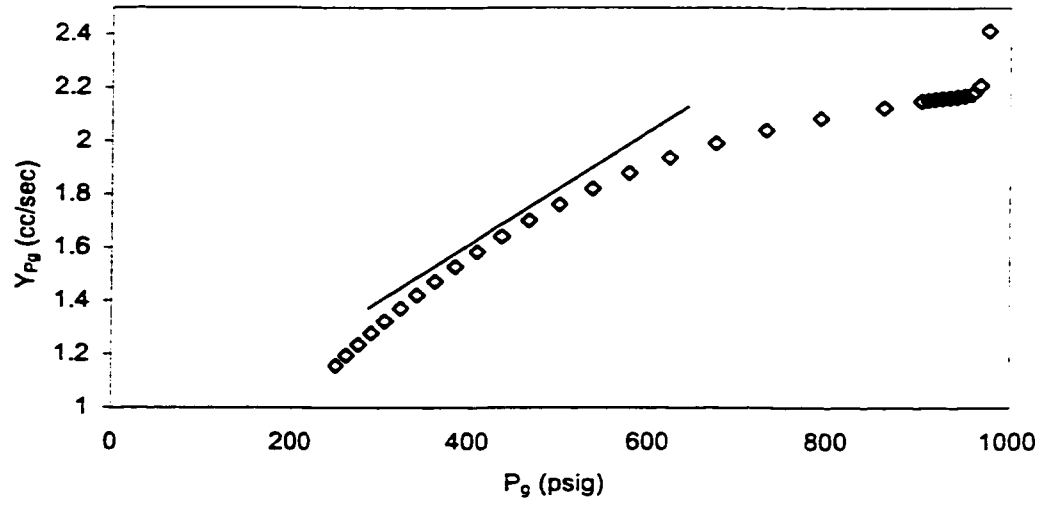

Figure 6.26 Comparison of simulation results with Jones' approximate solution to check the presence of NDF (k=1.0md & ΔPi=2000psi)

The limitation of ignoring early time data was also present in this case, and the slope and intercept of the straight line from which the three properties were determined, considered by ignoring the early time data. Jones [21] suggested to assume a value of the Klinkenberg constant and to plot Z vs X for each assumed value of b. When the upward or downward curvature of the late time data vanishes and a straight line is obtain (Figure 6.27 and 6.28), the values of permeability, Klinkenberg constant and Forchheimer constant can be evaluated from the slope and intercept of the line. The difference in permeability value is less than 1% and for gas-slippage constant varies form 1% for 1.0 md to 20% for 0.01 md, increasing with decreasing permeability. The value of Forchheimer constant is higher than the input value for synthetic data by a factor of 10.

The higher deviation in the parameter estimation, in the case of lower permeability value (Figure 6.27) is due to a negligible effect of non-Darcy flow. This could be predicted from figure 6.23, where for pressure difference value of as high as 2000 psi the deviation of the Y_{Pg} vs P_g straight line cannot be seen for 0.01 md case.

6.5.2.3 Determination of k and β from single test data using Jones method

The same data from one core sample as discussed in section 6.5.2.1, was analyzed by Jones method to find the values of permeability, Klinkenberg constant and Forchheimer constant.

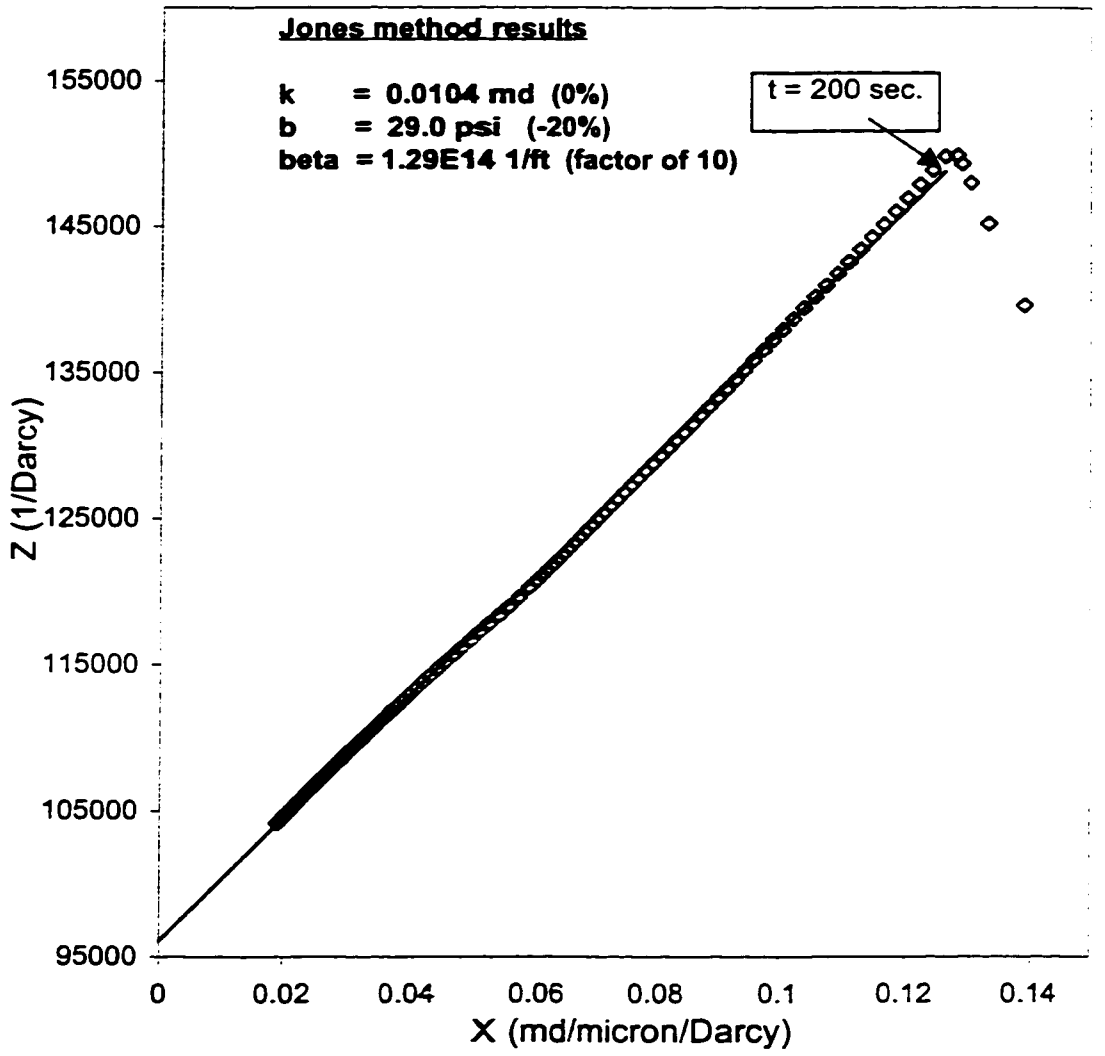

Figure 6.27 Comparison of the simulation results with Jones' approximate solution for the determination of k, b and beta. (k = 0.01 md)

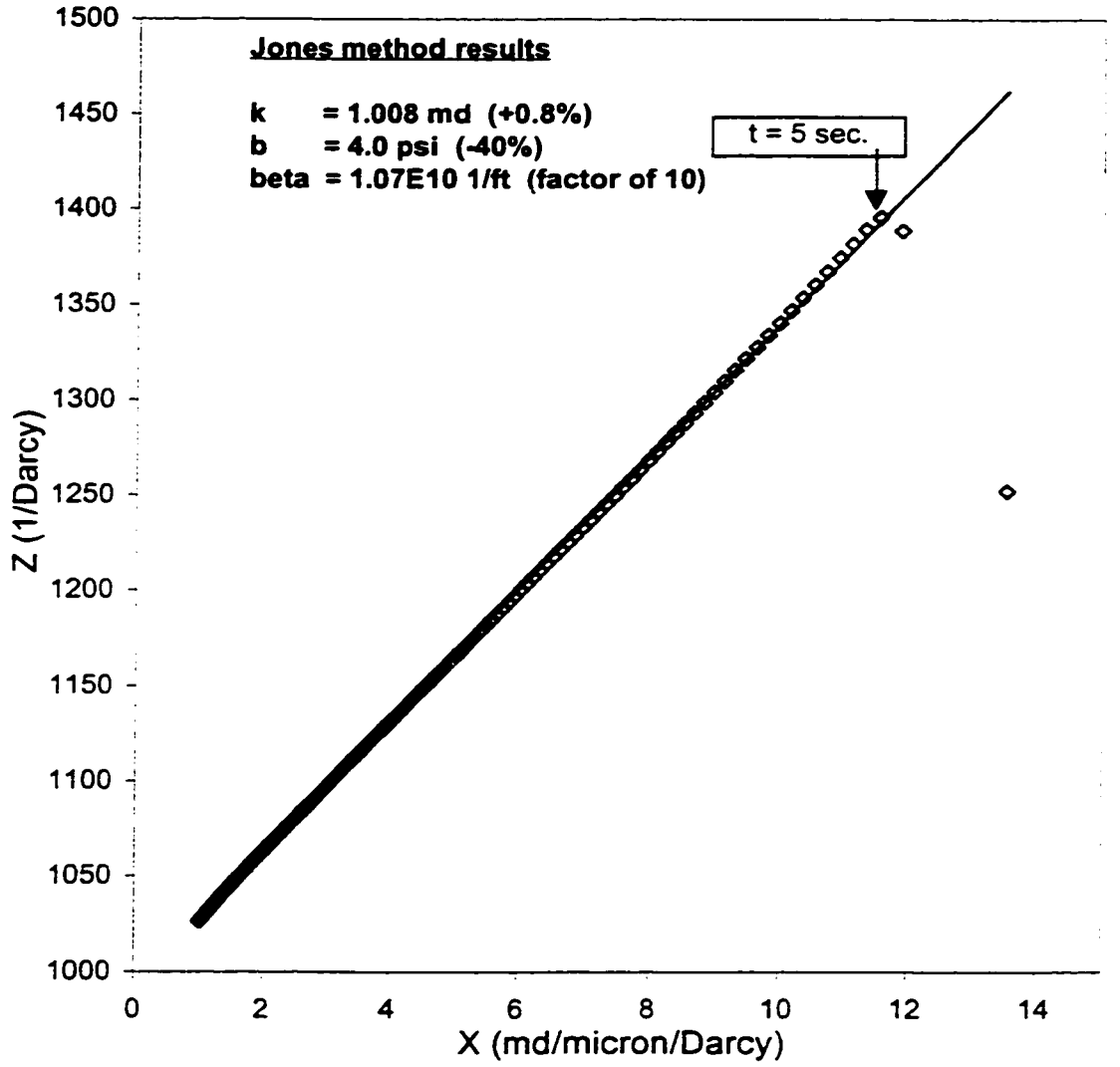

Figure 6.28 Comparison of the simulation results with Jones' approximate solution for the determination of k, b and beta. (k = 1.0 md)

Due to the scatter of the pressure derivative data for the X-Z plot, it was difficult to find the correct value of Klinkenberg constant. Thus assuming b=18.83 psi, as obtained in section 6.5.1.4 for the same core sample, and the values of k and β were determined (figure 6.29).

6.5.2.4 Comparison and discussion of the experimental results

In case of the conditions where PPD data is influenced by NDF effects and the values of permeability, Klinkenberg constant and Forchheimer constant are required to be estimated, it was difficult to apply Jones method to find simultaneously k, b and β. This was due to the difficulty in finding the straight line (X-Z plot), because of the scatter in the pressure derivative data (figure 6.28). The data analysis program gave values of permeability and Forchheimer constant that are comparable with the values from the Jones method (Table 6.9).

The permeability value obtained in this case is comparatively lower than the value obtained in section 6.5.1.4 for the case where slippage effect was dominant and NDF effect was negligible. To find the reason for this underestimation of permeability value when analyzing the PPD data that was influenced by NDF effect, further investigation is needed.

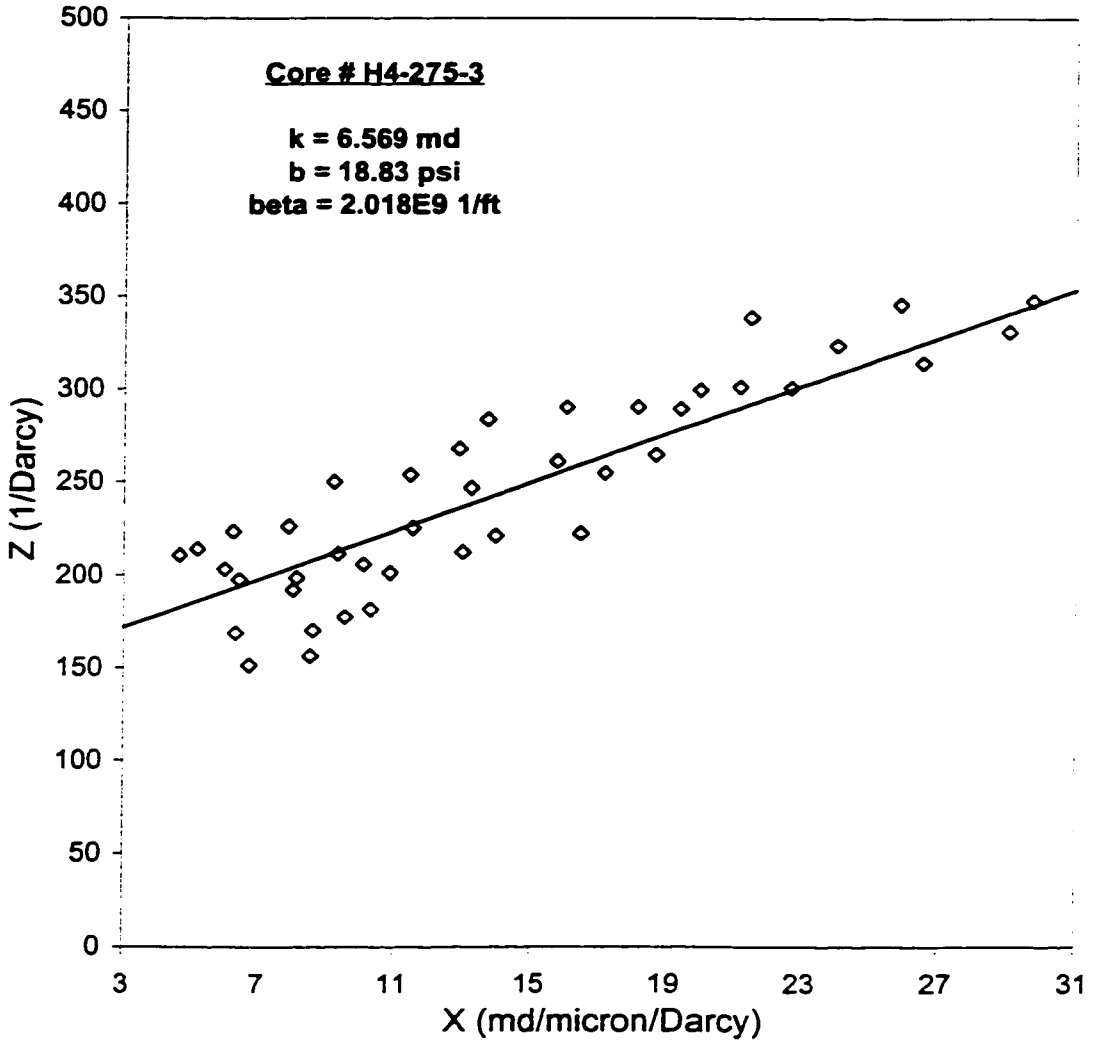

Figure 6.29 Jones approximate method applied on experimental data for the determination of k, b and beta

Table 6.9 Comparative results from the developed computer program and the Jones method for k, b and beta (Core # H4-275-3)

Graphical result		Numerical Model			Jones Approx results			Correlations*	
k (md)	b (psi)	k (md)	b (psi)	beta (1/ft)	k (md)	b (psi)	beta (1/ft)	b (psi)	beta (1/ft)
9.950	18.830	6.890	18.830	1.77E+08	6.569	18.830	2.01E+09	3.017	8.998E+08

Correlations

Jones : b=6.9 / K^(.36)

Geertsma: beta=4.85E4 / (Por^5.5*k^0.5)

CHAPTER 7

CONCLUSIONS AND RECOMMENDATIONS

7.1 CONSLUSIONS

Based on the results of this study, the following conclusions were reached,

1. A numerical simulator is developed to solve the transient, compressible fluid flow equation to describe pressure pulse decay in a porous media, taking into account the effects of gas-slippage and non-Darcy flow.

2. A computer program is developed that analyzes the pressure pulse decay data to estimate permeability, Klinkenberg constant and Forchheimer constant.

3. Gas-slippage and non-Darcy flow effects act in opposite directions. Pressure pulse decays faster if gas-slippage effect is present, while pressure pulse decays slower if non-Darcy flow effect is present.

4. Due to the opposite nature of the gas-slippage and non-Darcy flow effects, it is not reliable to find the values of Permeability (k), Klinkenberg constant (b) and Forchheimer constant (β) simultaneously from a single pressure pulse decay test.

Hence, separate tests should be designed and performed to find Klinkenberg constant (b) and permeability (k), and Forchheimer constant (β) and permeability (k), using pressure pulse decay technique.

5. A more reliable technique for the estimation of permeability (k) and Klinkenberg constant (b), simultaneously from multiple pressure pulse decay tests is proposed.

6. Experimental errors can significantly affect the correct estimation of the parameters (k, b and β).

7. Jones method for the analysis of pressure pulse decay data, is the most commonly used method in the laboratory estimation of permeability, Klinkenberg constant and Forchheimer constant form pressure pulse decay tests. Jones method is found to be unreliable for very tight core samples (< 0.1 md). This is because of the early time data of the pressure pulse decay experiment that cannot be analyzed by Jones method and identifying this early time data is very difficult, especially for the case of tight cores (<0.01 md).

7.2 RECOMMENDATION

Work is suggested to obtain more reliable correlation of b and β in terms of k and ϕ.

REFERENCES

1. A De Ville, "On the Properties of Compressible Gas Flow in a Porous Media", Transport in Porous Media 22: 287-306, 1996.

2. Al-Rumhy M. H. and Kalam M.Z., "Relationship of Core Scale Heterogeneity with Non-Darcy Flow Coefficients", SPE 25649, presented at the SPE Middle East Oil Tech. Conference and Exhibition held in Bahrain, 3-6April 1993.

3. API, Recommended Practice 40, Section 6, Permeability Determination.

4. Bourbie Thierry, Walls Joel, "Pulse Decay Permeability: Analytical Solution and Experimental Test", SPEJ Forum, Oct. 1982.

5. Brace W. F., Walsh J. B. and Frangos W. T., "Permeability of Granite under High Pressure", journal of Geophysical Research, Vol.73, No. 6, March 15, 1968.

6. Chen Techien and Stagg P. W., "Semilog Analysis of the Pulse Decay Technique of Permeability Measurement", SPEJ, Dec. 1984.

7. Coles M. E. and Hartman K. J., "Non-Darcy Measurements in Dry Core and the Effect of Immobile Liquid", SPE 39977 presented at the 1998 Gas Tech Symposium at Calgary, Alberta, Canada, 15-18 March 1998.

8. Cooper J., Wang X., and Mohanty K. K., "Non Darcy Flow Experiments in Anisotropic Porous Media", SPE 49224, presented at the 1998 SPE Annual Tech. Conference and Ex. held in New Orleans, LA, 27-30 Sept. 1998.

9. Dicker A. I. and Smits R. M., "A Practical Approach for Determining Permeability From Laboratory Pressure Pulse Decay Measurements", SPE 17578, presented at the SPE International Meeting on Petroleum Engineering, held in Tianjin, China, Nov. 1-4, 1988.

10. Dogru A.H. et al. "Confidence limits on the parameters and predictions of slightly compressible, single-phase reservoirs." SPEJ, Feb. 1977, Page 42-56.

11. Douglas C. Montgomery and George C. Runger, "Applied Statistics and Probability for Engineers." John Wiley & Sons, Inc., 1994.

12. Ertekin Turgay, King G. R., "Dynamic Gas Slippage: A Unique Dual Mechanism Approach to the Flow of Gas in Tight Formations", SPE 12045, presented at the 58th Annual Tech Conference and Exb. held in San Francisco, CA, Oct. 5-8, 1983.

13. Firoozabadi Abbas, Thomas L. K. and Todd Bert, "High Velocity Flow in Porous Media", SPE Reservoir Engineering, May 1995.

14. Freeman David Louis, Bush Darrell Cleo, "Low Permeability Laboratory Measurements by Non-Steady State and Conventional Methods", SPEJ, Dec.1983.

15. Geertsma J., "Estimating the coefficient of inertial resistance in fluid flow through porous media", SPEJ, October 1974.

16. Gracki, J. A., Flynn, G.P. and Ross, J., "Viscosity of Nitrogen, Helium, Hydrogen and Argon from -100 to 25 °C up to 150-250 atm." J. of Chemical Physics, Nov 1969, 51(9), 3856-63.

17. Grigg Reid B. and Hwang M. K., "High Velocity Gas Flow Effects in Porous Gas Water System", SPE 39978, presented at the 1998 SPE Gas Tech. Symp. held in Calgary, Alberta, Canada, 15-18 March 1998.

18. Haskett S. E., Narahara G. M. and Hoditch S. A., "A method for the Simultaneous Determination of Permeability and Porosity in Low Permeability Cores", SPE 15379, presented at the 61st Annual Tech. Conference and Exh. held in New Orleans, LA, Oct. 5-8, 1986.

19. Hougen, O.A. and Watson, K.M., "Chemical Process Principles, Part two, Thermodynamics," John Wiley and sons, New York, fifth printing, Sept. 1949, 482-3.

20. Hsieh P. A. et al, "A transient Laboratory Method for Determining the Hydraulic Properties of 'Tight' Rocks--I. Theory", Int. J. Rock Mech. Min. Sci. & Geomenc. Abstr. Vol.18, pp.245-252, 1981.

21. Jones, S. C., "A Rapid Accurate Unsteady-State Klinkenberg Permeameter", SPEJ, October 1972.

22. Jones S.C., "A technique for Faster Pulse Decay Permeability Measurements in Tight Rocks", SPE 28450, presented at the SPE 69th Annual Technical Conference and Exhibition held in New Orleans, LA, USA, 25-28 Sept. 1994.

23. Jones S. C., "Using Inertial Coefficient, β, to Characterize Heterogeneity in Reservoir Rock", SPE-16949 presented at the 62 Annual Tech. Conference and Exhibition of the SPE at Dallas, TX, 27-30 Sept. 1987.

24. Kaluarachchi Jagath J., "Analytical Solution to Two Dimensional Axisymmetric Gas Flow with Klinkenberg Effect", Journal of Environmental Engineering, May 1995.

25. Kamath Jairam, Boyer R. E. and Nakagawa F. M., "Characterization of Core Scale Heterogenities Using Laboratory Pressure Transients", SPE Formation Evaluation, Sept. 1992.

26. Klinkenberg L. J., "The permeability of porous media to liquids and gases", Drilling and Production Practice, API, pp. 200-213, 1941.

27. Licht willian Jr. and Stechert Dietrich G., " The variation of the viscosity of gases and vapors with temperature." J. of Physical Chemistry. 1944, Vol. 48, 223-47.

28. Lin Wunan, "Parametric Analyses of the Transient Method of Measuring Permeability", Journal of Geophysical Research, Vol.87, No.B2, February 10, 1981.

29. Liu X., Civan F., and Evans R. D., "Correlation of the Non Darcy Flow Coefficient", JCPT, Dec. 1995.

30. Milton-Tayler David, "Non Darcy Gas Flow: From Laboratory Data to Field Prediction", SPE 26146 presented at the SPE Gas Tech. Symp. In Calgary, Alberta, Canada, 28-30 June 1993.

31. Neilson Rudd, "Pressure Decay Measurement", SPE 1604, presented at the SPE Gas Tech. Symp., Omaha, Nebr., Sept 15-16, 1966.

32. Neuzil C. E. et al, " A transient Laboratory Method for Determining the Hydraulic Properties of 'Tight' Rocks--II. Application", Int. J. Rock Mech. Min. Sci. & Geomenc. Abstr. Vol.18, pp.253-258, 1981.

33. Thauvin F. and Mohanty K. K., "Network Modeling of Non-Darcy Flow Through Porous Media", Transport in Porous Media 31: 19-37, 1998.

34. Trimmer Donald A., "Design Criteria for Laboratory Measurements of Low Permeability Rocks", Geophysical Research Letters, Sept. 1981.

35. Yamada S. E. and Jones A. H., "A Review of a Pulse Technique for Permeability Measurements", SPEJ Forum, Oct. 1980.

36. Yildiz Turhan, "Analytical Treatment of Transient Non- Darcy Flow", SPE 22678, presented at the 66th Annual Tech. Conf. & Exb. At Dallas, TX, Oct 6-9, 1991.

37. Yu-Shu Wu, Pruess Karsten, and Persoff Peter, "Gas Flow in Porous Media with Klinkenberg Effects", Transport in Porous Media 32: 117-137, 1998.

Appendix A

The governing differential equation is derived as follows for transient flow of compressible fluid through porous media . The basic assumptions are:

(1) Single phase (gas) flow, Isothermal
(2) One dimensional flow
(3) Rock properties ϕ & k are constant

* Applying mass balance, we get

$$-\Delta t\left[(\rho A v)_x-(\rho A v)_{x+\Delta x}\right]=\left[\phi \rho A \Delta x\right]_{t+\Delta t}-\left[\phi A \rho \Delta x\right]_t$$

* Forchheimer Equation is given as

$$-\frac{dp}{dx}=\frac{\mu}{k}v+\rho\beta v^2$$

let,

$$\delta=\frac{1}{1+\frac{\beta\rho k}{\mu}(v)}$$

hence, we can write

$$v=-\frac{k}{\mu}\delta\frac{\partial p}{\partial x}$$

* Klinkenberg relation is given as

$$k_g=k_l(1+\frac{b}{p})$$

Combining the above equations we get

$$\left[-\left(\rho\frac{k_l\left(1+\frac{b}{p}\right)}{\mu}\delta\frac{\partial p}{\partial x}\right)_x+\left(\rho\frac{k_l\left(1+\frac{b}{p}\right)}{\mu}\delta\frac{\partial p}{\partial x}\right)_{x+\Delta x}\right]\Delta t=\Delta x\left[(\phi\rho)_{t+\Delta t}-(\phi\rho)_t\right]$$

$$\frac{\left[\frac{\rho}{\mu}k_l\left(1+\frac{b}{p}\right)\delta\frac{\partial p}{\partial x}\right]_{x+\Delta x}-\left[\frac{\rho}{\mu}k_l\left(1+\frac{b}{p}\right)\delta\frac{\partial p}{\partial x}\right]_{x}}{\Delta x}=\frac{(\phi\rho)_{t+\Delta t}-(\phi\rho)_t}{\Delta t}$$

Taking lim ($\Delta x \rightarrow 0$ and $\Delta t \rightarrow 0$), we get

$$\frac{\partial}{\partial x}\left[\frac{\rho}{\mu}k_l(1+\frac{b}{p})\delta\frac{\partial p}{\partial x}\right]=\frac{\partial}{\partial t}\left[\phi\rho\right]$$

For gases, we have

$$\rho=\frac{Mp}{zRT}$$

Therefore,

$$\frac{\partial}{\partial x}\left[\frac{Mp}{zRT\mu}k_l(1+\frac{b}{p})\delta\frac{\partial p}{\partial x}\right]=\frac{\partial}{\partial t}\left[\phi\frac{Mp}{zRT}\right]$$

$$\frac{M}{RT}k_l\frac{\partial}{\partial x}\left[\frac{p}{\mu z}(1+\frac{b}{p})\delta\frac{\partial p}{\partial x}\right]=\phi\frac{M}{RT}\frac{\partial}{\partial t}(\frac{p}{z})$$

$$\frac{\partial}{\partial x}\left[\frac{p}{\mu z}(1+\frac{b}{p})\delta\frac{\partial p}{\partial x}\right]=\frac{\phi}{k_l}\frac{\partial}{\partial t}(\frac{p}{z})\text{\_\_\_\_\_}(A-1)$$

Now finding the time derivative of (p/z)

$$\frac{\partial}{\partial t}(\frac{p}{z})=\frac{1}{z}\frac{\partial p}{\partial t}+p\frac{\partial}{\partial t}(\frac{1}{z})$$

$$\frac{\partial}{\partial t}(\frac{p}{z})=\frac{1}{z}\frac{\partial p}{\partial t}+p(-\frac{1}{z^2})\frac{\partial z}{\partial t}$$

$$\frac{\partial}{\partial t}(\frac{p}{z})=\frac{1}{z}\frac{\partial p}{\partial t}-\frac{p}{z^2}(\frac{\partial z}{\partial p}\times\frac{\partial p}{\partial t})$$

$$\frac{\partial}{\partial t}(\frac{p}{z})=\left[\frac{1}{z}-\frac{p}{z^2}\frac{\partial z}{\partial p}\right]\frac{\partial p}{\partial t}$$

$$\frac{\partial}{\partial t}(\frac{p}{z}) = \left[\frac{1}{p} - \frac{1}{z}\frac{\partial z}{\partial p}\right]\frac{p}{z}\frac{\partial p}{\partial t} \qquad \text{——————}(A-2)$$

Also we know that gas compressibility can be given as

$$c_g = -\frac{1}{V}\frac{\partial V}{\partial p}$$

$$c_g = -\frac{p}{z}\frac{1}{nRT}\left[\frac{\partial}{\partial p}(\frac{z}{p})nRT\right]$$

$$= -\frac{p}{z}\left[\frac{1}{p}\frac{\partial z}{\partial p} + (-\frac{z}{p^2})\right]$$

$$c_g = \frac{1}{p} - \frac{1}{z}\frac{\partial z}{\partial p} \qquad \text{——————}(A-3)$$

Substituting Equation A-3 into Equation A-2, we get

$$\frac{\partial}{\partial t}(\frac{p}{z}) = c_g\,\frac{p}{z}\,.\,\frac{\partial p}{\partial t} \qquad \text{——————————}(A-4)$$

Therefore, Equation A-1 becomes,

$$\frac{\partial}{\partial x}\left[\frac{p}{uz}(1+\frac{b}{p})\delta\frac{\partial p}{\partial x}\right] = \frac{\phi c_g}{k_l}.\frac{p}{z}.\frac{\partial P}{\partial t} \qquad \text{——————}(A-5)$$

Equation A-5 is the partial differential equation for the tranisient one-dimensional flow of gas through porous media with gas-slippage and non-Darcy flow effects.

Appendix B

The partial differential equation for the transit flow of gas through porous media with gas-slippage and non-Darcy flow effects is derived in appendix A and can be re-written as

$$\frac{1}{\alpha}\frac{\partial}{\partial x}\left[\frac{\delta}{\mu z}(p+b)\frac{\partial p}{\partial x}\right]=\frac{\phi}{k_l}.c_g\frac{p}{z}\frac{\partial p}{\partial t}$$

Where α is the unit conversion factor.

The finite difference representation of the above equation is presented below

For $I=3,...,N-2$

$$\frac{1}{\alpha}\frac{1}{\Delta x_i}\left\{\left[\frac{\delta}{\mu z}(p+b)\right]^n_{i-\frac{1}{2}}\frac{p^{n+1}_{i+1}-p^{n+1}_i}{\Delta x}-\left[\frac{\delta}{\mu z}(p+b)\right]^n_{i-\frac{1}{2}}\frac{p^{n+1}_i-p^{n+1}_{i-1}}{\Delta x}\right\}^{i-1}=\frac{\phi}{k_l}c_g\frac{p}{z}\frac{\partial p}{\partial t}$$

$$\frac{1}{\alpha}\frac{1}{\Delta x^2}\left\{\left[\frac{\delta(p+b)}{\mu z}\right]^n_{i+\frac{1}{2}}(p^{n+1}_{i+1}-p^{n+1}_i)-\left[\frac{\delta(p+b)}{\mu z}\right]^n_{i-\frac{1}{2}}(p^{n+1}_i-p^{n+1}_{i-1})\right\}=\frac{\phi}{k_l}c_g\frac{p}{z}(\frac{p^{n+1}_i-p^n_i}{\Delta t})$$

let

$$F=\frac{p+b}{\mu z}$$

$$G=\frac{p}{z}c_g$$

$$\frac{1}{\alpha}\frac{k_l}{\Delta x^2}\frac{\Delta t}{\phi}\left\{\delta^n_{i+\frac{1}{2}}F^n_{i+\frac{1}{2}}p^{n+1}_{i+1}-\delta^n_{i+\frac{1}{2}}F^n_{i+\frac{1}{2}}p^{n+1}_i-\delta^n_{i-\frac{1}{2}}F^n_{i-\frac{1}{2}}p^{n+1}_i+\delta^n_{i-\frac{1}{2}}F^n_{i-\frac{1}{2}}p^{n+1}_{i-1})\right\}-Gp^{n+1}_i=-Gp^n_i$$

Let

$$ccc=\frac{1}{\alpha\phi\Delta x^2}$$

and

$$cc=(ccc)\,k_l\Delta t=\frac{k_l\Delta t}{\alpha\phi\Delta x^2}$$

Therefore,

$$(cc)\,\delta_{i+\frac{1}{2}}F_{i+\frac{1}{2}}p^{n+1}_{i+1}-(cc)\left[\delta_{i+\frac{1}{2}}F_{i+\frac{1}{2}}p^{n+1}_i-\delta_{i-\frac{1}{2}}F_{i-\frac{1}{2}}p^{n+1}_i\right]-Gp^{n+1}_i+(cc)\,\delta_{i-\frac{1}{2}}F_{i-\frac{1}{2}}p^{n+1}_{i-1}=-Gp^n_i$$

Rearranging, we get

$$\left[(cc)\,\delta_{i-\frac{1}{2}}F_{i-\frac{1}{2}}\right]p_{i-1}^{n+1}-\left[(cc)\,\delta_{i+\frac{1}{2}}F_{i+\frac{1}{2}}+(cc)\,\delta_{i-\frac{1}{2}}F_{i-\frac{1}{2}}+G\right]p_i^{n+1}+\left[(cc)\,\delta_{i+\frac{1}{2}}F_{i+\frac{1}{2}}\right]p_{i+1}^{n+1}=-Gp_i^n.....(B-1)$$

For $i=2$

$$\frac{1}{\alpha}\,\frac{1}{\Delta x}\left\{\left[\frac{\delta}{\mu z}(p+b)\right]_{i+\frac{1}{2}}\left(\frac{p_{i+1}-p_i}{\Delta x}\right)-\left[\frac{\delta}{\mu z}(p+b)\right]_{i-\frac{1}{2}}\left(\frac{p_i-p_{i-\frac{1}{2}}}{\frac{\Delta x}{2}}\right)\right\}=\frac{\phi}{k_l}c_g\frac{p}{z}\frac{\partial p}{\partial t}$$

$$\frac{1}{\alpha}\,\frac{1}{\Delta x^2}\left\{\left[\frac{\delta(p+b)}{\mu z}\right]_{i+\frac{1}{2}}(p_{i+1}-p_i)-2\left[\frac{\delta(p+b)}{\mu z}\right]_{i-\frac{1}{2}}\left(p_i-p_{i-\frac{1}{2}}\right)\right\}=\frac{\phi}{k_l}\left(c_g\frac{p}{z}\right)\frac{p^{n+1}-p^n}{\Delta t}$$

$$\frac{1}{\alpha}\,\frac{k_l\Delta t}{\Delta x^2\phi}\left[\delta_{i+\frac{1}{2}}F_{i+\frac{1}{2}}p_{i+1}^{n+1}-\delta_{i+\frac{1}{2}}F_{i+\frac{1}{2}}p_i^{n+1}-2\delta_{i-\frac{1}{2}}F_{i-\frac{1}{2}}p_i^{n+1}+2\delta_{i-\frac{1}{2}}F_{i-\frac{1}{2}}p_{i-\frac{1}{2}}^{n+1}\right]-Gp_i^{n+1}=-Gp_i^n$$

$$\left[2(cc)\delta_{i-\frac{1}{2}}F_{i-\frac{1}{2}}\right]p_{i-1}^{n+1}-\left[(cc)\delta_{i+\frac{1}{2}}F_{i+\frac{1}{2}}+2(cc)\delta_{i-\frac{1}{2}}F_{i-\frac{1}{2}}+G\right]p_i^{n+1}+\left[(cc)\delta_{i+\frac{1}{2}}F_{i+\frac{1}{2}}\right]p_{i+1}^{n+1}=-Gp_i^n....(B-2)$$

For $i=N-1$

$$\frac{1}{\alpha}\,\frac{1}{\Delta x}\left\{\left[\frac{\delta}{\mu z}(p+b)\right]_{i+\frac{1}{2}}\left(\frac{p_{i+\frac{1}{2}}-p_i}{\frac{\Delta x}{2}}\right)-\left[\frac{\delta}{\mu z}(p+b)\right]_{i-\frac{1}{2}}\left(\frac{p_i-p_{i-1}}{\Delta x}\right)\right\}=\frac{\phi}{k_l}c_g\frac{p}{z}\frac{\partial p}{\partial t}$$

$$\frac{1}{\alpha}\,\frac{1}{\Delta x^2}\left\{2\left[\frac{\delta}{\mu z}(p+b)\right]_{i+\frac{1}{2}}\left(p_{i+\frac{1}{2}}-p_i\right)-\left[\frac{\delta}{\mu z}(p+b)\right]_{i-\frac{1}{2}}(p_i-p_{i-1})\right\}=\frac{\phi}{k_l}c_g\frac{p}{z}\frac{p^{n+1}-p^n}{\Delta t}$$

$$\frac{1}{\alpha}\,\frac{k_l\Delta t}{\Delta x^2\phi}\left[2\delta_{i+\frac{1}{2}}F_{i+\frac{1}{2}}p_{i+\frac{1}{2}}^{n+1}-2\delta_{i+\frac{1}{2}}F_{i+\frac{1}{2}}p_i^{n+1}-\delta_{i-\frac{1}{2}}F_{i-\frac{1}{2}}p_i+\delta_{i-\frac{1}{2}}F_{i-\frac{1}{2}}p_{i-1}\right]-Gp_i^{n+1}=-Gp_i^n$$

Let

$$cc=\frac{k_l\Delta t}{\alpha\Delta x^2\phi}$$

and rearranging with

$$p_{i+\frac{1}{2}}=p_{i+1}$$

$$\left[(cc)\delta_{i-\frac{1}{2}}F_{i-\frac{1}{2}}\right]p_{i-1}^{n+1}-\left[2(cc)\delta_{i+\frac{1}{2}}F_{i+\frac{1}{2}}+(cc)\delta_{i-\frac{1}{2}}F_{i-\frac{1}{2}}+G\right]p_i^{n+1}+\left[2(cc)\delta_{i+\frac{1}{2}}F_{i+\frac{1}{2}}\right]p_{i+1}^{n+1}=-Gp_i^n.....(B-3)$$

For Upstream Vessel we have the partial differential equation

$$c_gV_{cell}\frac{\partial p}{\partial t}=\frac{1}{\alpha}\,\frac{k_lA}{\mu}\frac{\delta(p+b)}{p}.\frac{\partial p}{\partial x}$$

$$c_g \frac{p}{z}\frac{\partial p}{\partial t} = \frac{1}{\alpha}\frac{k_l A}{V_u}\frac{p}{\mu z}\frac{\delta(p+b)}{p}.\frac{\partial p}{\partial x}$$

$$\Rightarrow \frac{1}{\alpha}\frac{k_l A}{V_u}\frac{\delta(p+b)}{\mu z}.\frac{\partial p}{\partial x} = c_g \frac{p}{z}\frac{\partial p}{\partial t}$$

let

$$F = \frac{p+b}{\mu z}$$

$$G = c_g \frac{p}{Z};$$

$$C_1 = 2\frac{k_l A \Delta t}{\alpha V_u \Delta x}$$

Therefore,

$$\frac{1}{\alpha}\frac{k_l A}{V_u} F\delta \frac{\partial p}{\partial x} = G\frac{\partial p}{\partial t}$$

$$\Rightarrow \frac{1}{\alpha}\frac{k_l A}{V_u} F_{i+\frac{1}{2}}\delta_{i+\frac{1}{2}}\left(\frac{p_{i+1} - p_{i+\frac{1}{2}}}{\frac{\Delta x}{2}}\right) = G\frac{p^{n+1} - p^n}{\Delta t}$$

since,

$$p_{i+\frac{1}{2}} = p_i$$

$$\frac{1}{\alpha}\frac{2k_l A \Delta t}{V_u \Delta x}\left[\delta_{i+\frac{1}{2}} F_{i+\frac{1}{2}} p_{i+1}^{n+1} - \delta_{i+\frac{1}{2}} F_{i+\frac{1}{2}} p_i^{n+1}\right] - G p_i^{n+1} = -G p_i^n$$

$$-\left[c_1 \delta_{i+\frac{1}{2}} F_{i+\frac{1}{2}} + G\right] p_i^{n+1} + \left[c_1 \delta_{i+\frac{1}{2}} F_{i+\frac{1}{2}}\right] p_{i+1}^{n+1} = -G p_i^n \quad \ldots\ldots\ldots\ldots\ldots\ldots\ldots\ldots\ldots\ldots (B-4)$$

For Downstream Vessel we have

$$c_g \frac{p}{z}\frac{\partial p}{\partial t} = -\frac{1}{\alpha}\frac{k_l A}{V_d}\frac{p}{\mu z}\frac{\delta(p+b)}{p}.\frac{\partial p}{\partial x}$$

$$-\frac{1}{\alpha}\frac{k_l A}{V_d} F\delta \frac{\partial p}{\partial x} = G\frac{\partial p}{\partial t}$$

$$-\frac{1}{\alpha}\frac{k_l A}{V_d} F_{i-\frac{1}{2}}\delta_{i-\frac{1}{2}}\left(\frac{p_{i-\frac{1}{2}} - p_{i-1}}{\frac{\Delta x}{2}}\right) = G\frac{p_i^{n+1} - p_i^n}{\Delta t}$$

since,

$$p_{i-\frac{1}{2}} = p_i$$

$$\frac{1}{\alpha}\ \frac{2k_l A\Delta t}{V_d \Delta x}\delta_{i-\frac{1}{2}} F_{i-\frac{1}{2}} \left[p_{i-1} - p_i\right] - G p_i^{n+1} = -G p_i^n$$

Let

$$c_2 = \frac{2k_l A\Delta t}{\alpha \Delta x V_d}$$

$$\left[c_2 \delta_{i-\frac{1}{2}} F_{i-\frac{1}{2}}\right] p_{i-1}^{n+1} - \left[c_1 \delta_{i-\frac{1}{2}} F_{i-\frac{1}{2}} + G\right] p_i^{n+1} = -G p_i^n \quad \ldots\ldots\ldots\ldots\ldots\ldots\ldots\ldots\ldots\ldots (B-5)$$

Equation B-1 to B-5 are the numerical scheme solution for equation A-5.

Appendix C

```
************************************************************************
**  COMPUTER SIMULATOR BASED ON THE NUMERICAL SOLUTION OF THE TRANSIENT  **
**   ONE-DIMENSIONAL COMPRESSIBLE FLUID FLOW EQUATION,INCORPORATING THE  **
**                  EFFECTS OF GAS-SLIPPAGE AND NON-DARCY FLOW.          **
************************************************************************

                         ********************
                             MAIN PROGRAM
                         ********************
      IMPLICIT REAL*8 (A-H,O-Z)
      PARAMETER (MX=102)
      DIMENSION P(MX)
      COMMON C1,C2,CC
      COMMON /BLK1/TEMP,BETA,BETA1
      COMMON /BLK3/PERM,POR,DX,AMW,R
      OPEN(UNIT=5,FILE='SLIPy2.DAT')
      OPEN(UNIT=6,FILE='SLIPN.OUT')
C
      READ(5,*)
      READ(5,*) TEMP,PA,PI,VU,VD,XL,DIAM,PERM,POR,BETA,BETA1,NX,AMW,R
C     GAS SLIPPAGE FACTOR (JONE'S, 1972)
      IF(BETA .LT. 0.) BETA=6.9/PERM**.36
C     NON-DARCY FLOW FACTOR (GEERTSMA'S)
      IF(BETA1 .LT. 0.AND.POR.GT.0.07)BETA1=4.85D4/(POR**5.5*PERM**0.5)
C     NON-DARCY FLOW FACTOR (JONE'S, 1987)
      IF(BETA1 .LT. 0.AND.POR.LT.0.07)BETA1=6.15D10/PERM**(1.55)
C
      AREA=3.14159*DIAM**2/4.
      DX=XL/NX
      DX2=DX*DX
      CC1=2.*PERM*AREA/(1.47D4*VU*DX)
      CC2=2.*PERM*AREA/(1.47D4*VD*DX)
      CCC=PERM/(1.47D4*POR*DX2)
      NN=NX+2

      WRITE(6,300)
      WRITE(6,400)TEMP,PA,PI,VU,VD,XL,DIAM,NX,AMW
      WRITE(6,*)
      WRITE(6,500)
      WRITE(6,600)PERM,POR,BETA,BETA1,R
      WRITE(6,*)
C
      WRITE(6,100)
      TM=0.
C     INITIALIZE THE PRESSURE DISTRIBUTION
      P(1)=PI
      DO 10 I=2,NN
 10   P(I)=PA
      READ(5,*)
 20   READ(5,*,END=50) DT,NDT,NP
```

```
      C1=CC1*DT
      C2=CC2*DT
      CC=CCC*DT
      DO 30 J=1,NP
      DO 35 I=1,NDT
      TM=TM+DT
      CALL SOLVE(NN,P)
 35   CONTINUE
      DP=P(1)-P(NN)
      WRITE(6,200) TM,P(1),P(NN),DP,DT,NDT
 30   CONTINUE
      GO TO 20
 100  FORMAT(5X,'Time(sec)',5X,'P(0)',11X,'P(L)',10X,'DP',8X,'DT',3X,
     *'NDT')
 200  FORMAT(F12.3,3F14.6,1x,F7.3,2X,I4)
300   FORMAT('Temp(C)',2X,'Pd(psi)',2x,'Pu(psi)',4x,'Vu(cc)',2x,'Vd(cc)'
     c,2x,'L(cm)',2x,'Dia(cm)',1x,'Grids',2x,'Mol.Wt')
400   FORMAT(F4.1,4X,F6.1,4X,F7.1,1X,2D9.3,1X,2F6.2,2X,I4,3X,F6.1)
500   FORMAT('Perm(md)',2X,'Porosity',2x,'Slippage(psi)',2x,'Beta(1/ft)
     c',2X,'R(psi.cc./gmole/K)')
600   FORMAT(2F8.4,6X,F7.2,8X,1D7.2,3X,F7.1)
 50   STOP
      END
```

```
                              **********************
                                SUBROUTINE SOLVE
                              **********************
```

```
      SUBROUTINE SOLVE(NN,P)
      IMPLICIT REAL*8 (A-H,O-Z)
      PARAMETER (MX=102)
      DIMENSION A(MX),B(MX),C(MX),R(MX),P(MX),PN(MX),F(MX),G(MX),DiPhalf
     *(MX)
      COMMON C1,C2,CC
C
      CC2=2.*CC
      DO 10 I=1,NN
 10   PN(I)=P(I)
      CALL FUNC(NN,P,F,G)
      CALL DELTA(NN,P,DiPhalf)

C *** HARMONIC AVERAGE OF i+-1/2 TERMS
      I=1
      C(I)=C1*F(1)*DIPHALF(1)
      B(I)=-C(I)
C
      I=2
      A(I)=CC2*F(I-1)*DIPHALF(I-1)
      C(I)=CC2*F(I)*F(I+1)/(F(I)+F(I+1))*DIPHALF(I)
      B(I)=-(A(I)+C(I))
C
      DO 20 I=3,NN-2
      A(I)=CC2*F(I-1)*F(I)/(F(I-1)+F(I))*DIPHALF(I-1)
      C(I)=CC2*F(I)*F(I+1)/(F(I)+F(I+1))*DIPHALF(I)
      B(I)=-(A(I)+C(I))
```

```
 20   CONTINUE
C
      I=NN-1
      A(I)=CC2*F(I-1)*F(I)/(F(I-1)+F(I))*DIPHALF(I-1)
      C(I)=CC2*F(I+1)*DIPHALF(I)
      B(I)=-(A(I)+C(I))
C
      I=NN
      A(I)=C2*F(I)*DIPHALF(I-1)
      B(I)=-A(I)
C
C***  COMPUTE THE MAIN DIAGONAL & RHS    ***
      DO 35 I=1,NN
      B(I)=B(I)-G(I)
      R(I)=-PN(I)*G(I)
 35   CONTINUE
      NM1=NN-1
C     SOLVE THE SYSTEM OF EQUATIONS
C     FORWARD ELIMINATION
      DO 60 I=1,NM1
      I1=I+1
      TT=A(I1)/B(I)
      B(I1)=B(I1)-TT*C(I)
      R(I1)=R(I1)-TT*R(I)
 60   CONTINUE
C     BACK SUBSTITUTION
      P(NN)=R(NN)/B(NN)
      DO 70 II=2,NN
      I=NN-II+1
      I1=I+1
      P(I)=(R(I)-C(I)*P(I1))/B(I)
 70   CONTINUE
      RETURN
      END
```

```
**********************
   SUBROUTINE FUNC
**********************
```

```
      SUBROUTINE FUNC(N,P,F,G)
      IMPLICIT REAL*8 (A-H,O-Z)
      PARAMETER (MX=102)
      DIMENSION P(MX),F(MX),G(MX)

      COMMON /BLK1/TEMP,BETA,BETA1
      COMMON /BLK2/ZG(MX),VG(MX)

      DATA CZ1/-.196929D-04/,CZ2/.150321D-07/,CZ3/-.673225D-12/
      T=TEMP+273.
      V1=13.85*T**1.5/(T+102.)
      DO 10 I=1,N
      PR=P(I)
      PATM=PR/14.7
      DV=-0.12474+0.123688*PATM+1.05452E-3*PATM**2-1.5052E-6*PATM**3
      VG(I)=1.E-4*(V1+DV)
```

```
      vG(i)=.0179

      ZG(I)=1.0+CZ1*PR+CZ2*PR**2+CZ3*PR**3
      DZ=CZ1+2.*CZ2*PR+3.*CZ3*PR**2

      zg(I)=0.9973

      CG=8.734E-3

C     CG=1./PR-DZ/ZG(I)
c      write(*,*)i,vg(I),zg(I)
c     pause
      F(I)=(P(I)+BETA)/(VG(I)*ZG(I))
      G(I)=CG*P(I)/ZG(I)
 10   CONTINUE
      RETURN
      END

                              **********************
                                 SUBROUTINE DELTA
                              **********************

      SUBROUTINE DELTA(NN,P,DiPhalf
      IMPLICIT REAL*8 (A-H,O-Z)
      PARAMETER (MX=102)
      DIMENSION ROWB(MX),B1(MX),VELOC(MX),DipHalf(MX),PGRAD(MX),
     &VKRATIO(MX),ROW1(MX),P(MX)
      COMMON /BLK1/TEMP,BETA,BETA1
      COMMON /BLK2/ZG(MX),VG(MX)
      COMMON /BLK3/PERM,POR,DX,AMW,R
C
      T=TEMP+273.
C     Coefficients of the quadratic equation at the cell boundaries (i+-1/2)
      ************************************************************************
      DO 102 I=1,NN
C
      ROW1(I)=P(I)/ZG(I)
      VKRatio(I)=VG(I)/(PERM*(1+(BETA/P(I))))
C       Pressure gradient at the boundaries (c)
c       ---------------------------------------
      IF(I.EQ.1) PGRAD(I)=2*(P(I+1)-P(I))/DX
      IF(I.GT.1.AND.I.LT.NN-1) PGRAD(I)=(P(I+1)-P(I))/DX
      IF(I.EQ.NN-1) PGRAD(I)=2*(P(I)-P(I))/DX
102   CONTINUE
C       Density X Beta factor (a)
c       -------------------------
      DO 101 I=1,NN-1
      ROWB(I)=(2*ROW1(I)*ROW1(I+1)/(ROW1(I)+ROW1(I+1)))*14.7*(AMW*BETA1
     c/(R*(TEMP+273.0)))/3.0883D7
C       Viscosity-permeability ratio (b)
c       --------------------------------
      B1(I)=2*14700*VKRatio(I)*VKRatio(I-1)/(VKRatio(I)+VKRatio(I+1))
c       Velocity at the Boundaries
c       **************************
```

```
      IF(ROWB(I).EQ.0)GOTO 200
      VELOC(I)=(-B1(I)+SQRT(B1(I)**2-4.0*ROWB(I)*PGRAD(I)))/(2*ROWB(I)
     C)
c        Delta at the Boundaries
c        **************************
 200   DiPhalf(I)=1/(1+(ROWB(I)*VELOC(I))/B1(I))
 101   CONTINUE
       RETURN
       END
```

Appendix D

```
*************************************************************************
**  COMPUTER PROGRAM FOR THE ANALYSIS OF PRESSURE PULSE DECAY DATA FOR   **
**  THE ESTIMATION OF PERMEABILITY AND KLINKENBERG CONSTANT  BASED ON    **
**                        THE NON-LINEAR REGRESSION TECHNIQUE            **
*************************************************************************

                                  *********************
                                      MAIN PROGRAM
                                  *********************
      USE MSIMSLMD
      USE MSIMSLSD
C
      IMPLICIT REAL*8 (A-H,O-Z)
      PARAMETER (NCOEF=2,NCOL=2,NOBS=600,LDX=NOBS)
      DIMENSION A(NCOEF),R(NCOEF,NCOEF)
      DIMENSION PM(LDX),PC(LDX)
      COMMON /BLK1/ V(LDX,NCOL),NP
      COMMON /BLK2/ TEMP,NN,PA,PI,CC1,CC2,CCC,DT(NOBS),NDT(NOBS)
      COMMON /BLK5/ POR,DX,AMW,R1,BETA1
      COMMON /BLK6/ TEMPER
      EXTERNAL EVAL
      DATA IDERIV/1/
      OPEN(UNIT=5,FILE='fin25
     .
     dat')
      OPEN(UNIT=7,FILE='LSQRSLIP1.OUT')
      OPEN(UNIT=8,FILE='LSQRSLIP1.RES')
C
C     READ THE EXPERIMENTAL PARAMETERS
      READ(5,*)
      READ(5,*) TEMP,PA,PI,VU,VD,XL,DIAM,NX,AMW
C     READ THE INITIAL ESTIMATE OF THE PARAMETERS
      READ(5,*)
      READ(5,*)
      READ(5,*) PERM,POR,BETA,BETA1,R1

      TEMPER=TEMP
      AREA=3.14159*DIAM**2/4.
      DX=XL/NX
      DX2=DX*DX
      NN=NX+2
      CC1=2.*AREA/(1.47D4*VU*DX)
      CC2=2.*AREA/(1.47D4*VD*DX)
      CCC=1./(1.47D4*POR*DX2)

C     GAS SLIPPAGE FACTOR (JONE'S)
      IF(BETA .LT. 0.) BETA=6.9/PERM**.36
C     NON-DARCY FLOW FACTOR (GEERTSMA'S)
      IF(BETA1 .LT. 0.AND.POR.GT.0.07)BETA1=4.85D4/(POR**5.5*PERM**0.5)
C     NON-DARCY FLOW FACTOR (JONE'S, 1987)
      IF(BETA1 .LT. 0.AND.POR.LT.0.07)BETA1=6.15D10/PERM**(1.55)
```

```
      A(1) = PERM
      A(2) = BETA
C     READ PRESSURE DROP EXPERIMENTAL DATA
      READ(5,*)
      READ(5,*)
      K=0
   10 K=K+1
      READ (5,*,END=15) V(K,1),P0,P1,DP,DT(K),NDT(K)
      V(K,2)=DP
      PM(K)=DP
      GO TO 10
   15 NP=K-1
      WRITE(7,100)
      WRITE(7,700) PERM,BETA,BETA1
      WRITE(7,140) NP
  100 FORMAT(/,5X,'INITIAL ESTIMATE OF THE UNKNOWN PARAMETERS')
  120 FORMAT(/,5X,'FINAL ESTIMATE OF THE UNKNOWN PARAMETERS')
  140 FORMAT(/,5X,'NUMBER OF DATA POINTS READ =',I4)
  220 FORMAT(/,5X,'INITIAL ESTIMATE OF THE NON-LINEAR PARAMETERS')
  230 FORMAT(5X,'A(',I1,')=',E12.5)
  240 FORMAT(/,5X,'FINAL ESTIMATE OF THE NON-LINEAR PARAMETERS')
  250 FORMAT(5X,'A(',I1,')=',E12.5,3X,'DA(',I1,')=',E12.5)
  300 FORMAT(5X,'SAE =',F10.2,3X,'NO. OF ITER =',I3)
  340 FORMAT(11X,'TIME    P(MEAS)   P(CALC)   ERROR %')
  350 FORMAT(5X,F10.2,3F10.2)
  400 FORMAT(5X,'AVERAGE ABSOLUTE RELATIVE ERROR =',F10.3)
  500 FORMAT(/,3X,'ESTIMATE OF THE PARAMETERS AT ITERATION NUMBER =',I2)
  600 FORMAT(5X,'SUM OF THE SQUARES OF THE ERROR =',F12.3)
  700 FORMAT(5X,'PERMEABILITY=',E12.5,3X,'BETA=',E12.5,3X,'BETA1=',E12.5
      *)
C     PRINT THE INITIAL ESTIMATES OF THE NON-LINEAR PARAMETERS
      WRITE(7,220)
      WRITE(7,230) (I,A(I),I=1,NCOEF)
      WRITE(*,*)'PLEASE WAIT FOR A WHILE, THE PROGRAM IS RUNNING'
C
C     NON-LINEAR REGRESSION - LEAST SQUARE METHOD
C
      CALL DRNLIN(EVAL,NCOEF,IDERIV,A,R,LDX,IRANK,DFE,SSE)
C
C     PRINT THE NON-LINEAR PARAMETERS
      WRITE(7,240)
      WRITE(7,230) (I,A(I),I=1,NCOEF)
C
      PERM = A(1)
      BETA = A(2)
      WRITE(7,120)
      WRITE(7,700) PERM,BETA,BETA1
C
      WRITE(8,340)
C     COMPUTE THE CALCULATED PRESSURES
      CALL FUNEVL(NP,PERM,BETA,PC)
C     CALCULATE ERRORS AND PRINT THE RESULTS
      CALL ERROR(PM,PC,NP,NCOEF,SSE)
      CALL CONF(A,SSE)
```

```
      DO 65 K=1,NP
      ERR=100.*(PM(K)-PC(K))/PM(K)
 65   WRITE(8,350) V(K,1),PM(K),PC(K),ERR
      STOP
      END

XXXXXXXXXXXXXXXXXXXXXXXXXXXXXXXXXXXXXXXXXXXXXXXXXXXXXXXXXXXXXXXXXXXXXXXXXXXXXXXXXXXXXXXXXXXXXXX
      SUBROUTINE EVAL(NPAR,A,IOPT,IOBS,FRQ,WT,E,DE,IEND)
      IMPLICIT REAL*8 (A-H,O-Z)
      PARAMETER (NCOEF=2,NCOL=2,NOBS=600,LDX=NOBS)
      DIMENSION A(NPAR),DE(NPAR)
      DIMENSION PP(LDX),PP1(LDX),PP2(LDX)
      COMMON /BLK1/ V(LDX,NCOL),NP
C     write(*,*) 'eval-1'
      PERM=A(1)
      BETA=A(2)
      IF(IOBS .EQ. 1 .AND. IOPT .EQ. 0) THEN
      CALL FUNEVL(NP,PERM,BETA,PP)
      ENDIF
      IF(IOBS .EQ. 1 .AND. IOPT .EQ. 1) THEN
      PERM=1.001*A(1)
      CALL FUNEVL(NP,PERM,BETA,PP1)
      PERM=A(1)
      BETA=1.001*A(2)
      CALL FUNEVL(NP,PERM,BETA,PP2)
      ENDIF
      IF(IOBS .LE. NP) THEN
      K=IOBS
      WT=1.0
      FRQ=1.0
      IEND=0
      IF(IOPT .EQ. 0) THEN
      E=V(K,2)-PP(K)
      ELSE
      DE(1)=-(PP1(K)-PP(K))/(0.001*A(1))
      DE(2)=-(PP2(K)-PP(K))/(0.001*A(2))
      ENDIF
      ELSE
      IEND=1
      ENDIF
      RETURN
      END

XXXXXXXXXXXXXXXXXXXXXXXXXXXXXXXXXXXXXXXXXXXXXXXXXXXXXXXXXXXXXXXXXXXXXXXXXXXXXXXXXXXXXXXXXXXXXXX
      SUBROUTINE FUNEVL(NP,PERM,BETA,PC)
      IMPLICIT REAL*8 (A-H,O-Z)
      PARAMETER (MX=102,NOBS=600)
      DIMENSION P(MX),PC(NOBS)
      COMMON /BLK2/ TEMP,NN,PA,PI,CC1,CC2,CCC,DT(NOBS),NDT(NOBS)
      COMMON /BLK3/ C1,C2,CC
C
      DPI=PI-PA
      P(1)=PI
      DO 30 I=2,NN
 30   P(I)=PA
```

```
      DO 40 K=1,NP
      C1=CC1*PERM*DT(K)
      C2=CC2*PERM*DT(K)
      CC=CCC*PERM*DT(K)
      DO 50 I=1,NDT(K)
      CALL SOLVE(NN,TEMP,PERM,BETA,P)
 50   CONTINUE
      DP=P(1)-P(NN)
      PC(K)=DP
 40   CONTINUE
      RETURN
      END

XXXXXXXXXXXXXXXXXXXXXXXXXXXXXXXXXXXXXXXXXXXXXXXXXXXXXXXXXXXXXXXXXXXXXXX
      SUBROUTINE SOLVE(NN,TEMP,PERM,BETA,P)
      IMPLICIT REAL*8 (A-H,O-Z)
      PARAMETER (MX=102)
      DIMENSION A(MX),B(MX),C(MX),R(MX),P(MX),PN(MX),F(MX),G(MX)
     &,DIPHALF(MX)
      COMMON /BLK3/ C1,C2,CC
      CC2=2.*CC
      DO 10 I=1,NN
 10   PN(I)=P(I)
      CALL FUNC(NN,TEMP,BETA,P,F,G)
      CALL SDELTA(P,NN,PERM,BETA,DIPHALF)
C *** HARMONIC AVERAGE OF i+-1/2 TERMS
      I=1
      C(I)=C1*F(1)*DIPHALF(1)
      B(I)=-C(I)

      I=2

      A(I)=CC2*F(I-1)*DIPHALF(I-1)
      C(I)=CC2*F(I)*F(I+1)/(F(I)+F(I+1))*DIPHALF(I)
      B(I)=-(A(I)+C(I))
C
      DO 20 I=3,NN-2
      A(I)=CC2*F(I-1)*F(I)/(F(I-1)+F(I))*DIPHALF(I-1)
      C(I)=CC2*F(I)*F(I+1)/(F(I)+F(I+1))*DIPHALF(I)
      B(I)=-(A(I)+C(I))
 20   CONTINUE
C
      I=NN-1
      A(I)=CC2*F(I-1)*F(I)/(F(I-1)+F(I))*DIPHALF(I-1)
      C(I)=CC2*F(I+1)*DIPHALF(I)
      B(I)=-(A(I)+C(I))
C
      I=NN
      A(I)=C2*F(I)*DIPHALF(I-1)
      B(I)=-A(I)
C
C***  COMPUTE THE MAIN DIAGONAL & RHS   ***
      DO 35 I=1,NN
      B(I)=B(I)-G(I)
      R(I)=-PN(I)*G(I)
```

```
 35    CONTINUE
       NM1=NN-1
C      SOLVE THE SYSTEM OF EQUATIONS
C      FORWARD ELIMINATION
       DO 60 I=1,NM1
       I1=I+1
       TT=A(I1)/B(I)
       B(I1)=B(I1)-TT*C(I)
       R(I1)=R(I1)-TT*R(I)
  60   CONTINUE
C      BACK SUBSTITUTION
       P(NN)=R(NN)/B(NN)
       DO 70 II=2,NN
       I=NN-II+1
       I1=I+1
       P(I)=(R(I)-C(I)*P(I1))/B(I)
  70   CONTINUE
       RETURN
       END

XXXXXXXXXXXXXXXXXXXXXXXXXXXXXXXXXXXXXXXXXXXXXXXXXXXXXXXXXXXXXXXXXXXXXX
       SUBROUTINE FUNC(NN,TEMP,BETA,P,F,G)
       IMPLICIT REAL*8 (A-H,O-Z)
       PARAMETER (MX=102)
       COMMON /BLK4/ZG(MX),VG(MX)
       DIMENSION P(MX),F(MX),G(MX)
       DATA CZ1/-.196929D-04/,CZ2/.150321D-07/,CZ3/-.673225D-12/
C
       T=TEMP+273.
       V1=13.85*T**1.5/(T+102.)
       DO 10 I=1,NN
       PR=P(I)
       PATM=PR/14.7
       DV=-0.12474+0.123688*PATM+1.05452E-3*PATM**2-1.5052E-6*PATM**3
       VG(I)=1.E-4*(V1+DV)
       PZ=PR
       ZG(I)=1.0+CZ1*PZ+CZ2*PZ**2+CZ3*PZ**3
       DZ=CZ1+2.*CZ2*PZ+3.*CZ3*PZ**2
       CG=1./PR-DZ/ZG(I)
       F(I)=(P(I)+BETA)/(VG(I)*ZG(I))
       G(I)=CG*P(I)/ZG(I)
 10    CONTINUE
       RETURN
       END

XXXXXXXXXXXXXXXXXXXXXXXXXXXXXXXXXXXXXXXXXXXXXXXXXXXXXXXXXXXXXXXXXXXXXX
       SUBROUTINE CONF(A,SSE)
       IMPLICIT REAL*8 (A-H,O-Z)
       PARAMETER (NCOEF=2,NCOL=2,NOBS=600,LDX=NOBS)
       DIMENSION A(NCOEF),F(LDX,NCOEF),R(NCOEF,NCOEF)
       DIMENSION PP(LDX),PP1(LDX),PP2(LDX)
       COMMON /BLK1/ V(LDX,NCOL),NP
       PERM=A(1)
       BETA=A(2)
       CALL FUNEVL(NP,PERM,BETA,PP)
```

```
      PERM=1.001*A(1)
      CALL FUNEVL(NP,PERM,BETA,PP1)
      PERM=A(1)
      BETA=1.001*A(2)
      CALL FUNEVL(NP,PERM,BETA,PP2)
      SUMX=0.
      DO 10 K=1,NP
      SUMX=SUMX+V(K,1)
      F(K,1)=(PP1(K)-PP(K))/(0.001*A(1))
      F(K,2)=(PP2(K)-PP(K))/(0.001*A(2))
 10   CONTINUE
      XAVG=SUMX/(NP-1)
      SGMX=0.
      DO 20 I=1,NP
 20   SGMX=SGMX+(V(I,1)-XAVG)**2
C     CALCULATE THE CONFIDENCE LIMITS
      CALL DMXTXF (NP,NCOEF,F,LDX,NCOEF,R,NCOEF)
      CALL DLINRG (NCOEF,R,NCOEF,R,NCOEF)
      PROB=1.0 - 0.05/2.0
      DF = NP - NCOEF
      TSTAT=DTIN(PROB,DF)
      WRITE(7,100)
      DO 50 I=1,NCOEF
 50   WRITE(7,400) I,(R(I,J),J=1,NCOEF)
      WRITE(7,200)
      RMS=DSQRT(SSE/DF)
      DO 55 I=1,NCOEF
      DELA=RMS*DSQRT(DABS(R(I,I)))*TSTAT
      PERC=100.*DELA/DABS(A(I))
 55   WRITE(7,400) I,A(I),DELA,PERC
 100  FORMAT(/,5X,'INVERSE OF THE SENSITIVITY MATRIX')
 200  FORMAT(/,2X,'NO',5X,'PARAMETER     CONF. INTERVAL  CONF. INT.%')
 400  FORMAT(I4,5E15.6)
      RETURN
      END

XXXXXXXXXXXXXXXXXXXXXXXXXXXXXXXXXXXXXXXXXXXXXXXXXXXXXXXXXXXXXXXXXXXXXXXXXXXXXXX
      SUBROUTINE ERROR(XM,XC,N,M,SSE
      IMPLICIT REAL*8 (A-H,O-Z)
      PARAMETER (NOBS=600)
      DIMENSION  XM(1),XC(1),E(NOBS)
      SUMER=0.0
      SUMEA=0.0
      SS=0.0
      SSR=0.0
      SSE=0.0
      SST=0.0
      SUMXM=0.0
      EMAX=0.0
      EMIN=1.0D9
      DO  10  K=1,N
   10 SUMXM    =SUMXM+XM(K)
      XMAVG    =SUMXM/N
      DO  20  I=1,N
      E(I)=0.0
```

```
      IF(XC(I) .NE. 0.) E(I)=100.0
      IF(XM(I) .NE. 0.) E(I)=100.0*(XM(I)-XC(I))/XM(I)
      SUMER=SUMER+E(I)
      SUMEA=SUMEA+DABS(E(I))
      SS   =SS   + E(I)*E(I)
      SSE  =SSE  +(XM(I)-XC(I))**2
      SSR  =SSR  +(XC(I)-XMAVG)**2
   20 SST  =SST  +(XM(I)-XMAVG)**2
      ER =SUMER/N
      EA =SUMEA/N
      NM = N-M-1
      SD=DSQRT(SS /NM)
      R2=1.0-SSE/SST
      F0=((SST-SSE)/M)/(SSE/NM)
      DO 30    K=1,N
      IF(DABS(E(K)).LT.EMIN ) EMIN = DABS(E(K))
      IF(DABS(E(K)).GT.EMAX ) EMAX = DABS(E(K))
   30 CONTINUE
      WRITE(7,700)
  700 FORMAT(/,7X,'ER',10X,'EA',6X,'MIN ER-',4X,'MAX ER+',4X,'SSE')
      WRITE(7,750)ER,EA,EMIN,EMAX,SSE
  750 FORMAT(4(1X,F10.3),1X,E10.3)
      WRITE(7,800)
  800 FORMAT(/,6X,'SSR',8X,'SST',10X,'SD',7X,'R**2',7X,'F0')
      WRITE(7,850)SSR,SST,SD,R2,F0
  850 FORMAT(2(1X,E10.3),2(1X,F10.4),1X,E12.4)
      RETURN
      END

XXXXXXXXXXXXXXXXXXXXXXXXXXXXXXXXXXXXXXXXXXXXXXXXXXXXXXXXXXXXXXXXXXXXXXX
      SUBROUTINE SDELTA(P,NN,PERM,BETA,DiPhalf)
      IMPLICIT REAL*8 (A-H,O-Z)
      PARAMETER (MX=102)
      DIMENSION ROWB(MX),B1(MX),VELOC(MX),DipHalf(MX),PGRAD(MX),VKRATIO
     C(MX),ROW1(MX),P(MX)
      COMMON /BLK6/TEMPER
      COMMON /BLK4/ZG(MX),VG(MX)
      COMMON /BLK5/POR,DX,AMW,R1,BETA1

C     Coefficients of the quadratic equation at the cell boundaries (i+-1/2)
c     **********************************************************************
      DO 102 I=1,NN
      IDELTA=IDELTA+1
      ROW1(I)=P(I)/ZG(I)
      VKRatio(I)=VG(I)/(PERM*(1+(BETA/P(I))))
C           Pressure gradient at the boundaries (c)
c           -------------------------------------
      IF(I.EQ.1) PGRAD(I)=2*(P(I+1)-P(I))/DX
      IF(I.GT.1.0.AND.I.LT.NN-1) PGRAD(I)=(P(I+1)-P(I))/DX
      IF(I.EQ.NN-1) PGRAD(I)=2*(P(I-1)-P(I))/DX
  102 CONTINUE
C           Density X Beta factor  a
c           ------------------------
      DO 101 I=1,NN-1
      ROWB(I)=(2*ROW1(I)*ROW1(I+1)/(ROW1(I)+ROW1(I+1)))*(AMW*BETA1/(R1*
```

```
     c(TEMPER+273.0)))*14.7/3.0883D7
C            Viscosity-permeability ratio (b)
c            --------------------------------
      B1(I)=2*14700*VKRatio(I)*VKRatio(I+1)/(VKRatio(I)+VKRatio(I+1))
c     Velocity at the Boundaries
c     **************************
      VELOC(I)=(-B1(I)+DSQRT(B1(I)**2-4.0*ROWB(I)*PGRAD(I)))/(2*ROWB(I)
     C)
c     Delta at the Boundaries
c     ***********************
      DiPhalf(I)=1/(1+(ROWB(I)*VELOC(I))/B1(I))

 101  CONTINUE
      RETURN
      END
```